“Plasticity of the Phosphatidylcholine Biogenesis in the Obligate Intracellular Parasite *Toxoplasma gondii*”

D i s s e r t a t i o n

Zur Erlangung des Akademischen Grades
doctor rerum naturalium
(Dr. rer. nat.)
im Fach Biologie

eingereicht an der
Mathematisch-Naturwissenschaftlichen Fakultät I
der Humboldt Universität zu Berlin

von Diplom-Biologin Vera Sampels

Präsidentin/Präsident der Humboldt Universität zu Berlin:
Prof. Dr. Jan-Hendrik Olbertz

Dekanin/Dekan der Mathematisch Naturwissenschaftlichen Fakultät I:
Prof. Dr. Andreas Herrmann

Gutachter: 1. Prof. Thomas Pomorski

2. Prof. Richard Lucius

3. Prof. Kai Matuschewski

Tag der mündlichen Prüfung: 27.03.2012

ACKNOWLEDGEMENTS

First, I would like to thank Dr. Nishith Gupta for the supervision of my research and the guidance throughout the thesis.

I am also very greatful to Prof. Richard Lucius for giving me the opportunity to do this work in his department and making this work possible.

Moreover, I want to thank Prof. Thomas Pomorski, Prof. Kai Matuschewski and Prof. Richard Lucius for agreeing to review this thesis.

My co-workers in the lab, both past and present, have contributed a lot to this work and certainly kept the lab lively. I very much appreciate the friendship and help from all of you and thank you for the great atmosphere. Moreover, I want to especially acknowledge Grit for managing the lab and her incredible patience and technical and mental support.

I also owe my gratitude to Prof. Isabelle Coppens for letting me spend 3 months in her lab. It was a wonderful and inspiring time and I feel grateful for the technical and personal support. I also thank EMBO for granting a short-term fellowship to this end.

Moreover, I want to thank our collaborators Prof. Isabelle Coppens, Prof. Boris Striepen and Prof. Andreas Herrmann for their advice and for sharing resources.

Finally, I feel very fortunate having been part of the ZIBI graduate school, and I want to thank not only for the financial support, but also for generating a wonderful environment for the personel and scientific exchange.

Last, but for sure not least, I would like to express my gratitude to my family and my partner for their unconditioned support. Thanks for sharing in the good days and providing me with the necessary support and encouragement to get me through the not so good days.

ABSTRACT

Toxoplasma gondii is an obligate intracellular apicomplexan parasite that causes life-threatening disease in neonates and in immunocompromised people. Successful replication of *Toxoplasma* requires substantial membrane biogenesis, which must be satisfied irrespective of the host-cell milieu. Like in other eukaryotes, the two most abundant phospholipids in the *T. gondii* membrane are phosphatidylcholine (PtdCho) and phosphatidylethanolamine (PtdEtn). Bioinformatics and precursor labeling analyses confirm their synthesis *via* the CDP-choline and CDP-ethanolamine pathway, respectively. This work shows that the 3-step CDP-choline pathway, involving the activities of *Tg*CK, *Tg*CCT and *Tg*CPT, localizes to the cytosol, nucleus and ER membrane, respectively. The initial reaction is catalyzed by a dual-specificity choline kinase (*Tg*CK, ~70-kDa), capable of phosphorylating choline as well as ethanolamine. The purified full-length *Tg*CK displayed a low affinity for choline (K_m ~0.77 mM). *Tg*CK harbors a unique N-terminal hydrophobic peptide that is required for the formation of enzyme oligomers in the parasite cytosol but not for activity. The displacement of the *Tg*CK promoter in a conditional mutant of *T. gondii* ($\Delta tgck_i$) attenuated the enzyme expression by ~80%. Unexpectedly, the $\Delta tgck_i$ mutant was not impaired in intracellular growth, and exhibited a normal PtdCho biogenesis. To recompense for the loss of full-length *Tg*CK, the mutant appears to make use of an alternative promoter and/or start codon, resulting in the expression of a shorter but active *Tg*CK isoform identified by the anti-*Tg*CK antiserum, which correlated with its persistent choline kinase activity. Accordingly, the $\Delta tgck_i$ showed an expected incorporation of choline into PtdCho, and susceptibility to dimethylethanolamine (a choline analog). Interestingly, the conditional mutant displayed a regular growth in *off state* despite a 25% decline in PtdCho content, which suggests a compositional flexibility in *T. gondii* membranes and insignificant salvage of host-derived PtdCho. The two-step conditional mutagenesis of *Tg*CCT, which caused a reduced growth rate to about 50%, further substantiated this finding. The enzymatic activity of *Tg*CCT and its role in PtdCho synthesis remain to be proven, however.

Taken together, the results demonstrate that the CDP-route is likely essential in *T. gondii*. The competitive inhibition of choline kinase to block the parasite replication appears a potential therapeutic application.The work also reveals a remarkably adaptable membrane biogenesis in *T. gondii*, which may underly the evolution of *Toxoplasma* as a promiscuous pathogen.

ZUSAMMENFASSUNG

Der obligat intrazelluläre Parasit *Toxoplasma gondii* ist der Erreger der Toxoplasmose, und dient zugleich als wichtiger Modellorganismus für weitere Human- und Tierpathogene, wie z.B. *Plasmodium* oder *Eimeria*. Die Vermehrung von *T. gondii* erfordert eine effiziente Biosynthese von Phospholipiden für die Herstellung neuer Membranen, was durch die *de novo* Synthese durch den Parasiten, und/oder den Import von Lipiden aus der umgebenden Wirtszelle gewährleistet werden kann. Während der Parasit zahlreiche Möglichkeiten für Synthese oder Import von PtdEtn und PtdSer verwendet, scheint die Biosynthese des abundantesten Membranlipids PtdCho auschließlich über den CDP-Cholin Weg zu erfolgen. Dieser erstreckt sich in *T. gondii* über 3 zelluläre Kompartimente, mit einer cytosolischen Cholin-Kinase (*Tg*CK), einer im Zellkern lokalisierenden Cholin-Cytidylyltransferase (*Tg*CCT) und einer Cholin-Phosphotransferase (*Tg*CPT) im ER. Anders als die substrat-spezifische Ethanolamin-Kinase (*Tg*EK), kann *Tg*CK neben Cholin außerdem Ethanolamin phosphorylieren. *Tg*CK zeigt eine geringe Affinität zu Cholin (K_m ~0.77 mM), während eine verkürzte *Tg*CK (*Tg*CK$_S$), welcher eine als Signalpeptid vorhergesagte N-terminale Sequenz (20 Aminosäuren) fehlt, eine etwa 3-fach höhere Aktivität aufweist (K_m ~0.26 mM). Während jedoch die Wildtyp-*Tg*CK cytosolische Cluster in *Toxoplasma* bildet, zeigt die verkürzte *Tg*CK eine gleichmäßigere cytosolische Lokalisierung. Wir schlussfolgern daraus, dass der hydrophobe N-Terminus nicht notwendig ist für eine funktionale *Tg*CK, sondern eine strukturelle Funktion bei der Protein-Lokalisierung hat. Eine konitionelle Mutante, in welcher der *Tg*CK Promoter gegen den Tetracyclin-regulierbaren Promoter *pTetO7Sag4* ausgetauscht wurde (*Δtgck$_i$*), zeigt erstaunlicherweise normales Wachstum und PtdCho Biosynthese. Die *Tg*CK Aktivität und die daraus resultierende PtdCho Synthese sind nur zu ~30% regulierbar. Unsere Ergebnisse deuten auf die Verwendung eines alternativen Startcodons bzw. Promoters hin, welcher zur Expression einer verkürzten (~53-kDa) aber vermutlich aktiven Cholin Kinase führt, wodurch der Verlust der *Tg*CK (~70-kDa) kompensiert wird.

Der konditionelle Knockout von *Tg*CCT, dem regulatorischen Enzym des CDP-Cholin Wegs, hatte einen 50%igen Wachstumsdefekt zur Folge.

Diese Studie zeigt eine erstaunliche Flexibilität des Parasiten bezüglich seiner Membranzusammensetzung, und bestätigt zugleich die Annahme, dass PtdCho nicht von der Wirtszelle importiert werden kann. Diese Anpassungsfähigkeit stellt einen möglichen Faktor dar, der es *T. gondii* erlaubt sich in einem breiten Spektrum von Wirten zu vermehren.

ABBREVIATIONS

APR	Apical polar ring
ATc	Anhydro-tetracycline
ATP	Adenosine triphosphate
CAT	Chloramphenicol acetyltransferase
CCT	Choline cytidylyltransferase
cDNA	complementary deoxyribonucleic acid
$CHCl_3$	Chloroform
CK	Choline kinase
CPT	CDP-choline phosphotransferase
DAPI	4',6-diamidino-2-phenylindole
DHFR-TS	Dihydrofolate reductase thymidylate synthase
DME	Dimethylethanolamine
DMEM	Dulbeccos's modified Eagle medium
DNA	Deoxyribonucleic acid
EDTA	Ethylendiamine tetraacetate
EK	Ethanolamine kinase
ER	Endoplasmic reticulum
EtOH	Ethanol
FAS I/II	Fatty acid synthase type I/II
FCS	Fetal calf serum
FUdR	5-Fluoro-2'-deoxyuridine
HFF	Human foreskin fibroblast

H.O.S.T.	Host Organelle Sequestering Tubulo-Structures
HXGPRT	Hypoxanthine-xanthine-guanine phosphoribosyl transferase
IEM	Immunoelectron microscopy
IFA	Indirect immunofluorescence assay
IMC	Inner membrane complex
IPTG	Isopropyl-ß-D-1-thiogalactopyranoside
IVN	Intravacuolar network
LDL	Low-density lipoprotein
LiAc	Lithium acetate
MeOH (CH_3OH)	Methanol
MTOC	Microtubule organizing center
NADH	Nicotinamide adenine dinucleotide
NLS	Nuclear localization signal
NBD	7-nitrobenz-2-oxa-1,3-diazol-4-yl
ORF	Open reading frame
PBS	Phosphate buffered saline
PCR	Polymerase chain reaction
PEG	Polyethylene glycol
PEMT	Phosphatidylethanolamine methyltransferase
*Pf*PMT	phosphoethanolamine methyltransferase (*Plasmodium falciparum*)
PSD	Phosphatidylserine decarboxylase
PtdCho	Phosphatidylcholine
PtdEtn	Phopshatidylethanolamine
PtdSer	Phosphatidylserine

PV	Parasitophorous vacuole
PVM	PV membrane
RNA	Ribonucleic acid
SDS	Sodium dodecyl sulfate
TaTi	Trans-activator trap identified
TLC	Thin layer chromatography
UPRT	Uracil phosphoribosyl transferase
UTR	Untranslated region

TABLE OF CONTENTS

FIGURES

APPENDICES

1 Introduction

1.1 Introduction to *Toxoplasma gondii*

1.1.1 *Toxoplasma gondii*: life cycle and disease

Toxoplasma belongs to the phylum Apicomplexa, a diverse group of obligate intracellular parasites, many of which inflict devastating diseases in human and animals, such as malaria, toxoplasmosis and coccidiosis (1). Unlike other intracellular parasites, which usually have a narrow host range, *T. gondii* has an exceptional ability to replicate in most vertebrate cells. The wide host range of *T. gondii* makes toxoplasmosis one of the most common parasitic infections of humans and animals. Up to one third of the population worldwide is estimated to harbor the parasite. The seroprevalence, however, varies strongly between countries, with about 20-80% in Europe and 23% in the USA (2,3). Infection with *T. gondii* is usually asymptomatic but it can cause life-threatening encephalitis and systemic infections in neonates and in immunocompromised individuals.

The natural life cycle of *Toxoplasma* involves a sexual phase in feline species, and an asexual phase, which can occur in virtually all warm-blooded hosts (Fig. 1). The intermediate host can acquire the parasite by ingestion of the infected feed or undercooked meat. Upon ingestion, the parasite immediately invades host cells to commence its asexual and lytic cycle. The invasive tachyzoite stage is capable of converting into the dormant bradyzoite stage, preferentially in the central nervous system or muscle tissue, which can persist as tissue cysts for life. These cysts can be reactivated to become actively replicating tachyzoites upon decay of the host immune response. Tachyzoites have a doubling time between 8-10 hrs, and cause a tissue lysis by sequential events of invasion, replication, egression and re-invasion of neighboring host cells. The ingestion of infected mice carrying tissue cysts by cats results in parasite invasion into the gut epithelium cells of the feline host and subsequent onset of sexual stages (Fig. 1). The merozoites in the intestine differentiate into macro- and microgametes, which fuse to form the oocyst. These oocysts are shed into the environment and harbor 2 sporocysts each enclosing 4 sporozoites. Accidental ingestion of the sporulated oocysts indicates the asexual life cycle.

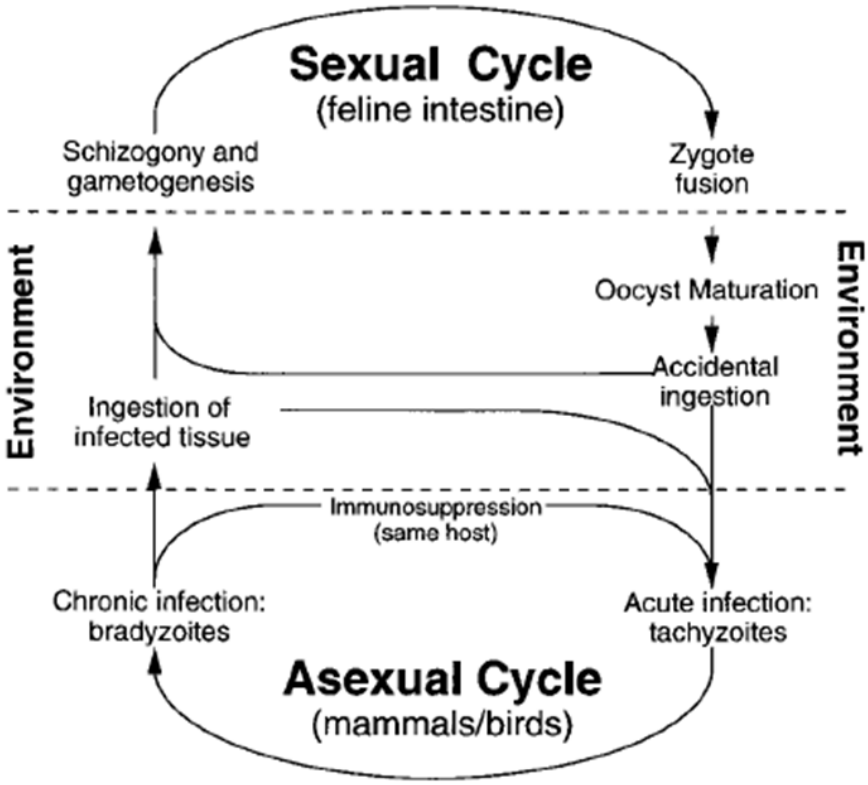

Fig. 1: **Life cycle of *Toxoplasma gondii.*** The life cycle involves a sexual phase, which is resticted to feline species only. The asexual phase can occur in most warm-blooded animals including human. Oocysts shed in the environment can be ingested by an intermediate host, where sporozoites are released and develop into the replicative tachyzoite stage. Tachyzoites undergo a lytic life cyle (acute infection) and can transform into bradyzoites (chronic infection) in response to host immune system (1).

1.1.2 Subcellular organelles and cell division

Members of the phylum apicomplexa are higly polarized cells and share an apical complex harboring the conoid and a set of unique secretory organelles, micronemes, rhoptries and dense granules. These organelles play a crucial role in the active invasion and subsequent modification of the host environment (4). *Toxoplasma* displays a typical eukaryotic morphology comprising of a nucleus, perinuclear endoplasmic reticulum, an elongated lunate-shaped mitochondrion, and a single Golgi stack. The apicoplast, a plastid of cyanobacterial origin acquired by secondary endosymbiosis and therefore enclosed by 4 membranes, is also present in most apicomplexans except in *Cryptosporidium* (5). The structural integrity of the parasite is ensured by a pellicle, consisting of the subpellicular microtubules and the inner membrane complex (IMC), a system of flattened membrane cisternae underlying the plasma membrane (6). The microtubules emerge from an apical microtubule organizing center

(MTOC) located at the basal end of the conoid (7). *T. gondii* possesses a haploid genome throughout its asexual replication. Two extrachromosomal genomes are present in the apicoplast and mitochondrion of *T. gondii* (8).

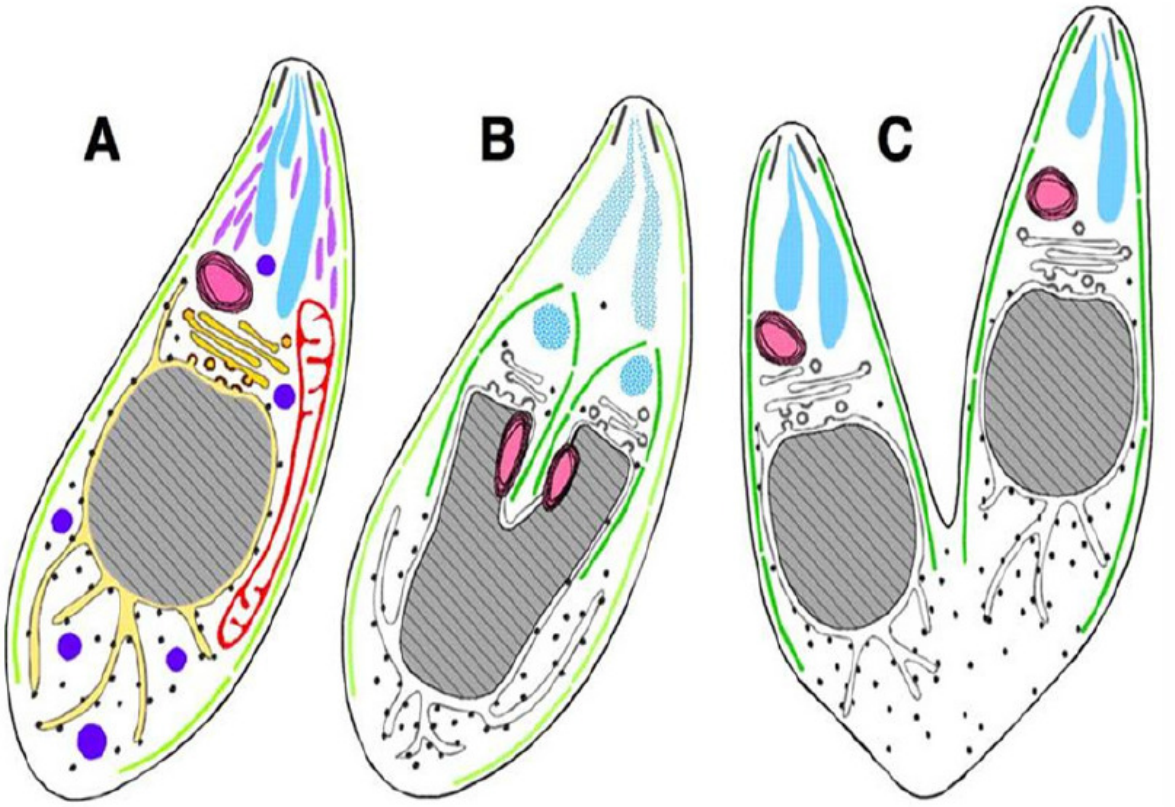

Fig. 2: **Schematic depiction of structure and cell division of *T. gondii*.** (A) conoid (black lines), inner membrane complex (light green lines), rhoptries (turquoise), micronemes (lavender), dense granules (blue), apicoplast (pink), mitochondrion (red), Golgi (gold), nucleus (grey), endoplasmic reticulum (yellow); (B) developing daughter IMC scaffolds (dark green). Adapted from Nishi *et al*. (9)

The cell division in tachyzoites proceeds *via* endodyogeny, in which two progenies are formed within an intact mother cell (Fig. 2). First indication of cell division is the duplication of centrioles, which definines a mitotic spindle (10). Centriole duplication occurs with the concurrent elongation and fission of the Golgi (11). The DNA replication is initiated and the IMC scaffold emerges from the apical polar ring (APR)-MTOC (10). The extension of the microtubule network from the APR towards the posterior end of the budding parasite causes the partitioning of the mother nucleus and cytoplasm. The division of maternal mitochondrion and ER occurs late during the division, which are distributed equally in the daughter cells. Unlike other organelles, rhoptries and micronemes are formed *de novo* in each daughter cell presumably by vesicular budding from the Golgi stack. The mitochondrion and apicoplast

harbor their own genomes, which undergo division before (apicoplast) or immediately after (mitochondrion) the karyokinesis (9,12). The newly formed daughter parasites acquire their plasma membrane from the mother cell, leaving behind only a small residual body.

1.2 Genetic manipulation of *T. gondii*

1.2.1 Selection markers

Over the last two decades a wide spectrum of methods to manipulate the haploid genome of *Toxoplasma* tachyzoites has been established. The two crucial achievements were the establishment of transfection *via* electroporation of tachyzoites (13) and the completion of the genome sequencing (www.ToxoDB.org). *Toxoplasma* serves as an excellent model organism to study the biology of apicomplexan parasites, due to relative ease of genetic manipulation and well established culture of the infectious tachyzoite stage. (14).

The stable transfection makes use of selection markers to generate transgenic parasites. An observation that wild-type strains of *T. gondii* are sensitive to inhibitors of prokaryotic translation, such as chloramphenicol, and introduction of the chloramphenicol acetyltransferase (CAT) gene renders the parasite resistant to drug, led to the development of CAT as a positive selection marker (15). Based on pyrimethamine-resistance in *Plasmodium*, introduction of point mutations in the *Tg*DHFR-TS protein provided a positive selection system for transgenic work (16). Significantly higher frequency of stable transformation was achieved by exploitation of the parasite's dihydrofolate reductase-thymidylate synthase (DHFR-TS). A yet another approach exploits the parasite purine salvage pathway. The hypoxanthine-xanthine-guanine phosphoribosyl transferase (HXGPRT) can be used as a positive as well as a negative selection marker, because its absence confers resistance to 6-thioxanthine (6-TX), whereas the ectopic expression of HXGPRT in null background can rescue the parasite from mycophenolic acid in the presence of exogenous xanthine (17). Uracil phosphoribosyl transferase (UPRT) is largely dispensable for *T. gondii* tachyzoite survival and its replacement by foreign DNA renders the tachyzoites resistant to 5-fluoro-deoxyuridine (FUDR) (18). This phenomenon can be exploited to target genes of interest to the UPRT locus by negative selection.

Other selection methods include the *Streptoalloteichos* or Tn5 *ble* gene product, which can protect from the DNA-damaging activity of phleomycin. The selection must be applied on extracellular tachyzoites, which makes it inconvenient and thus a less common marker.

1.2.2 Conditional *versus* direct gene deletion

The haploid genome of *T. gondii* tachyzoites makes it easier to study the gene function by direct deletion mediated by double homologous recombination. The constructs harboring the 5'- and 3'-UTRs of the gene of interest flanking a resistance cassette allow replacement or disruption of the open reading frames. The resultant clonal transgenic parasite lines can be phenotyped. The deletion of essential genes, however, is lethal to the parasite due to its haploid nature. To this end, conditional manipulation of *T. gondii* has been established, which permits regulation of gene expression in response to specific ligands. The tetracycline transactivator-based "*tet-off*" method controls the gene expression at the transcriptional level (19,20). Fusion of a *Toxoplasma* transactivation domain with the *E. coli* Tet-repressor (TetR) in the TATi (trans-activator trap identified) tachyzoites allows a controlled gene expression through a minimal parasite promoter fused with "tetO" (Tet operator) elements. Transcription is reversibly blocked by anhydro-tetracycline (ATc), which displaces the transactivator from the operator. Conditional mutagenesis can be performed by direct replacement of the native gene promoter by the tetracycline regulatable promoter. Alternatively, a regulatable cassette can be introduced into the parasite genome, and then the native locus can be ablated by double crossover.

The essential genes can also be examined by modulation of the protein stability. Fusion of a destabilization domain (ddFKBP) with the target protein leads to its proteasomal degradation, unless the domain is masked by a ligand known as Shield-1 (21,22). This system allows a fast and efficient control of proteins fused with ddFKBP-domain.

1.2.3 Recombination *versus* random integration

The ablation of gene function by direct deletion in *Toxoplasma gondii* has proven difficult due to a lower frequency of crossover, which could only be counteracted by constructs with longer (>2kb) crossover sequences. This was recently attributed to the presence of non-homologous end-joining (NHEJ) pathways in *T. gondii*, mediated by a protein complex, which facilitate the direct repair of double strand breaks in DNA (23,24). A heterodimer of Ku70 and Ku80 binds to the broken and free DNA ends, and subsequently recruits a DNA-dependent protein kinase and the DNA-ligase-IV-XRCC4 complex. This results in ligation of the DNA breaks (25). The attempts to delete Ku70 and DNA-ligase-IV genes have failed which appear to be essential in *T. gondii*. The type I and type II (23,24,26) strain lacking the Ku80 gene have

been generated, which show a much improved efficiency of homologous recombination. These strains are now widely used for genetic manipulation to study the biology of tachyzoite and bradyzoite stages, respectively.

1.3 Membrane biogenesis in eukaryotic cells

1.3.1 Introduction to neutral and polar lipids

Lipids are defined as hydrophobic ingredients of biological membranes, which are readily soluble in the organic solvents. There is a great diversity of lipid species differing in their structure and function, which can be broadly classified as triacylglycerols, phospholipids, sphingolipids and neutral lipids (Fig. 3). The main constituents of biological membranes are phospholipids and neutral lipids the former of which are amphipathic molecules with two fatty acid chains at the *sn*-1 and *sn*-2 positions of a glycerol backbone and a phosphate or polar head group at *sn*-3 position. The polar head group is usually choline, ethanolamine, serine or inositol. In a hydrophilic milieu, e.g. the cell cytosol, phospholipids spontaneously self-assemble to form a bilayer, in which the acyl chains face the hydrophobic interior and the hydrophilic phosphate and head groups interact with the aqueous milieu. The primary role of lipids is the formation of lipid bilayers surrounding the organelles, in addition to their functions as energy store or as signaling molecules.

The second most abundant class of membrane lipids is cholesterol, which differs significantly from phospholipids. Cholesterol is a member of the steroid lipids and is composed of 20 carbon atoms arranged as four hydrocarbon rings, 3 cyclohexanes and 1 cyclopentane. A hydroxyl group is attached to the C3 position, and the C17 in the cyclopentane ring harbors an alkyl side chain. Its amphipathic character allows interaction with the polar headgroups of neighboring phospholipids through the hydroxyl group, while the hydrophobic ring and alkyl chain are embedded in the core of the bilayer. Cholesterol provides rigidity to the membrane and regulates its permeability for small molecules.

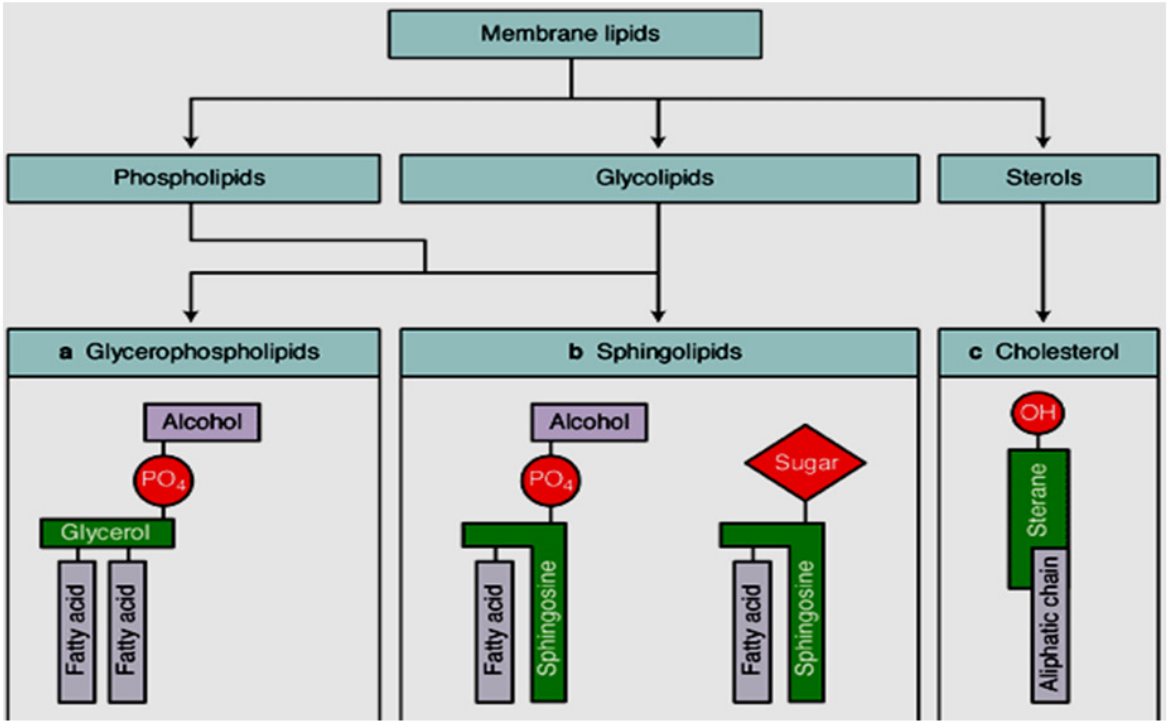

Fig. 3: **Major classes of lipids present in most eukaryotic membranes.** Lipids are broadly classified into phospholipids, glycolipids and sterols. Phospholipids are composed of a glycerol backbone, which carries two fatty acid chains and a phosphate or polar head group (choline, etc.). Sphingolipids consist of a sphingosine moiety, which harbors an acyl chain and a sugar residue or a phosphorylated head group. Sterols are generally composed of four carbon rings, an alkyl chain, and a hydroxyl group.

1.3.2 *De novo* synthesis of lipids in mammalian cells

Lipids synthesis in mammalian cells is highly interconnected and consists of two independent pathways for the formation of each phospholipid. It begins with cytosolic and/or nuclear enzymes; however, the eventual sites of lipid biosynthesis are the endoplasmic reticulum and the mitochondria. PtdEtn, PtdCho and PtdSer are synthesized from their respective precursors ethanolamine, choline and serine, and further interconverted into eachother (Fig. 4).

Choline is metabolized into PtdCho *via* the CDP-choline pathway (27,28). Choline, an essential nutrient, is phosphorylated to phosphocholine by a choline kinase (CK) in the cytosol. The phosphocholine cytidylyltransferase (CCT) then catalyzes the fusion of phosphocholine with CTP to produce CDP-choline. The product is finally converted into PtdCho *via* transfer of the phosphocholine moiety to diacylglycerol (DAG) catalyzed by CDP-choline phosphotransferase (CPT). PtdCho can also be made from PtdEtn *via* a three-step methylation reaction catalyzed by a PtdEtn methyltransferase (PEMT). The CDP-

ethanolamine pathway is analogous to the above pathway and involves activity of EK, ECT and EPT to generate PtdEtn from ethanolamine (27). Alternatively, PtdEtn can be made from PtdSer using a PtdSer decarboxylase, which is localized in the mitochondria. PtdSer in mammalian cells is produced by a PtdSer synthase, exchanging serine for the head group from PtdCho (PSS-1) or PtdEtn (PSS-2) (27). The DAG is mainly derived from phosphatidic acid (PtdOH) by the action of a phosphatase.

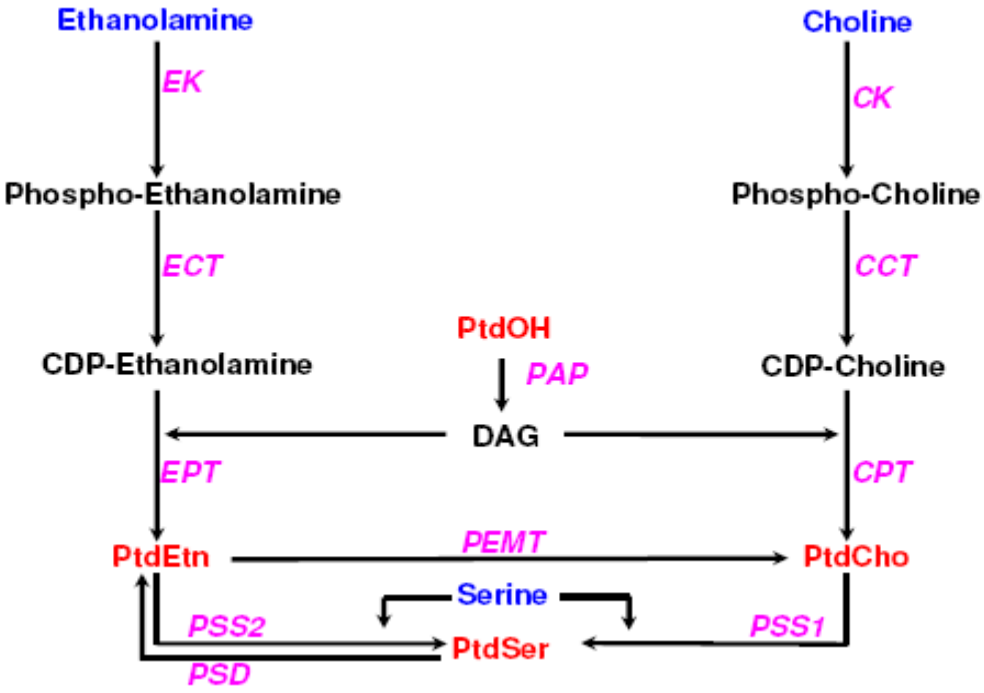

Fig. 4: ***De novo*** **synthesis of phospholipids in mammalian cells.** CK, choline kinase; CPT, CDP-choline phosphotransferase; DAG, diacylglycerol; EK, ethanolamine kinase; EPT, CDP-ethanolamine phosphotransferase; PCT, phosphocholine cytidylyltransferase; PET, phospho-ethanolamine cytidylyltransferase; PEMT, phosphatidylethanolamine methyltransferase; PSD, phosphatidylserine decarboxylase; PSS, phosphatidylserine synthase; PtdCho, phosphatidylcholine; PtdEtn, phosphatidylethanolamine; PtdOH, phosphatidic acid; PtdSer, phosphatidylserine

Mammalian cells are also capable of synthesizing cholesterol *via* the mevalonate pathway, a multi-step pathway named after a key metabolic intermediate of the rate-limiting reaction catalyzed by hydroxymethyl-glutaryl (HMG)-CoA reductase (29). The cholesterol biosynthesis is tissue-specific and mainly occurs in the liver, from where it is exported *via* low-density lipoproteins (LDL) to other tissues in esterified form. The LDL can be internalized by other cells using LDL-receptor mediated endocytosis (30). The cholesterol is utilized for membrane biogenesis, in the formation of vitamins and steroid hormones, and for cellular signalling.

1.3.3 Intracellular trafficking of lipids in eukaryotic cells

Not only do the subcellular membranes vary in their lipid composition, the two leaflets of the bilayer are selectively enriched in individual lipids. Moreover, the final reactions of lipid synthesis occur in the ER- or mitochondrial membranes from where lipids must be distributed to other cellular organelles. To facilitate the process, lipids can shuttle between the organelles *via* carrier vesicles (31).

The lipid trafficking, however, is partially insensitive to drugs blocking vesicular transport, which indicates the presence of alternative non-vesicular routes for lipid movement (32). Tight apposition of two membranes can provide contact zones for lipid exchange, such as the mitochondria-associated membranes (MAM), the contact sites between the ER and mitochondria (33). Finally, lipid trafficking and movement can also occur *via* specific carrier proteins. This includes lipoproteins for cholesterol, the ceramide transport protein (CERT), and the ATPases between the membrane leaflets. The plasma membrane shows an asymmetric distribution of phospholipids, in which PtdCho and sphingolipids are enriched in the outer exoplasmic leaflet, and PtdSer and PtdEtn on the inner cytoplasmic face of the membrane (34). This lipid asymmetry is mainly due to two types of flippases, the ABC (ATP-binding cassette)-transporter catalyzing the outward-directed movement ("flop") of lipids, and the P4-type ATPases, which translocate lipids to the inner leaflet ("flip") (35).

1.3.4 Phospholipid synthesis in *Toxoplasma*

Successful replication of *T. gondii* requires substantial biogenesis of the parasite organelle and plasma membranes. Further, the parasite growth must be accompanied by enlargement of the enclosing parasitophorous vacuolar membrane (PVM). The *T. gondii* membrane consists primarily of phospholipids and neutral lipids, and minor plant-like lipids (36,37). Similar to other eukaryotic cells, PtdCho is the most abundant lipid in *T. gondii*. The lipid analyses of human host cell (HFF) and the tachyzoites have revealed a higher content of PtdCho in the parasite. PtdCho accounts for ~75% of total phospholipids in *T. gondii*, which is followed by PtdEtn (10%), PtdIns (7.5%), PtdSer (6%) and PtdOH (1.5%) (38). Moreover, the parasite phospholipids preferentially contain shorter-chain and more saturated fatty acid (37). The precursor labeling assays have shown that *Toxoplasma* can utilize choline, ethanolamine and serine into PtdCho, PtdEtn and PtdSer, respectively (38,39). This has been substantiated by enzyme assays and bioinformatic analyses. Unlike other eukaryotes, however, *Toxoplasma*

does not possess gene annotations or activity for PEMT, and appears incompetent in making PtdCho from PtdEtn (38). There is also no evidence for a plant-type phospho-ethanolamine methyltransferase in *T. gondii*, which has been identified exclusively in *P. falciparum* (40). These findings suggest a strict dependence of *T. gondii* on its CDP-choline pathway (i.e. choline auxotrophy) to sustain its PtdCho biogenesis.

Shortly after invasion dense granule proteins are released into the PV lumen lumen, of which a complex of Gra2, Gra4 and Gra6 proteins is implicated in biogenesis of the intravacuolar network (IVN), which originates from multi-lamellar vesicles, secreted at the posterior end of the parasite (41,42). The IVN is thought to provide a large surface area and potentially serves as a conduit for nutritional exchange between *T. gondii* and its host. The selective labeling of host or parasite lipids indicated the flow and assimilation of host-derived lipids across the PVM to the IVN, which might contribute to enlargement of the PVM (43). However, whether the PVM expansion is accomplished by translocation of parasite-derived lipids or *via* recruitment of host lipids is not fully understood.

The intracellular parasite extensively modifies its host cell to gain access to a variety of nutritional compounds, which are either imported *via* specific transporters, or can freely diffuse through the 1.3 kDa pores in the PVM (44). The PVM is juxtaposed with host endoplasmic reticulum and mitochondria (45), which are the major sites of lipid synthesis in the mammalian host. These organelles can therefore potentially offer a source for host-derived lipid for the parasite.

1.4 Objective of this study

Toxoplasma gondii as an obligate intracellular parasite requires biogenesis of subcellular membranes to ensure a faithful replication. Whether the parasite fulfills the demand of phospholipids by *de novo* synthesis and/or salvaging of host-derived lipids is not understood. Axenic *T. gondii* can incorporate free choline into its most abundant lipid PtdCho; however, at much lower rate (~9%) than required for the cell doubling (38). The aim of this work was to investigate the relative dependence of *T. gondii* on *de novo* CDP-choline pathway and host-derived LDL for PtdCho biogenesis.

2 Materials and Methods

2.1 Materials

2.1.1 Biological resources

Cell Line	Source
Human Foreskin Fibroblasts (HFF)	Carsten Lüder, University of Göttingen, Germany
T. gondii tachyzoites (RH *hxgprt*$^-$)	Dominique Soldati-Favre, University of Geneva, Switzerland
T. gondii tachyzoites (TaTi-*Δku80* strain)	Boris Striepen, University of Georgia, USA
T. gondii tachyzoites (*Δku80* strain)	Vern Carruthers, University of Michigan, Ann Arbor, USA
COS-7	Isabelle Coppens, Johns Hopkins University, Baltimore, USA
E.coli (XL-1blue, Rosetta)	Stratagene, Germany
Saccharomyces cerevisiae (KS106) (*MATα eki1Δ::TRP1 cki1Δ::HIS3 leu2-3,112 ura3-1 trp1-1 his3-11,15 ade2-1 can1-100*)	George Carman, Rutgers University, New Brunswick, USA
Saccharomyces cerevisiae Y04832 (*MAT a; his3Δ1; leu2Δ0; met15Δ0; ura3Δ0; YGR202c::kanMX4*)	Euroscarf, Frankfurt
Saccharomyces cerevisiae Y04637 (*MAT a; his3Δ1; leu2Δ0; met15Δ0; ura3Δ0; YGR007w::kanMX4*)	Euroscarf, Frankfurt
Saccharomyces cerevisiae HJ000 *MATa his3-Δ1 leu2-3,112 ura3-52 trp1-289 cpt1::LEU2 ept1-Δ1::URA3*	Christopher McMaster, Dalhousie University, Canada

2.1.2 Chemical reagents

Product	Manufacturer
Adenosinetriphosphate (ATP)	Sigma, Germany
Albumin Fraction V	Applichem, Germany
Aluminium hydroxide Fluid Gel	Reheis, Ireland
Ammonium acetate	Roth, Germany
Ammonium molybdate	Applichem, Germany
Ammonium persulfate	Sigma, Germany
Ammonium Reineckate salt	Sigma, Germany
Ammonium sulphate	Roth, Germany
Ampicillin	Sigma, Germany
Ascorbic acid	Applichem, Germany
Bromophenol blue	Merck, Germany
Calcium carbonate	Merck, Germany
Calcium chloride	Applichem, Germany
Chloramphenicol	Roth, Germany
Chloroform	Roth, Germany
Choline chloride	Applichem, Germany
Coomassie brilliant blue	Applichem, Germany
Crystal violet	Sigma, Germany
Deoxynucleotide-triphospate (dNTPs)	Rapidozym, Germany
Dimethylethanolamine	Sigma, Germany
Dimethyl sulfoxide (DMSO)	Sigma, Germany
DNA marker (1 kb ladder)	Fermentas, Germany

Dragendorff's reagent	Sigma, Germany
Distilled water (HPLC-purified)	Roth, Germany
Dithiothreitol (DTT)	Applichem, Germany
Dubecco's Modified Eagle Media (DMEM) (w/o Na-pyruvate, w/o L-glutamine, 4.5 g/l D-glucose)	Biochrom, Germany
EDTA	Applichem, Germany
Ethanol	Applichem, Germany
Ethanolamine chloride	Applichem, Germany
Ethidium bromide	Applichem, Germany
Fetal calf serum	Biochrom, Germany
Fluoromount G / DAPI	SouthernBiotech, USA
5-Fluoro-2'-deoxyuridine (FUDR)	Sigma, Germany
Glacial acetic acid (99 %)	Applichem, Germany
D(+)-Galactose	Applichem, Germany
α-D(+)-Glucose monohydrate	Applichem, Germany
Glutathione	Applichem, Germany
Glycerol	Applichem, Germany
Human Serum (1 unit)	Interstate Blood Bank, Memphis, TN, USA
Iodine (anhydrous beads)	Sigma, Germany
IPTG	Applichem, Germany
L-glutamine (200 mM)	Biochrom, Germany
Lipofectamine 2000	Invitrogen, USA
Lithium acetate	Applichem, Germany
Mangan(II)-chloride-tetrahydrate	Applichem, Germany

Magnesium chloride hexahydrate	Applichem, Germany
Methanol	Roth, Germany
MOPS (3-(N-Morpholino)-Propansulfonsäure)	Applichem, Germany
Mycophenolic acid	Applichem, Germany
NADH, Disodium salt	Calbiochem, Germany
Na-pyruvate (100 mM)	Biochrom, Germany
NBD-labeled phospholipids	Avanti Polar Lipids, USA
Non-essential amino acids (100x)	Biochrom, Germany
Paraformaldehyde	Roth, Germany
PBS	Biochrom, Germany
Penicillin / Streptomycin	Biochrom, Germany
Penicillin / Streptomycin	Invitrogen, Germany
Perchloric acid	Applichem, Germany
Phosphocholine	Sigma, Germany
Phosphoethanolamine	Sigma, Germany
Polyethylenglycol 3350	Applichem, Germany
Potassium acetate	Roth, Germany
Potassium chloride	Roth, Germany
Potassium dihydrogen phosphate	Applichem, Germany
Potassium hydrogen carbonate	Applichem, Germany
Di-potassium hydrogen phosphate	Applichem, Germany
Potassium hydroxide	Merck, Germany
Potassium sulphate	Applichem, Germany

Protein marker (prestained)	New England Biolabs, Germany
N-Propanol	Applichem, Germany
Roti-phenol/Chloroform/Isoamyl alcohol (25:24:1)	Roth, Germany
Rotiphorese Gel 30	Roth, Germany
Phosphoenolpyruvate	Applichem, Germany
Primers (see Table 1)	Invitrogen, Germany
Pyrimethamine	Sigma, Germany
Pyruvate kinase/Lactic dehydrogenase	Sigma, Germany
Salmon sperm DNA (10 mg/ml)	Invitrogen, Germany
Salts	Roth, Applichem, Germany
Sodium dodecyl sulfate (SDS)	Roth, Germany
TEMED	Roth, Germany
TLC plates (silica 60)	VWR, Germany
Tris-HCl	Applichem, Germany
Triton X-100	Applichem, Germany
Trizol	Invitrogen, Germany
Trypsin / EDTA	Biochrom, Germany
Tryptone	Applichem, Germany
Xanthine	Applichem, Germany
X-Gal	Applichem, Germany
Yeast extract	Roth, Germany
Yeast nitrogen base (YNB)	Sigma, Germany

2.1.3 Materials for radioactive work

Product	Manufacturer
[methyl-^{14}C]-Cytidine diphosphocholine	Biotrend, Germany
[^{3}H]-Choline chloride	Perkin Elmer, USA
[^{14}C]-Choline chloride	Biotrend, Germany
[1,2-^{3}H]-Ethanolamine	Hartmann Analytic, Germany
Liquid scintillation cocktail	Perkin-Elmer, USA
[^{14}C]-Phosphocholine	Biotrend, Germany
24-well scintillation plate	Perkin Elmer, Germany

2.1.4 Vectors

Plasmid	Source
pcDNA3.1^{+}	Isabelle Coppens, Johns Hopkins University, Baltimore, USA
p2854 DFHR-TS	Dominique Soldati, University of Geneva, Switzerland
pDT7S4	Boris Striepen, University of Georgia, USA
pESC-Ura, *pESC-His*	Stratagene, USA
pET22b^{+}	Novagen, Germany
pET28b^{+}	Novagen, Germany
pET41b^{+}	Novagen, Germany
pNTP3	Isabelle Coppens, Johns Hopkins University, Baltimore, USA
pNTP3TetO7Sag1	modified *pNTP3*
pTetO7Sag1-NTP3-UPKO (*pTetUPKO*)	modified *pNTP3*

pTKO	John Boothroyd, Stanford University School of Medicine, USA

2.1.5 Antibodies and working dilutions

Antibody and dilution factor	**Source**
Alexa 594, Alexa 488 (anti-mouse, anti-rabbit) (1:3000)	Invitrogen, Germany
α-HA (rabbit, mouse) (1:1000)	Invitrogen, Germany
Anti-6xHis-tag mAb IgG1 (mouse)	Dianova, Germany
Phalloidin-Alexa595	Invitrogen, USA
α-*Tg*Actin	Dominique Soldati, University of Geneva, Switzerland
α-*Tg*Gap45 (1:3000)	Plattner *et al*. (46)
α-*Tg*Gra3 (1:500)	Dubremetz *et al*. (47)
α-*Tg*Sag1 (1:1000)	Kim and Boothroyd (48)
α-Ty1 (BB2 hybridoma culture supernatant, 1:50)	Bastin *et al.* (49)
α-V5 (1:1000)	John Leslie, Immunology Consultants Laboratory, OR, USA

2.1.6 Enzymes

Enzyme	**Manufacturer**
Antartic phosphatase	NEB, Germany
Dream Taq polymerase	Fermentas, Germany
Pfu Ultra II Fusion HS DNA polymerase	Stratagene, Germany

Proteinase K	Sigma, Germany
Restriction endonucleases, Klenow enzyme	NEB, Germany
T4 ligase	Invitrogen, Germany
Thrombin protease	Novagen, Germany

2.1.7 Instruments

Instrument	**Manufacturer**
BioPhotometer	Eppendorf, Germany
BTX square wave electroporator (ECM 830)	BTX, USA
Gel documentation & EASY Enhanced Analysis	Herolab, Germany
Gel electrophoresis chamber and power supply	Amersham Biosciences, USA
Microscope (Apotome Imager.Z2)	Zeiss, Germany
Nanodrop (ND 1000)	Wilmington, USA
PCR Thermocycler (FlexCycler)	JenaAnalytic, Germany
Scintillation counter (1450 MicroBeta TriLux)	PerkinElmer, USA
TLC developing tank	Sigma, Germany
Western Blotting chamber	Peqlab, Germany

2.1.8 Plasticware and disposables

Product	**Manufacturer**
Cover slips	Roth, Germany
Cryo tubes	Biochrom, Nalgene, Germany
Disposable pipettes (10 ml, 25 ml, 50 ml)	Greiner Bio-One, Austria
Eppendorf tubes (1.5 ml, 2 ml)	Greiner Bio-One, Austria

Electroporation cuvettes (4 mm gap)	Eppendorf, Germany
Falcon tubes (15 ml, 50 ml)	Greiner Bio-One, Austria
Filter sterilizer (0.22 µm)	Schleicher Schuell, Germany
Glass beads (0.45 – 0.6 mm)	Sartorius, Göttingen, Germany
High performance chemiluminescence film	GE Healthcare, Germany
LabTek chamber slides	ThermoScientific, Germany
Microscopy slides	Menzel, Germany
Needles	BD, Germany
Nitrocellulose transfer membrane	Applichem, Germany
Improved Neubauer counting chamber	Neubauer, Germany
Parafilm	Pechiney, USA
PCR tubes	Rapidozym, Germany
Pipette tips	Greiner Bio-One, Austria
Polypropylene tubes (12 ml)	Greiner Bio-One, Austria
RNAase-free barrier tips	Sorenson BioScience, USA
Syringes	BD, Germany
Tissue culture flasks, Petridishes, Multi-well plates	Greiner Bio-One, Austria
Whatman (3 MM)	A. Hartenstein, Germany
X-ray film (FUJI Medical)	A. Hartenstein, Germany

2.1.9 Commercial kits

Product	**Manufacturer**
DNA purification (plasmid preps)	Jena Analytic, Invitrogen, Germany

pDrive cloning kit	Qiagen, Germany
ECL Western blotting and analysis system	GE Healthcare, Germany
µMACS mRNA isolation	Miltenyi Biotec, Germany
µMACS one-step cDNA synthesis	Miltenyi Biotec, Germany
Platinum SYBR Green qPCR Superscript-UDG	Invitrogen, Germany
Protein Assay Kit (BCA)	Thermo Scientific, USA
Pure Link RNA Mini Kit	Ambion, Germany
Reverse transcription PCR (SuperScript III)	Invitrogen, Germany
SuperScript III First-strand synthesis supermix for qRT-PCR	Invitrogen, Germany

2.1.10 Reagent preparations

Solution	**Composition**
D10	DMEM (high glucose) supplemented with 10% FCS, 2 mM L-Glutamine, 1x NEAA, 1 mM Sodium pyruvate, 100 U/ml Penicillin and 100 µg/ml Streptomycin
LB media	10 g tryptone, 5 g yeast extract and 10 g NaCl in 1 liter ddH_2O (15 g of agar-agar optional for plates)
SOB media	20 g tryptone, 5 g yeast extract, 0.5 g NaCl, 186 mg KCl and 10 mM $MgCl_2$ in 1 liter ddH_2O
SOC-media	2% tryptone (w/v), 0.5 % yeast extract (w/v), 10 mM NaCl, 2.5 mM KCl and 20 mM glucose in ddH_2O

TFB I	30 mM KOAc (pH 5.8), 50 mM $MnCl_2$ x 4 H_2O, 10 mM $CaCl_2$, 100 mM RbCl, 15% glycerol Filter sterilize
TFB II	10 mM MOPS (pH 7), 75 mM $CaCl_2$, 10 mM RbCl, 15% glycerol Filter sterilize
YPD-media	20 g peptone, 10 g yeast extract and 20 g agar-agar (optional) in 950 ml ddH_2O. Filter-sterile glucose (40% stock) was added to obtain a final concentration of 2%
10x amino acid mix	adenine hemisulfate (400 mg), L-Arg (200 mg), L-Asp (1000 mg), L-Gln (1000 mg), L-His (200 mg), L-Leu (600 mg), L-Lys (300 mg), L-Met (200 mg), L-Phe (500 mg), L-Ser (3750 mg), L-Thr (2000 mg), L-Try (400 mg), L-Tyr (300 mg), L-Val (1500 mg) and Uracil (200 mg) in 500 ml ddH_2O. Uracil or histidine was omitted for selective media.
Synthetic drop-out media	1.7 g YNB (free of ammonium sulphate and amino acids) and 5 g ammonium sulphate in 500 ml ddH_2O. The 10x amino acid mix and 40% sugar (final 2 %) stocks were added to obtain synthetic drop-out media
Cytomix for *T. gondii* transfection	120 mM KCl, 0.15 mM $CaCl_2$, 100 mM K_2HPO_4/KH_2PO_4, 500 mM HEPES, 100 mM EGTA and 100 mM $MgCl_2$. 30 µl ATP (100 mM stock), 12 µl GSH (250 mM stock) and 10-50 µg DNA were added to 700 µl prior to the parasite transfection
Transformation buffers for *S. cerevisiae*	10x TE buffer

	100 mM Tris (pH 7.5), 10 mM EDTA Buffer was filter sterilized and stored at 4°C. The 1x TE buffer was freshly prepared from 10x TE buffer.
	LiAc / TE buffer The 1x LiAc / TE buffer was prepared by diluting 10x LiAc (1 M lithium acetate, pH 7.5) and 10x TE solutions in sterile water.
	PEG3350 / LiAc / TE buffer This solution was prepared fresh from 10x TE, 10x LiAc and filter-sterilized PEG3350 (50 %, w/v) in a ratio of 1:1:8.
TAE buffer for agarose gel electrophoresis	The 1x TAE buffer was prepared from 50x buffer, which contained 242 g/l of Tris base, 57.1 ml/l of glacial acetic acid and 18.6 g/l of EDTA.
Lysis buffer for genomic DNA	10 mM Tris-HCl (pH 8), 5 mM EDTA, 0.5% SDS, 200 mM NaCl in ddH_2O. 100 µg/ml proteinase K solution was added prior to use.
Choline/Ethanolamine kinase assay solutions	Assay buffer (1x) ATP (10 mM), DTT (1.3 mM), $MgCl_2$ (11 mM), Tris (67 mM, pH 8.5) Prepare as 5x stock and supplement with enzyme preparation, [^{3}H]- or [^{14}C]-choline + choline chloride or [1,2-^{3}H]-ethanolamine chloride + ethanolamine chloride prior to use
	Prepare 100 mM choline chloride stock in ddH_2O
	Prepare 100 mM choline chloride stock in 0.5 N NaOH for ammonium reineckate

	precipitation and dilute (final 10 mM and 40 mM choline chloride) prior to use
	Prepare 5 M ethanolamine chloride stock in 5 M HCl for ethanolamine kinase assay
	Prepare 5 M dimethylethanolamine chloride stock in 5 M HCl for choline kinase inhibition
	5 % Ammonium reineckate salt in methanol (prepare fresh)

2.1.11 Primer Table 1

Primer Name (restriction site)	**Primer Sequence (restriction site underlined)**	**Cloning Vector (research objective)**
Functional Expression in *E. coli*		
*Tg*CK-F (*NdeI*) *Tg*CK-R (*HindIII*)	CTCCATATGCAGGTACTCGCGTGTGT CTCAAGCTTCTTTCGAGCCGGGAAGAGT	*pET22b*$^+$(*Tg*CK-6xHis in Rosetta strain)
*Tg*CK-wo-HP-F (*NdeI*) *Tg*CK-R (*BglII*)	CTCATCCATATGTCCCCTTCAGGCGCTGGCT CTCAGATCTTCACTTTCGAGCCGGGAAGAGTCC	*pET28b*$^+$(6xHis-*Tg*CK$_S$ in Rosetta strain)
*Tg*EK-F (*NcoI*) *Tg*EK-R (*HindIII*)	CTCCCATGGCCAGCAAGGCAGAGAGAAC CTCAAGCTTGAACGACAAATGCGGGACT	*pET28b*$^+$ (*Tg*EK-6xHis in Rosetta strain)
*Tg*CCT-F1 (*NdeI*) *Tg*CCT-R1 (*NotI*)	CTCATCCATATGGAGGCTGTTAGCAGTTCTTC CTCATCGCGGCCGCCTGTCATGCGTCAGATGCTG	*pET41b*$^+$(*Tg*CCT-6xHis in Rosetta strain)
*Tg*CPT-F1 (*NdeI*) *Tg*CPT-R1 (*NotI*)	CTCATCCATATGATGGTCGGTGGCGTT CTCATCGCGGCCGCGGAGCTCTTTTTGAGAGCATTAAG	*pET41b*$^+$(*Tg*CPT-6xHis in Rosetta strain)
*Tg*EPT-F1 (*NdeI*)	CTCATCCATATGGTGTTTGGACACTACATTCCCCCT	*pET41b*$^+$ (*Tg*EPT-6xHis in

*Tg*EPT-R1 (*NotI*)	CTCATCGCGGCCGCAGCCCCGCGCCGTCTGCT	Rosetta strain)
Functional Expression in *S. cerevisiae*		
*Sc*CK1-F (*NotI*) *Sc*CK1-R (*NotI*)	CTCGCGGCCGCATGGTACAAGAATCACGTCCA CTCGCGGCCGCTTACAAATAACTAGTATCGAGGAACTT	*pESC-Ura* (*Sc*CK1 in KS106 strain)
*Sc*EK1-F (*SpeI*) *Sc*EK1-R (*BglII*)	CTCACTAGTATGTACACCAATTATTCACTTAC CTCAGATCTTTAAAAAATAAGTTTAGTGTCTAAG	*pESC-Ura* (*Sc*EK1 in KS106 strain)
*Tg*CCT-F2 (*NotI*) *Tg*CCT-R2 (*NotI*)	CTCATCGCGGCCGCATGGAGGCTGTTAGCAGTTCTTC CTCATCGCGGCCGCTTACTGTGATGCGTCAGATGCT	*pESC-His* (*Tg*CCT in Y04832 or Y04637 strain)
*Tg*CPT-F2 (*NotI*) *Tg*CPT-R2 (*NotI*)	CTCATCGCGGCCGCATGATGGTCGGTGGCGTT CTCATCGCGGCCGCTTAGGAGCTCTTTTTGAGAGCATTAA	*pESC-His* (*Tg*CPT in Y04832, Y04637 or HJ000 strain)
*Tg*EPT-F2 (*NotI*) *Tg*EPT-R2 (*NotI*)	CTCATCGCGGCCGCATGGTGTTTGGACACTACATTCCCCC CTCATCGCGGCCGCCTAAGCCCCGCGCCGTCT	*pESC-His* (*Tg*CPT in Y04832, Y04637 or HJ000 strain)
*Sc*CCT1-F (*NotI*) *Sc*CCT1-R (*NotI*)	CTCATCGCGGCCGCATGGCAAACCCAACAACAG CTCATCGCGGCCGCTCAGTTCGCTGATTGTTTCTTC	*pESC-His* (*Sc*CCT1 in Y04832 strain)
*Sc*CPT1-F (*NotI*) *Sc*CPT1-R (*NotI*)	CTCATCGCGGCCGCATGGGATTCTTTATTCCTCAGAGT CTCATCGCGGCCGCCTAAATTTCTTTTGGATGTTTAATTGA	*pESC-His* (*Sc*CPT1 in HJ000 strain)
*Sc*ECT1-F (*NotI*) *Sc*ECT1-R (*NotI*)	CTCATCGCGGCCGCATGACGGTAAACTTAGATCCGGAT CTCATCGCGGCCGCTTATATGGACATTCCCTTTTTTTGG	*pESC-His* (*Sc*ECT1 in Y04637 strain)
*Sc*EPT1-F (*NotI*) *Sc*EPT1-R (*NotI*)	CTCATCGCGGCCGCATGGGATATTTTGTTCCGGATT CTCATCGCGGCCGCTTATGTCAGCTTGGAGCGC	*pESC-His* (*Sc*CPT1 in HJ000 strain)

Subcellular Localization in *T. gondii*		
*Tg*CK-Term-F (*HindIII*) *Tg*CK-Term-R (*NheI*)	CTCAAGCTTCTGGAATTTGGAGTCAACGC CTCGCTAGCCAAGCAGAAGTCGGATATTAGCG	Step # 1 for expressing *Tg*CK-HA under the *pTgCK* promoter in tachyzoites
*Tg*CK-Prom-F (*ApaI*) *Tg*CK-Prom-R (*HindIII*)	CTCGGGCCCGGCAGGTGGTTTTGCTTC CTACTGAAGCTTGAATACTCTCGAAC	Step # 2 for expressing *Tg*CK-HA under the *pTgCK* promoter in tachyzoites
*Tg*CK-ORF-F (*HindIII*) *Tg*CK-ORF-HA-R (*HindIII*)	GTATTCAAGCTTCAGTAGCACCAAC CTCAAGCTTTCAAGCGTAATCTGGAACATCGTATG GGTACTTTCGAGCCGGGAAGAG	Step # 3 for expressing *Tg*CK-HA under the *pTgCK* promoter in tachyzoites
*Tg*CK-Prom-HP-Ty1-F (*NheI*) *Tg*CK-Prom-HP-Ty1-R (*ApaI*)	CTCTCTGCTAGCCTGGATAAATACCCGATGCTACA AATC CTCTCTGGGCCCATCGAGCGGGTCCTGGTTCGTGT GGACCTCAGCGCCTGAAGGGGACGC	Step # 1 for expressing *Tg*CK-Ty1 under the *pTgCK* promoter in tachyzoites
*Tg*CK-ORF-Term-F (*ApaI*) *Tg*CK-ORF-Term-R (*ApaI*)	CTCTCTGGGCCCGGCTCTTTGTTTCTGGTGGC CTCTCTGGGCCCCAAGCAGAAGTCGGATATTAGC G	Step # 2 for expressing *Tg*CK-Ty1 under the *pTgCK* promoter in tachyzoites
TgCK_S-F (*SbfI*) *Tg*CK_S-myc-R (*PacI*)	CTCATCCCTGCAGGCCCCTTCAGGCGCTGGCT CTCATCTTAATTAACTAGAGGTCTTCTTCGGAAATC AACTTCTGTTCCTTTCGAGCCGGGAAGAGTCCA	*pTKO* (For expressing *Tg*CK_S-myc in tachyzoites)
*Tg*EK-F (*NcoI*) *Tg*EK-HA-R (*PacI*)	CTCCCATGGCCAGCAAGGCAGAGAGAAC CTCTTAATTAATCAAGCGTAATCTGGAACATCGTAT GGGTAGAACGACAAATGCGGGACT	*pNTP3* (For expressing *Tg*EK-HA in tachyzoites)
*Tg*CCT-F3 (*EcoRV*) *Tg*CCT-HA-R3 (*PacI*)	CTCATCGATATCATGGAGGCTGTTAGCAGTTCTTC CTCTTAATTAATCAAGCGTAATCTGGAACATCGTAT GGGTACTGTGATGCTGCAGATGCTG	*pTetUPKO* or *pNTP3TetO7Sag1* (*Tg*CCT-HA under the *pTetO7Sag1* promoter in tachyzoites)
*Tg*CPT-F3 (*EcoRV*)	CTCATCGATATCATGATGGTCGGTGGCGTT	*pNTP3TetO7Sag1*

*Tg*CPT-HA-R3 (*PacI*)	CTCATCTTAATTAATCAAGCGTAATCTGGAACATC GTATGGGTAGGAGCTCTTTTTGAGAGCATTAAG	(*Tg*CPT-HA under the *pTetO7Sag1* promoter in tachyzoites)
Functional Expression in COS-7 Cells		
*Tg*CK-F4 (*HindIII*) *Tg*CK-R4 (*XbaI*)	CTCATCAAGCTTATGCAGGTACTCGCGTGTGT CTCATCTCTAGACTTTCGAGCCGGGAAGAGT	*pcDNA3.1*$^+$ (*Tg*CK-V5 under the *pCMV* promoter in COS-7 cells)
*Tg*CCT-F4 (*HindIII*) *Tg*CCT-R4 (*XbaI*)	CTCATCAAGCTTATGGAGGCTGTTAGCAGTTCTTC CTCATCTCTAGACTGTGATGCGTCAGATGCTG	*pcDNA3.1*$^+$ (*Tg*CCT-V5 under the *pCMV* promoter in COS-7 cells)
*Tg*CPT-F4 (*HindIII*) *Tg*CPT-R4 (*XbaI*)	CTCATCAAGCTTATGATGGTCGGTGGCGTT CTCATCTCTAGAGGAGCTCTTTTTGAGAGCATTAA G	*pcDNA3.1*$^+$ (*Tg*CPT-V5 under the *pCMV* promoter) in COS-7 cells
*Tg*EPT-F4 (*HindIII*) *Tg*EPT-R4 (*XbaI*)	CTCATCAAGCTTATGGTGTTTGGACACTACATTCC CCC CTCATCTCTAGAAGCCCCGCGCCGTCTGCT	*pcDNA3.1*$^+$ (*Tg*EPT-V5 under the *pCMV* promoter in COS-7 cells)
Promoter Displacement of *Tg*CK in *T. gondii*		
*Tg*CK-PD-5'UTR-F (*NdeI*) *Tg*CK-PD-5'UTR-R (*NdeI*)	CTCATCCATATGGGATGAAGTGTGTGTGGTCTG CTCATCCATATGTGTAAACTTAGGCGACTACACAG C	*pDT7S4* (promoter displacement of *Tg*CK in the TaTi-*Δku80* strain)
*Tg*CK-PD-3'UTR-F (*BglII*) *Tg*CK-PD-3'UTR-R (*AvrII*)	CTCATCAGATCTATGCAGGTACTCGCGTGTG CTCATCCCTAGGGAACGGGTACTCCATCAGGTAGT	*pDT7S4* (promoter displacement of *Tg*CK in the TaTi-*Δku80* strain)
*Tg*CK-PD-5'Scr-F DHFR-R	CATTCCGAGGCGGATAAA CGGGTTTGAATGCAAGGTT	Screening for 5'-crossover in transgenic TaTi-*Δku80* strain
DHFR-F *Tg*CK-PD-3'Scr-R	CTCTCTTTTCGGAGGGATCAG ACAACCTGTCTCTGCACCG	Screening for 3'-crossover in transgenic TaTi-*Δku80* strain
Conventional Knockout of *Tg*CK in *T. gondii*		

*Tg*CK-KO-5'UTR-F (*HindIII*) *Tg*CK-KO-5'UTR-R (*NheI*)	CTCAAGCTTCGTAGGATAGAAGCGAGTCGTT CTCGCTAGCCGTCTAGGAGGTTCAAATTTGC	*p2854-DHFR-TS* (conventional knockout of *Tg*CK in the *Δku80* or *hxgprt*$^-$ strain)
*Tg*CK-KO-3'UTR-F (*NotI*) *Tg*CK-KO-3'UTR-R (*NotI*)	CTCGCGGCCGCTCGGATAACACAGTGGAACTTGG CTCGCGGCCGCTCACACCAAAGAGGGCCG	*p2854-DHFR-TS* (conventional knockout of *Tg*CK in the *Δku80* or *hxgprt*$^-$ strain)
*Tg*CK-KO-5'Scr-F DHFR-R2	CCTCGTTTCTAGATAAAAGGCTGC ATGCAAGGTTTCGTGCTGTC	Screening of 5'-crossover in transgenic *Δku80* or *hxgprt*$^-$ strain
DHFR-F2 *Tg*CK-KO-3'Scr-R	CGAATCCAGATGGAGATGGCTGTC AGAATGCGAGTGTCTGGCAA	Screening of 3'-crossover in transgenic *Δku80* or *hxgprt*$^-$ strain
Conditional Knockout of *Tg*CCT in *T. gondii*		
*Tg*CCT-KO-5'UTR-F (*ApaI*) *Tg*CCT-KO-5'UTR-R (*ApaI*)	CTCATCGGGCCCCACTGGGGATTCTTGTGCG CTCGGGCCCCAGAATTCCCTGTTAATCTCTGTGC	*p2854* (conditional knockout of *Tg*CCT in the TaTi-*Δku80* strain)
*Tg*CCT-KO-3'UTR-F (*XbaI*) *Tg*CCT-KO-3'UTR-R (*NotI*)	CTCATCTCTAGAGACGTAATGTCTACGCTTTCATGG CTCGCGGCCGCGTGTCTCAATGCCGTTATTCGT	*p2854* (conditional knockout of *Tg*CCT in the TaTi-*Δku80* strain)
*Tg*CCT-KO-5'Scr-F DHFR-R	AACATTGGAAGAAAAATACTTTGACTT CGGGTTTGAATGCAAGGTT	Screening of 5'-crossover in transgenic TaTi-*Δku80* strain
DHFR-F *Tg*CCT-KO-3'Scr-R	CTCTCTTTTCGGAGGGATCAG GTTGATGACGTTGGCAACC	Screening of 3'-crossover in transgenic TaTi-*Δku80* strain
Quantitative PCR of *Tg*CK		
*Tg*CK-Ex1-F1 *Tg*CK-Ex1-R1	TAAAGGGCTGGGAAAACCTT CTCTTGCCTCGAATTTCCAC	qPCR of Exon1 (368-576 bp) in *Tg*CK transcript

*Tg*CK-Ex1-F2 *Tg*CK-Ex1-R2	CTTTGTTTCTGGTGGCCAGT CCCGATAAACGACTGCACTT	qPCR of Exon1 (80-360 bp) in *Tg*CK transcript
*Tg*CK-Ex6-F *Tg*CK-Ex6-R	TCTTCTCCGTCCACTTGACC GTCCACCATAGCCTTGGAAA	qPCR of Exon6 (1547-1698 bp) in *Tg*CK transcript
*Tg*GT1-EST-F *Tg*GT1-EST-R	GGCTATTTTGGCACCTTTCA AACGGGAAGACAAACCACAG	qPCR of *Tg*GT1 (Housekeeping gene)
*Tg*Elf1a-EST-F *Tg*Elf1a-EST-R	AGTCGACCACTACCGGACAC CTCGGCCTTCAGTTTATCCA	qPCR of *Tg*Elf1a (Housekeeping gene)

2.2 Methods - Culture and Transfection

2.2.1 Propagation of mammalian cells

The primary human foreskin fibroblasts (HFF) were cultured in Dulbecco's modified Eagle's medium with 10% fetal calf serum, 2 mM glutamine, 1x MEM non-essential amino acids, 100 units/ml penicillin and 100 µg/ml streptomycin in a humidified incubator (37°C at 10% CO_2). The cells were harvested using Trypsin/EDTA and seeded into flasks and dishes.

2.2.2 Propagation of *Toxoplasma gondii* tachyzoites

All strains of *T. gondii* tachyzoites were maintained by serial passage in confluent HFF monolayers. Transgenic parasites were selected in 25 µg/ml mycophenolic acid (MPA) with 50 µg/ml xanthine or 1 µM pyrimethamine or 5 µM FUDR. The tranfected parasites were added to the host monolayer and allowed to invade. Selection with pyrimethamine or MPA and xanthine was started 12-24 hrs post-transfection by adding fresh medium containing the indicated amounts of the respective drugs. Medium was then changed and fresh drug was added every day and after about 1 week stable transgenic parasites were obtained. For selection with FUDR, transfected parasites were passaged for 4 cycles in medium without drug. Then, D10 medium supplemented with 5 µM FUDR was added to the intracellular parasites. Fresh medium containing drug was added after 1 week, and the cultures were

incubated for 2 weeks or until the lysed-out vacuoles were observed. The stable parasites were pooled and subjected to cloning by limiting dilution.

2.2.3 Transfection of *T. gondii* tachyzoites

Freshly egressed or syringe-released parasites (10 to 30x10^6) were centrifuged at 300 g for 10 min at RT, washed once in 1x PBS, and the pellet was suspended in 700 µl of cytomix. This mixture was complemented with 5-50 µg of linearized or circular plasmid DNA, 30 µl ATP (sterile 100 mM stock) and 12 µl GSH (sterile 250 mM stock). Electroporation was done by two 1.7 kV pulses at an interval of 100 msec using a BTX square wave electroporator. Transfected parasites were used to infect confluent HFF monolayers for further experiments.

2.2.4 Transformation of *Saccharomyces cerevisiae*

The YPM media containing 2 % glucose (50 ml) was inoculated (OD_{600} of 0.1) with an over-night-grown pre-culture of *S. cerevisiae* and grown at 30°C with shaking until an OD_{600} of 0.4 was reached. Yeast cells were pelleted by centrifugation (1000g, 5 min, RT), followed by 1x washing with 25 ml of sterile TE-buffer and then with 10 ml of LiAc / TE buffer. The final pellet was resuspended in N*100 µl of LiaAc / TE buffer (N number of transformations) and incubated at RT for 30 min. 100-200 ng of plasmid preparation and 100 µg of salmon sperm DNA were added to the 100 µl of competent yeast suspension and mixed by finger tapping. The 0.6ml of PEG / LiAc / TE (8:1:1) solution was added to the transformation mix followed by vortexing for 10 seconds and horizontal incubation for 30 min (200 rpm, 30°C). Then, 70 µl of DMSO were added to each reaction and the suspension was mixed by inverting the tube. A heat-shock was performed for 15 min at 42°C in water bath followed by immediate cooling on ice for 2 min. Cells were pelleted at 14000 g for 15 sec and washed with 1x TE buffer prior to suspension in 100 µl of TE buffer. Finally, cells were plated on selective SD plates (-ura or -his) with 2 % glucose and incubated at 30°C for three to four days. One colony was picked from each plate and streaked onto a master plate for subsequent experiments. Freezer stocks were made in 2% glycerol by snap freezing in liquid N_2.

2.3 Methods - Molecular Cloning

2.3.1 PCR reactions

10-500 ng of the template DNA was used for PCR. The Dream-Taq polymerase (Fermentas) was employed for standard analytical PCR, and the Pfu-Ultra FusionII high-fidelity polymerase (Stratagene) was used for expression cloning. PCR composition and conditions were set according to the primers, polymerase and the length of amplification targets. The PCR reaction was tested for amplification using 0.8-1% agarose gel with0.4% ethidium bromide ran in 1x TAE buffer. The DNA product was mixed with 6x loading dye and resolved at 80-100V followed by UV-visualization.

2.3.2 Ligation of DNA

The PCR amplified inserts were evaluated for their purity on agarose gel and subsequently purified either by gel extraction or by column purification according to the kits' manual. The vector DNA was isolated from *E. coli* according to the kits' protocol (plasmid miniprep) and concentration was determined by NanoDrop instrument. Insert and plasmid were subjected to digestion with appropriate restriction enzymes. In case of non-directional gene cloning, prior to ligation, the plasmid was dephosphorylated using Antartic Phosphatase (NEB) for 1 hr at 37°C followed by heat inactivation (65°C, 30 min). Digested vector and insert were mixed in molar ratios of 1:3 or 1:5 (10 fmol of vector and 30 or 50 fmol of insert) and ligated using 1U of T4 ligase (1 hr at RT or at 4°C over-night), prior to transformation of the competent *E. coli* (Xl1-blue) cells.

2.3.3 Competent *Escherichia coli* cells

A 5 ml over-night-grown culture of *E. coli* (XL-1blue or the Rosetta strain) was used to inoculate 200 ml SOB culture, which was grown at 37°C until an OD_{600} of 0.4 to 0.5 was reached. The culture was pelleted (1300 g, 10 min, 4°C) and washed once in 50 ml of ice-cold TFB-I buffer. Cells were resuspended in 6.4 ml of TFB-II buffer and snap-frozen into aliquots at -80°C.

2.3.4 Transformation of *Escherichia coli*

Each ligation reaction was mixed with a 10-fold higher volume of freshly-thawed competent *E. coli*. The samples were incubated on ice for 30 min, followed by a heat shock (45 sec, 42°C), and 2 min cooling on ice. Prewarmed SOC media (750 µl) was added to each transformation reaction and the mix was shaked at 37°C for 1 hr. The cells were pelleted (3 min, 6000 rpm), resuspended in fresh LB media and plated on Amp or Kan plates according to the plasmid. The plates were incubated at 37°C overnight.

2.3.5 Purification of recombinant proteins from *Escherichia coli*

The full-length choline kinase (*Tg*CK) and ethanolamine kinase (*Tg*EK) proteins with a C-terminal 6xHis tag (*Tg*CK-6xHis, *Tg*EK-6xHis) and a truncated *Tg*CK lacking its first 20 residues with an N-terminal histidine tag (6xHis-*Tg*CK_S) were cloned in the *pET22b*$^+$(*Tg*CK-6xHis) or in the *pET28b*$^+$(*Tg*EK-6xHis, 6xHis-*Tg*CK_S) plasmids, and expressed in the *E. coli* Rosetta strain. The cultures were grown at 37°C until an OD_{600} of 0.3-0.5 was reached, and induced with 1 mM IPTG for 4 hrs at 25 °C. Cells were pelleted (5000xg, 10 min, 4 °C), and suspended in 6 ml of binding buffer (20 mM NaH_2PO_4 (pH 7.4) with 500 mM NaCl, 10 mM imidazole, 10% glycerol and protease inhibitors). Samples were lysed by probe sonication (3 phases, 30sec each), and the cell debris was removed (5000xg, 10 min, 4°C). The cell-free extracts were re-centrifuged (15000xg, 30 min, 4 °C), and the supernatant was used to affinity-purify *Tg*EK-6xHis, *Tg*CK-6xHis and 6xHis-*Tg*CK_S proteins using the Ni-NTA resin (Qiagen) and 20 mM NaH_2PO_4 (pH 7.4), with 500 mM NaCl and 100 mM imidazole. Purified proteins were concentrated using 50-kDa cut-off centrifugal filters (Amicon), and quantified by Bradford method (50).

2.3.6 Nucleic acid preparation

The genomic DNA was prepared from lysed-out *T. gondii* tachyzoites according to Rotureau *et al.* (51). Briefly, the cell pellet was lysed in 200 µl of lysis buffer and incubated for 30 min at 65°C prior to precipitation with 450 µl of absolute cold ethanol. The DNA pellet was dried at RT and dissolved in sterile water.

To prepare the RNA, RNAase-free material was used throughout the procedure. *Toxoplasma gondii*-infected cells were washed with PBS and dissolved in 1 ml of Trizol and stored at -

80°C until use. The sample was thawed and RNA was isolated using the Pur Link RNA Mini kit according to the kit`s protocol. In brief, 200 µl of $CHCl_3$ were added to each sample and the tubes shaked by hand for 15 seconds, followed by incubation at RT for 2 min. Phase separation was achieved by centrifugation (12000 x g, 15 min, 4°C) and 400 µl of the upper RNA-containing phase were transferred to a fresh RNase-free tube. An equal volume of 70% ethanol was added, the mixture was transferred to a spin cartridge and subsequently centrifuged at 12000 x g for 15 seconds and RT. An on-column DNase I treatment was performed for 15 min at RT, prior to two washing steps and elution of the RNA in RNAase-free water. The RNA isolated by this method was used for quantitative PCR. For expression cloning, mRNA was isolated from fresh syringe-released tachyzoites and transcribed into first-strand cDNA using the µMACS mRNA isolation and the cDNA synthesis kits (Miltenyi Biotec, Germany). The cDNA was synthesised using SuperScript III first-strand cDNA synthesis kit (Invitrogen) using oligo-dT primers and stored at -20°C. Subsequent amplification of specific ORFs was performed using Pfu-Ultra FusionII high fidelity Polymerase (Stratagene, Germany) and the indicated cDNA-specific primers (Primer Table 1).

2.4 Methods – Assays

2.4.1 Indirect immuno-fluorescence assay (IFA)

The HFF were grown on glass coverslips in a 24-well plate and infected with parasites. The parasite-infected cells were fixed with 2% paraformaldehyde (PFA) for 15 min at RT, followed by 5 min neutralization in 0.1 M Glycine/PBS. Cells were permeabilized in 0.2% Triton-X100/PBS for 20 min, and non-specific binding was blocked with 2% BSA in 0.2% Triton-X100. Samples were stained with primary antibodies (anti-*Tg*Gap45 1:3000; anti-*Tg*CK serum 1:200; anti-HA 1:1000; anti-Ty1 1:50; anti-Myc 1:1000, anti-V5 1:1000 dilutions) followed by three washes with 0.2% Triton-X100 in PBS. Finally, the corresponding secondary antibodies (mouse or rabbit Alexa488 or Alexa594) were applied (1:3000), and after three PBS washes slides were mounted in DAPI-Fluoromount G for fluorescent imaging (Apotome, Carl-Zeiss, Germany). Pictures were taken at 63x mgnification using filtersets 38HE eGFP (green), 43HE Cy3 (red) and 49 DAPI (blue) and processed with the Axiovision software (Carl-Zeiss).

2.4.2 Immuno-electron microscopy (IEM)

T. gondii-containing fibroblasts were fixed with 4% PFA (Electron Microscopy Sciences, PA) in 0.25 M HEPES (pH 7.4) for 1 hr at RT and then with 8% PFA in the same buffer overnight at 4°C. They were infiltrated, frozen and sectioned as previously described (52) In brief, cell preparations were scraped, pelleted, and embedded in 10% bovine skin gelatin in PBS. The pellet sections were infiltrated overnight with 2.3 M sucrose in PBS at 4°C, mounted on aluminum studs, and frozen in liquid nitrogen. Samples were sectioned at -108°C using a cryo-ultramicrotome (Leica). The 60-nm thick sections were collected using a mixture of 2.3 M sucrose and 2% methyl cellulose (1:1) and then transferred onto formvar- and carbon-coated nickel grids. Ultrathin sections were incubated with 0.1 M NH_4Cl in PBS for 10 min and then with 0.5% fish skin gelatin in PBS for 20 min. The sections were immuno-labeled with mouse anti-*Tg*CK antiserum (1:250 in PBS/1% fish skin gelatin), and then with anti-mouse IgG antibody, which was immediately followed by 10 nm protein A-gold particles (Department of Cell Biology, Medical School, Utrecht University, Netherlands). Samples were examinated with a Philips CM120 Electron Microscope (Eindhoven, Netherlands) under 80 kV. For double immuno-staining, the sections were labeled with the mouse anti-*Tg*CK antiserum revealed by 10 nm protein A-gold particles, and the rat anti-HA antibody (1:200) detected by 5 nm protein A-gold particles.

2.4.3 Plaque and replication assays

Plaque assay recapitulates all events of the parasite's lytic cycle including host cell invasion, intracellular replication, and re-invasion of neighboring cells. HFF cells in the 6-well plates were infected with 200 tachyzoites, cultured for 7 days without perturbation, fixed with -80°C methanol and stained with crystal violet for 10 min followed by 2x washing with PBS. The images were documented at 4x magnification using an inverted Leica microscope. The mean area of the plaque images from three independent biological replicates (50 plaques each) was calculated for evaluating the parasite growth. For replication assays, HFFs grown on glass coverslips were infected with parasites (MOI=3) and subjected to IFA using anti-*Tg*Gap45 (1:3000) antibody 29 hrs post-infection. The parasite replication was deduced from the number of parasites in their vacuoles. The three independent experiments each with 50 vacuoles were performed.

2.4.4 Radioactive and photometric choline kinase assays

Choline kinase activity was determined by measuring the formation of [^{3}H]- or [^{14}C]-phosphocholine from [^{3}H]- or [^{14}C]-choline. The [^{3}H]- or [^{14}C]-choline (2.5 nCi/nmol; 0.25 nCi/nmol) and increasing concentrations of choline chloride (0-3.2 mM) were mixed with 5x reaction buffer (final concentrations 67 mM Tris-Cl (pH 8.5), 10 mM ATP, 11 mM $MgCl_2$, 1.3 mM DTT) in a total volume of 60 µl. The 0.2-2 µg of cell-free extract or purified protein were added and the reaction mix was incubated at 37°C for 4 min following. Initial optimization assays had confirmed a linear enzyme activity in this range. The reaction was stopped by adding 20 µl of 10 mM choline chloride prepared in 0.5 N NaOH. The residual substrate was then removed from the radiolabeled product (phosphocholine) as choline reineckate by precipitation with 50 µl ammonium reineckate (250 mg in 4-5 ml CH_3OH) (53). The reaction products were separated on silica gel 60 plates using the solvent system containing 95% ethanol/2% ammonium hydroxide (1:1). The activity was determined by phospho-imaging and quantified by scintillation counting.

To study the inhibitory effect of DME on *Tg*CK, the formation of radioactive phosphocholine from [^{3}H]-choline was monitored in the presence of a constant concentration of choline (2.5 nCi/nmol, 0.2 mM) and increasing amounts of DME (0-4 mM). The reactions were run for 4 min at 37 °C in water bath. Residual choline was precipitated as reineckate salt and the amount of [^{3}H]-phosphocholine was determined by radioactive scintillation counting. To study the mechanism of inhibition, the *Tg*CK assay was performed with purified enzyme in the absence or presence of 2 mM DME, and the formation of phosphocholine was quantified by scintillation counting.

A similar assay was performed with [^{3}H]-ethanolamine. 5 µl of [1,2-^{3}H]-ethanolamine (50 nCi/nmol) were dissolved in 100 µl of 1 mM ethanolamine chloride. 10 µl of this suspension was mixed with the 5x choline kinase buffer and purified protein (as described above) in a total volume of 100 µl. Reactions were incubated for 30 min at 37°C and then terminated by 10 µl of glacial acetic acid. The product formation was evaluated by TLC without any precipitation.

Choline kinase was also assayed by a spectrophotometric method adapted from a pyruvate kinase/lactate dehydrogenase-coupled system (54). The phosphorylation of choline by an active choline kinase produces ADP, which reacts with phosphoenol-pyruvate to form pyruvate and ATP, a reaction catalyzed by pyruvate kinase. Finally, the lactate dehydrogenase converts pyruvate into lactate, thereby oxidizing NADH to NAD^{+}. A choline-dependent

decrease in the NADH absorption (340 nm) represents the enzyme activity of choline kinase. The 200-µl reaction in a 96-well plate contained indicated amounts of choline, 100 mM Tris-Cl (pH 8.5), 100 mM KCl, 10 mM $MgCl_2$, 0.4 mM NADH, 5 mM ATP, 1 mM phosphoenol-pyruvate, pyruvate kinase (30 U), lactate dehydrogenase (37 U) and purified protein (1-2 µg). The choline-independent ATPase activity of choline kinase was recorded and subtracted from the choline-dependent ATP turnover. To measure the steady-state kinetics, one substrate was kept constant (5 mM ATP; 4 mM choline or DME), whereas the other was varied (0–4 mM choline or DME). Data were fitted to the Michaelis-Menten equation using a robust fit nonlinear regression (GraphPad Prism v5.0).

2.4.5 Genetic manipulation of the *Tg*CK gene

The *TgCK* promoter was displaced using a tetracycline-regulatable promoter (*pTetO7Sag4*). Primers used for the genetic manipulation are depicted in Primer Table 1 (page 36). The 5'UTR fragment (2-kb), amplified from tachyzoite gDNA using the primers (*Tg*CK-PD-5'UTR-F/R), was cloned into the *pDT7S4* vector at the *NdeI* site. The 1-kb region downstream to the initiating ATG of the *Tg*CK gene was amplified (primers *Tg*CK-PD-3'UTR-F/R), and cloned at *BglII* and *AvrII* to achieve the promoter-displacement construct. The TaTi-*Δku80* strain of *T. gondii* was transfected with 50 µg of the linearized construct (*ApaI*) using the BTX630 instrument (1.7 kV, 50 Ohm, 25 µF, 100 µs), and stable transgenic parasites were selected with 1 µM pyrimethamine (16). The drug-resistant parasites were apparent within ~2 weeks, which were cloned by limiting dilution in the 96-well plates, and screened for 5'- and 3'-recombination using *Tg*CK-PD-5'Scr-F/DHFR-R or DHFR-F/*Tg*CK-PD-3'Scr-R primers. The knockout of *Tg*CK was attempted using *p2854-DHFR-TS* vector containing about 3.3-kb of 5'- (*HindIII*/*NheI*) and 3'-UTR (*NotI*/*NotI*) sequences flanking the DHFR-TS resistance cassette. The *ApaI*- or *PsiI*-linearized construct was transfected in -*Δku80* or *hxgprt*$^-$ strain, and the parasites were selected using pyrimethamine (16). The transgenic parasites were cloned, and screened using 5'- and 3'-crossover-specific primers (*Tg*CK-KO-5'Scr-F/DHFR-R2 or DHFR-F2/*Tg*CK-KO-3'Scr-R).

2.4.6 Genetic manipulation of the *Tg*CCT gene

A tetracycline-regulatable copy of the C-terminally HA-tagged *Tg*CCT ORF (*Tg*CCT_i-HA) was inserted at the *Tg*UPRT locus *via* double homologous recombination. To generate the

construct, the *Tg*CCT cDNA (987 bp) was amplified from the tachyzoite mRNA using primers *Tg*CCT-F3/-R3 and digested with *EcoRV* and *PacI*. The vector *pTetUPKO* was first digested with *NcoI* followed by treatment with Klenow enzyme and *PacI* digestion for blunt-cohesive ligation of the *Tg*CCT_i-HA ORF. The *NotI*-linearized construct was transfected into TaTi-*Δku80* strain, and the resistant parasites were selected with 5µM FUDR. The expression and tetrycycline regulation of *Tg*CCT-HA was confirmed by IFA using the mouse anti-HA antibody (1:1000). The *p2854-DHFR-TS* plasmid was modified to generate a knockout construct to subsequently delete the endogenous *Tg*CCT locus. The 1 kb of the 5'- and 3'-UTR fragments were amplified using the *Tg*CCT-KO-5'UTR-F/-R and *Tg*CCT-KO-3'UTR-F/-R primers. The inserts were cloned at the *ApaI/ApaI* and *XbaI*/*NotI* sites of *p2854-DHFR-TS*, respectively, flanking the DHFR-TS resistance cassette. The construct (50 µg) was linearized with *NotI* prior to transfection into tachyzoites. Stable selection was achieved using 1 µM pyrimethamine within 12 days (16) and 20 clones were screened for homologous crossover at the *Tg*CCT locus by genomic PCR using the crossover-specific primers (*Tg*CCT-KO-5'Scr-F/DHFR-R and DHFR-F/*Tg*CCT-KO-3'Scr-R).

2.4.7 Precursor labeling and lipid analyses

Choline labeling (0.1 µCi/ml media) of intracellular parasites was performed for 40-hrs in the parasitized HFF (MOI of 3) cultures. Total lipids were extracted from PBS-washed axenic parasites according to Bligh and Dyer (55). Briefly, the 1-ml parasite suspension in PBS was mixed with 1.1 ml each of CH_3OH and $CHCl_3$ followed by 10 min incubation at room temperature to allow the phase separation. The resultant chloroform phase was washed 3 times with 1.9 ml of CH_3OH/0.2 M KCl/$CHCl_3$ (10:9:1, v/v). The final chloroform phase containing lipids was dried in vials, and the radioactivity was quantified by liquid scintillation method. Alternatively, lipids were dried and suspended in 100 µl of $CHCl_3$ for the TLC analysis on silica gel H plates in $CHCl_3$/CH_3OH/H_2O (65:25:4, v/v). Lipids were visualized by iodine staining and/or radiographic imaging. All lipids were identified based on their co-migration with standards.

The chemical amounts of phospholipids were determined by lipid phosphorous assay. Freshly-egressed tachyzoites were washed twice with PBS and counted. The samples were normalized to the number of parasites and subjected to lipid extraction (55), followed by TLC in $CHCl_3$/CH_3OH/H_2O (65:25:4, v/v). Lipids in silica gel were scraped off from iodine-stained plate into glas vials. In addition, a phosphate standard was prepared from sodium

phosphate (Na_2HPO_4, 0-40 nM) and 40 µl of the individual concentrations were pipetted into fresh glass tubes. Then, 180 µl of perchloric acid (70%) were added to each tube, which were incubated at 200°C for 30 min with a marble put on top. The tube walls were rinsed with phosphate-free water (1040 µl for samples, 1000 µl for the standards) followed by addition of 200 µl ammonium molybdate (2.5%, w/v) and 200 µl of the fresh ascorbic acid (10%, w/v), with gentle vortexing after each step. Subsequently, the solution was incubated in the water bath (15 min, 50°C), and the lipid phosphorous content was quantified by spectrometry (820 nm).

2.4.8 Preparation of LDLconjugated with NBD-phospholipids

The C6-NBD-phospholipids were conjugated to human LDL-particles. 50 µl of the individual C6-NBD-phospholipids (PtdCho 8.5 mg/ml; PtdEtn 8.03 mg/ml; PtdSer 11.5 mg/ml) were mixed with 10 ml of fresh human serum and incubated overnight at 37°C. The NBD-lipid-conjugated LDL was isolated by zonal density-gradient ultracentrifugation as described before (56). The density was adjusted to 1.25 g/ml with KBr followed by 16 hrs centrifugation (40000 rpm, 4°C). The lipoprotein fraction in the interphase was transferred to a fresh tube and the density was adjusted to 1.3 g/ml with KBr. The lipoproteins were then added to the bottom of centrifugation tubes containing 0.9% NaCl (ratio of 1 ml lipoproteins and 7 ml NaCl) followed by 4-6 hrs centrifugation (50000 rpm, 4°C). The upper orange phase containing the LDL-particles was transferred to a fresh tube, buffer-exchanged against PBS, and stored at 4°C in N_2-flushed vials.

To test for the trafficking of host LDL-derived phospholipids to the *Toxoplasma* membranes, HFF monolayers on glass coverslips in a 24-well plate grown in lipoprotein-deficient serum were infected (MOI = 3), and 0.1 mg/ml of the NBD-loaded LDL were added to the cultures 28 hrs post infection. Samples were fixed after 1 hr incubation at 37°C, and lipid transport was analyzed by fluorescence microscopy.

2.4.9 Stable transfection of COS-7 cells

The cDNAs of *Tg*CK, *Tg*CCT, *Tg*CPT and *Tg*EPT were amplified from the tachyzoite mRNA and cloned at *HindIII* and *XbaI* sites in the mammalian expression plasmid *pcDNA3.1*$^+$. The cloning resulted in expression of C-terminally V5-tagged proteins under the *pCMV* promoter. For transfection of COS-7 cells the *BglII*-linearized plasmid (4 µg) was diluted in 250 µl of

Opti-MEM I (Reduced Serum) Medium. Another batch of 250 µl medium was mixed with 10 µl Lipofectamine 2000 and incubated for 5 min at room temperature. Both solutions (500 µl) were mixed and incubated for 20 min at room temperature. Meanwhile, a 6-well plate containing cultures of COS-7 cells was washed 3 times with PBS and prepared with antibiotic-free medium. The DNA-lipofectamine solution was added to the COS-7 cells and incubated at 37°C for 24 hrs. Cells were harvested by trypsine/EDTA treatment and diluted by at least 10-fold into T150 flasks. Selection of stable transgenic cells was started 48 hrs post-transfection using 800 µg/µl geneticin. Medium with fresh antibiotic was changed twice a week until cells were confluent and stable expression of V5-tagged proteins was tested by IFA.

2.4.10 CCT/CPT Enzyme Assay

The enzyme activity of CCT and CPT was tested in total protein extract prepared from transgenic COS-7 cells, *Toxoplasma* (*hxgprt*$^-$ strain) or *S. cerevisiae* strains Y04637, Y04832 or HJ000 expressing *Tg*CCT, *Tg*CPT and *Tg*EPT.

To test for the CCT activity, 10 µl protein extract was incubated for 5 min at 37°C in reaction buffer (58 mM Tris-Cl pH 7.5, 40 mM NaCl, 1.8 mM EDTA, 8.9 mM Magnesium acetate) supplemented with 3 mM CTP and 0.1 µCi [^{14}C]-phosphocholine (reaction volume 100 µl). The reaction was stopped by heat-inactivation in boiling water (2 min) and the product formation was analyzed by TLC (solvent 95% EtOH/2% NH_4OH, 1:1) and radio-imaging.

The CPT activity was assayed in a 200 µl reaction buffer containing 100 mM Tris-Cl (pH 8), 20 mM $MgCl_2$ and 1 mM EDTA. Diacylglycerol (2.5mg/ml prepared in 0.015% Tween20) was diluted 1:4 in the reaction buffer and supplemented with 3 mM CTP and protein extract, prior to 5 min pre-incubation at RT. 0.1 µCi [^{14}C]-phosphocholine were added and incubated for 30 min at 37°C. The reaction was terminated by addition of 1.5 ml $CH_3OH/CHCl_3$ (2:1, v/v) followed by 0.7 ml PBS and 0.5 ml $CHCl_3$. The organic phase was washed 3 times with 1.8 ml of CH_3OH/0.2 M KCl/$CHCl_3$ (10:9:1, v/v) and radioactivity in the resulting lipid phase was quantified by scintillation counting or analyzed by TLC (solvent 95% EtOH/2% NH_4OH, 1:1).

3 RESULTS

3.1 The *Toxoplasma* genome encodes enzymes of the CDP-Choline pathway

To study the parasite CDP-choline pathway, we first searched the *Toxoplasma* database (www.ToxoDB.org) and performed protein alignments using orthologs from *S. cerevisiae*, *P. falciparum* and *H. sapiens*. Our bioinformatic analyses identified 3 putative choline and/or ethanolamine kinases annotated and/or expressed in *T. gondii* (TGGT1_120660, TGGT1_040800, and TGGT1_058210). Our multiple attempts to amplify TGGT1_058210 from the tachyzoite mRNA were futile, leading to the assumption that either the gene annotation is incorrect or this gene might be silent in the tachyzoites. The ORFs of TGGT1_120660 (1.9 kb) and TGGT1_040800 (1.6 kb) were cloned using the first-strand cDNA prepared from the tachyzoite mRNA, which encoded *Tg*CK and *Tg*EK proteins with 630 and 547 residues, respectively (Fig. 5, Appendix 1A, Appendix 2A). PCR amplification of the upstream flanking regions confirmed the presence of an in-frame stop codon before the initiating ATG in both kinases. Both ORFs harbor a choline/ethanolamine kinase domain (PF01633), and also contain the Brenner's and typical choline kinase motifs. The former is a phosphotransferase motif, and the choline kinase motif is located downstream to the Brenner's motif (57). *Tg*CK protein shows 19%, 16% and 10% identity with *Hs*CKα1, *Pf*CK and *Sc*CK1 with best homology observed in the conserved regions (Appendix 1B). *Tg*EK is 21%, 20% and 14% identical to *Hs*EK, *Pf*EK and *Sc*EK1 proteins (Appendix 2B). Notably, *Tg*CK possesses a peculiar N-terminal hydrophobic sequence (first 20 amino acids) with no homology to any known protein in the NCBI database, and long stretches of amino acid insertions compared to its orthologs (Appendix 1A).

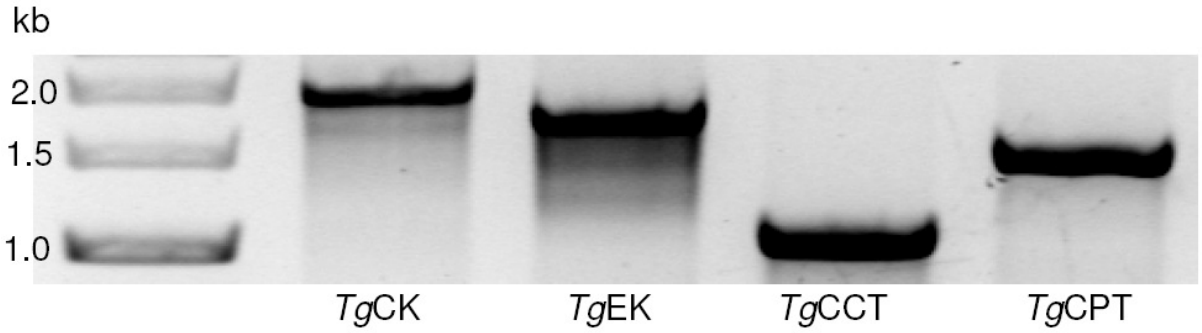

Fig. 5: **PCR amplification of *Tg*CK, *Tg*EK, *Tg*CCT and *Tg*CPT transcripts.** The tachyzoite mRNA was transcribed into first-strand cDNA, which was used to amplify the transcripts of *Tg*CK (1.9 kb), *Tg*EK (1.6 kb), *Tg*CCT (1 kb) and *Tg*CPT (1.4 kb) using the cDNA-specific primers (Primer Table 1).

Our database searches also revealed annotations for a choline-phosphate cytidylyltransferase (*Tg*CCT; TGGT1_098200) and a choline-phosphotransferase (*Tg*CPT; TGGT1_013180), which catalyze the second and third reactions of PtdCho synthesis in *T. gondii*, respectively. Their cDNAs (*Tg*CCT, 1 kb; *Tg*CPT, 1.4 kb; Fig. 5), amplified from the tachyzoite mRNA, encode proteins of 329 and 467 amino acids, respectively (Appendix 3A, Appendix 4A). Mammalian cells express 2 isoforms of CCT, of which the alpha-isoform harbors an N-terminal nuclear localization signal (NLS), whereas the CCT-beta is localized in the cytosol (58). The *Tg*CCT appears proximal to the CCT-alpha with 30% and 26% identity to its human and yeast (*S. cerevisiae*) orthologs, respectively. A NLS between the amino acids 154 and 166 of *Tg*CCT could also be identified (red box Appendix 3A).

*Tg*CPT, catalyzing the fusion of the phosphocholine moiety from CDP-choline with the diacylglycerol (DAG) (27), displayed 20%, 19% and 26% identity to its human, yeast and *Plasmodium* orthologs, respectively (Appendix 4B). *Tg*CPT showed best homologies to its orthologs in the catalytic domain ($DG(X)_2AR(X)_8G(X)_3D(X)_3D$) between the residues 104 and 126 (Appendix 4B, red box).

3.2 *Tg*CK is punctate intracellular, whereas *Tg*EK is uniformely cytosolic

To investigate the localization of *Tg*CK and *Tg*EK in *T. gondii*, the HA- and/or Ty1-tagged constructs of both enzymes were ectopically expressed in tachyzoites and localized by immuno-fluorescence. *Tg*EK with the C-terminal HA-tag (*Tg*EK-HA) under control of the *pNTP3* promoter displayed a uniform cytosolic pattern, which co-localized with a *bona fide* cytosolic marker protein, actin (*Tg*Actin) (Fig. 6).

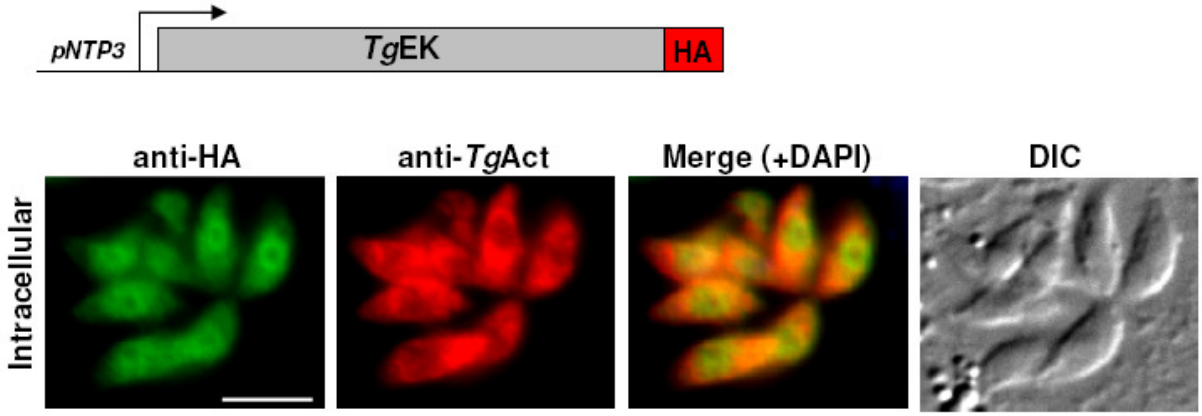

Fig. 6: ***Tg*EK is uniformly cytosolic in *T. gondii*.** *Tg*EK harboring the C-terminal HA-tag (*Tg*EK-HA) was expressed under the control of the *pNTP3* promoter, and co-localized with the parasite actin (*Tg*Act). The HFF infected with transfected tachyzoites were immuno-stained 29 hrs post-infection using the mouse anti-*Tg*Actin (*Tg*Act, red, 1:1000) and rabbit anti-HA (green, 1:1000) antibodies. Bar, 5 µm.

Interestingly, *Tg*CK possesses an N-terminal hydrophobic sequence, which is predicted to act as a signal peptide in the database. Our attempts to localize *Tg*CK with the N- or C-terminal HA-tag in stable transgenic parasites using a strong promoter such as *pNTP3* were unproductive. Hence, we designed a construct expressing *Tg*CK under the control of its native regulatory elements and harboring the C-terminal HA-tag (*Tg*CK-HA), which allowed us to assess its localization. Unexpectedly, *Tg*CK-HA demonstrated a punctate intracellular staining, which did not co-localize with the known dense granule or cytosolic proteins such as *Tg*Gra1, *Tg*Gra3 or *Tg*Actin. (Fig. 7A) To exclude a localization artifact due to interference with the C-terminal epitope, we performed the N-terminal-tagging of *Tg*CK, which rendered the protein undetectable suggesting that the N-terminus is required for localization. The atypical subcellular distribution and the possible requirement of the N-terminus for optimal targeting prompted us to express *Tg*CK fused with a Ty1 epitope after the N-terminal hydrophobic peptide (HP). *Tg*CK-Ty1 also showed a similar dotted intracellular presence, which co-localized with *Tg*CK-HA (Fig. 7B).

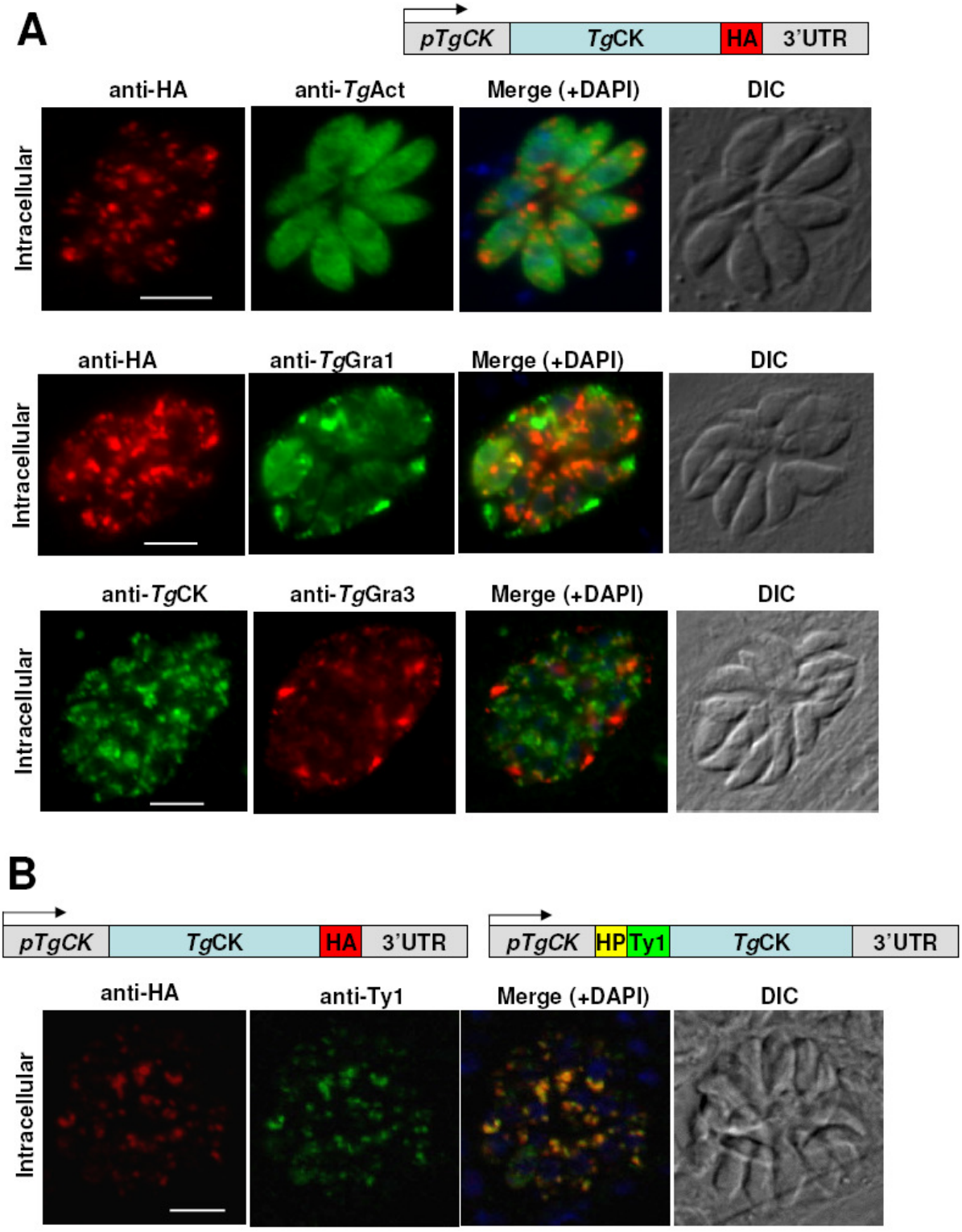

Fig. 7: ***Tg*CK displays a punctate intracellular distribution.** (A) *Tg*CK does not co-localize with dense granule (*Tg*Gra1, *Tg*Gra3) or cytosolic (*Tg*Act) marker proteins. (B) *Tg*CK isoforms with the C-terminal HA-tag (*Tg*CK-HA) or a Ty1-epitope (*Tg*CK-Ty1) following the hydrophobic peptide (HP) were co-expressed under the control of the native regulatory elements. The parasititized HFF were immuno-stained 29 hrs post-infection using anti-HA (from mouse or rabbit, 1:1000), the mouse anti-*Tg*CK serum (1:200), mouse anti-*Tg*Actin (1:1000), mouse anti-*Tg*Gra1 (1:500), mouse anti-Ty1 (1:50), and rabbit anti-*Tg*Gra3 (1:500) antibodies. Bar, 5 µm.

To further substantiate these findings, we generated the mouse antiserum against the purified and truncated *Tg*CK (see below). An N-terminally 6xHis-tagged *Tg*CK_S (6xHis-*Tg*CK_S) lacking its hydrophobic N-terminal sequence (first 20 amino acids), was subjected to thrombin protease treatment to remove the 6xHis epitope and subsequently injected into BALB/c mice (with alum as adjuvant) 3 times at 2 weeks intervals. The antiserum specifically identified a 70-kDa band corresponding to choline kinase in the protein extract prepared from parasitized human fibroblasts and free parasites but not from uninfected cells (Fig. 8).

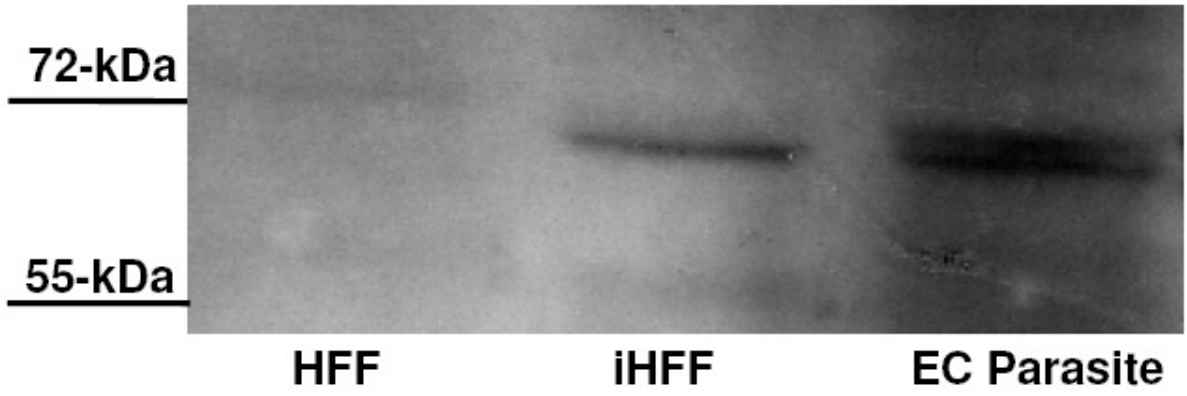

Fig. 8: **Anti-*Tg*CK-serum specifically identifies a 70-kDa choline kinase in *T. gondii* lysate.** Western blot of uninfected or infected HFFs or the axenic tachyzoite using the mouse *Tg*CK antiserum (1:200). 30 µg of the protein extract was resolved by 12% SDS-PAGE and blotted to identify the parasite choline kinase using anti-*Tg*CK serum (1:200) and HRP-conjugated secondary antibodies (1:3000).

Yet again, we observed a punctate intracellular pattern in wild-type parasites when stained with anti-*Tg*CK serum (Fig. 9A), which remained unchanged in extracellular parasites (Fig. 9B). Immuno-staining of the transgenic parasites expressing *Tg*CK-HA with *Tg*CK antiserum and anti-HA antibody revealed a perfect co-localization (Fig. 9C). Taken together, our results demonstrate that *Tg*CK has a distinct punctate intracellular distribution, whereas *Tg*EK is uniformly cytosolic in *T. gondii* tachyzoites.

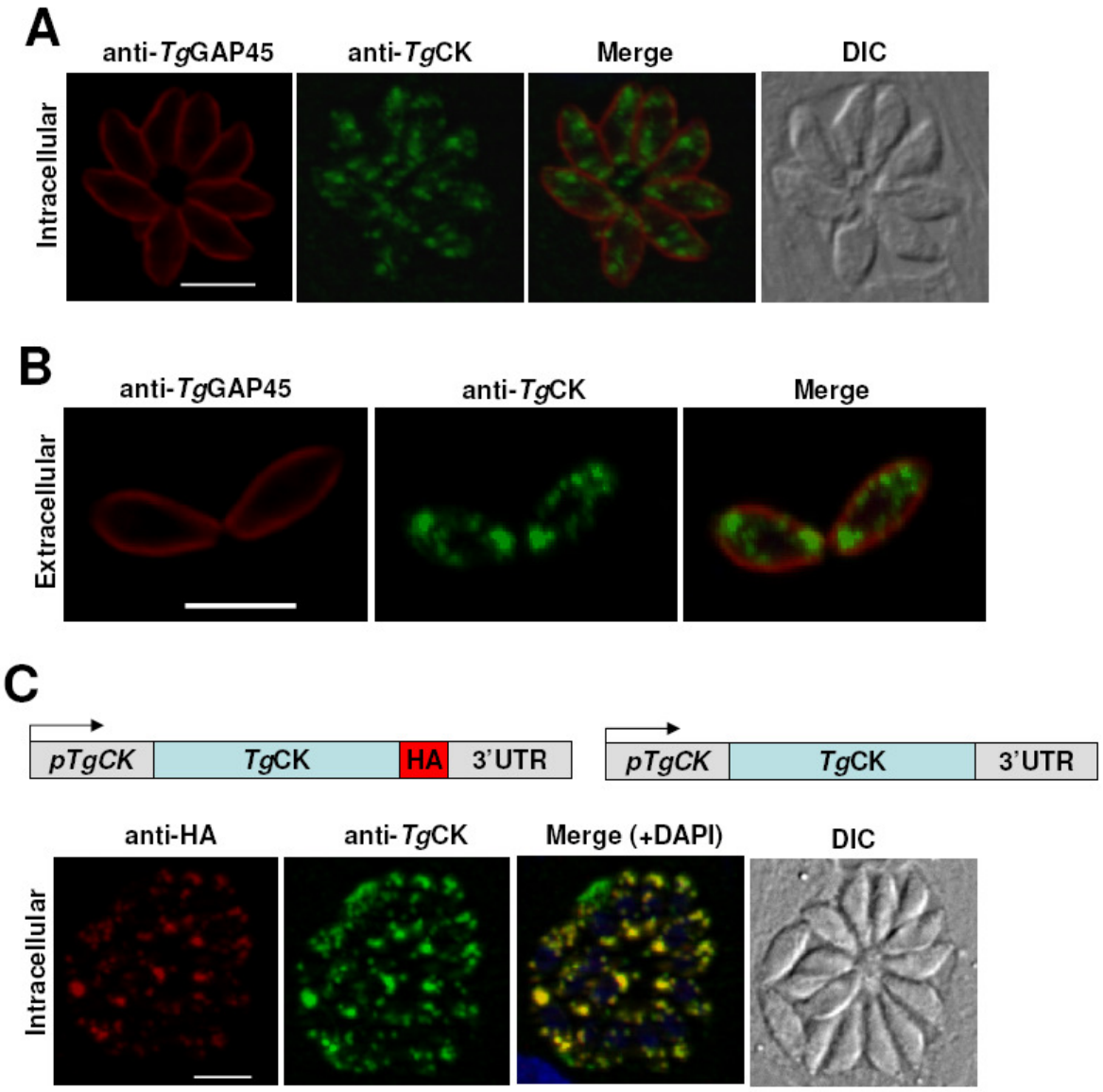

Fig. 9: **Anti-*Tg*CK serum confirms a punctuate intracellular localization.** The intracellular (A) and extracellular (B) *hxgprt*$^-$ parasites were immuno-stained using anti-*Tg*CK serum (green, 1:200) and anti-*Tg*Gap45 (red, 1:3000). Intracellular parasites were fixed 29 hrs post-infection. (C) *Tg*CK-HA was expressed under its native relulatory elements in the *T. gondii hxgprt*$^-$ strain and stained with mouse anti-*Tg*CK serum (green, 1:200) and rabbit anti-HA antibody (red, 1:1000) 29 hrs post-infection. Bar, 5 µm.

3.3 *Tg*CCT is nuclear, whereas *Tg*CPT resides in the ER

Next, we expressed the C-terminally HA-tagged *Tg*CCT (*Tg*CCT-HA) under *pTetO7Sag1* promoter, which localized to the parasite nucleus as determined by its co-staining with DAPI (Fig. 10A).

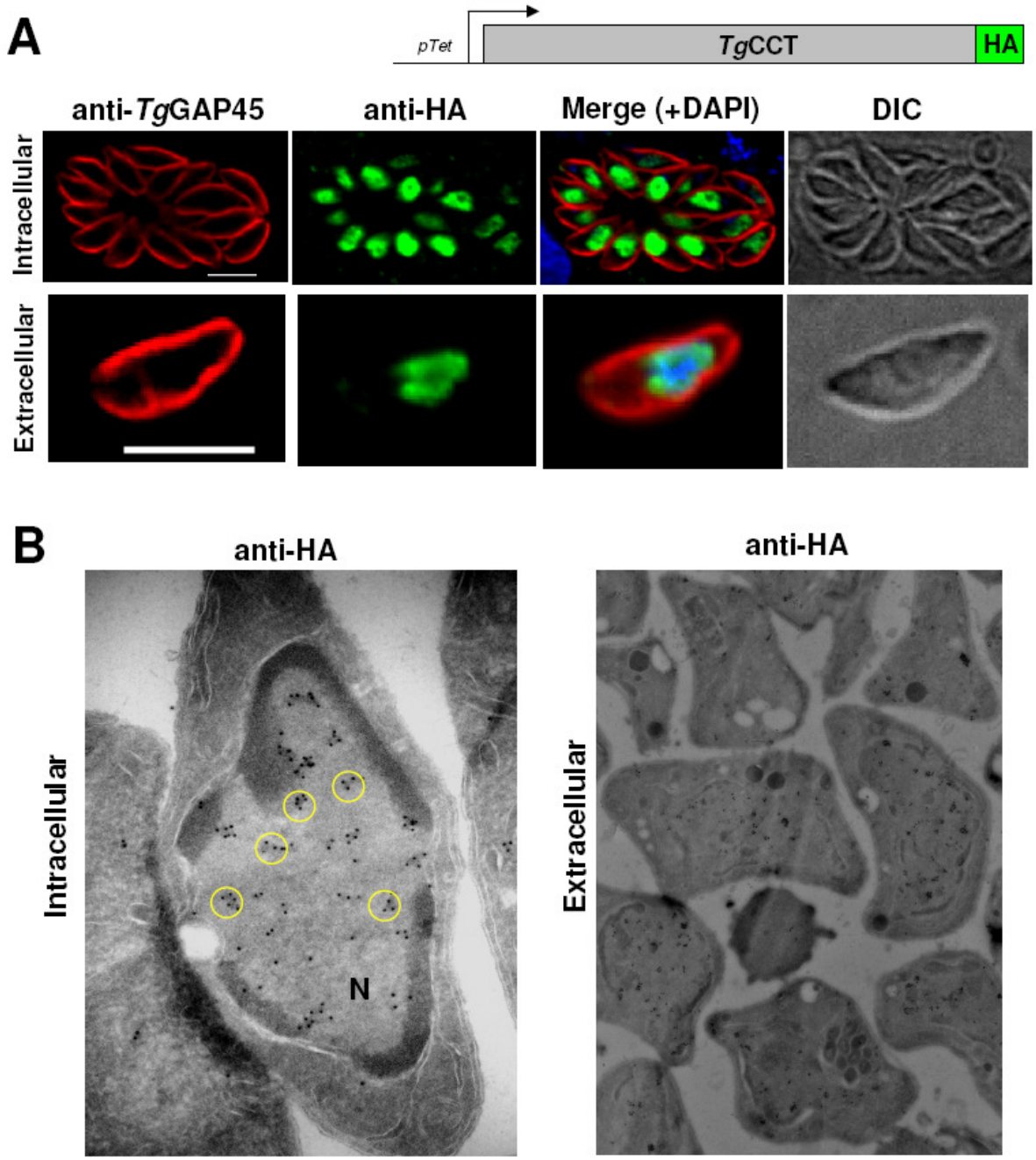

Fig. 10: ***Tg*CCT localizes to the nucleus in intracellular and extracellular tachyzoites.** The C-terminally HA-tagged *Tg*CCT (*Tg*CCT-HA) was expressed under the *pTetO7Sag1* promoter and *NTP3*-3'UTR and localized in intracellular and extracellular parasites by IFA (A) or IEM (B) using mouse anti-HA antibody (green, 1:1000; co-localization with rabbit anti-*Tg*Gap45, red, 1:3000; and DAPI, blue). For IEM the anti-HA (1:200) and the protein A-gold (10 nm)-conjugated secondary antibody were used. N, nucleus.

CCT catalyzes the rate-limiting reaction of PtdCho synthesis and the activity of mammalian CCT is regulated by its reversible binding to the nuclear membrane (59). External triggers, such as depletion of cellular PtdCho, can cause the translocation and activation of the soluble and nuclear CCT into a membrane-bound form. Surprisingly, *Tg*CCT showed a persistent

localization in the parasite nucleoplasm in intracellular as well as extracellular tachyzoites with no indication of redistribution to the nuclear membrane (Fig. 10A). This was further supported by immuno-gold electron microscopy (IEM) using the rat anti-HA and protein A-gold (10 nm)-labeled antibodies, which confirmed a nucleuar expression of *Tg*CCT-HA (Fig. 10B).

*Tg*CPT-HA, on the other hand, was confined to the ER as shown by immuno-fluorescence assays (Fig. 11). The co-localization studies with *Tg*CPT could not be performed due to unavailability of an antibody against a *bona fide* ER protein. The results, however, are consistent with the expression of mammalian CPT in the ER (27).

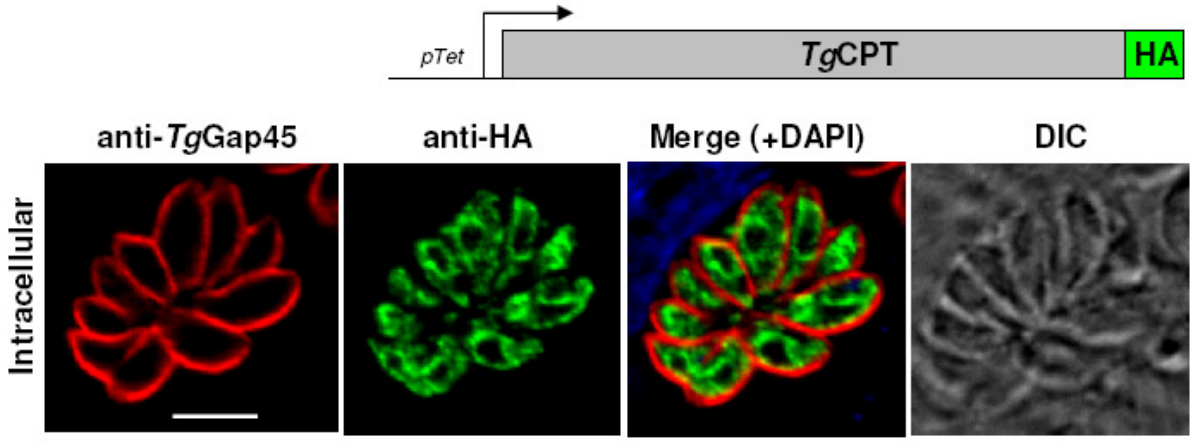

Fig. 11: ***Tg*CPT-HA localizes to the endoplasmic reticulum of *T. gondii* tachyzoites.** The *Tg*CPT-HA was expressed under the *pTetO7Sag1* promoter and NTP3-3'UTR, and IFA of parasitized HFF was performed using the mouse anti-HA (green, 1:1000) and rabbit anti-*Tg*Gap45 (red, 1:3000) antibodies 29 hrs post infection. Bar, 5 µm.

3.4 The N-terminal peptide is required for oligomerization of *Tg*CK

To identify the organelle underlying the punctate intracellular presence of *Tg*CK, we performed IEM using the anti-*Tg*CK serum. Notably, this revealed the formation of enzyme clusters in the parasite cytosol, and no association with any organelle and/or membrane was detectable in the wild-type RH strain (Fig. 12A). Further, IEM of the transgenic *hxgprt*$^-$ parasites stably expressing *Tg*CK-HA revealed a perfect co-localization of both, the native and ectopic forms of choline kinases, when labeled with the rat anti-HA and mouse anti-*Tg*CK serum as primary antibodies and protein A/gold (anti-rat, 5 nm; anti-mouse, 10 nm)-conjugated secondary antibodies (Fig. 12B)

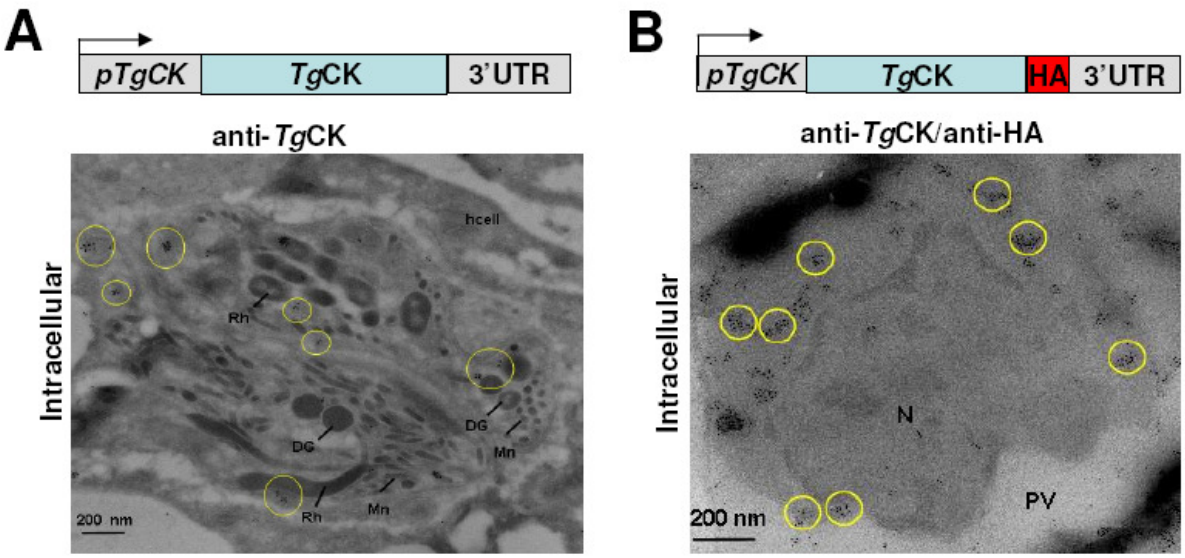

Fig. 12: ***Tg*CK forms clusters in the *T. gondii* cytosol.** (A) Immuno-gold electron microscopy of wild-type parasites using *Tg*CK antiserum (primary, 1:250) and protein A/gold (10 nm)-conjugated (secondary) antibodies. (B) The transgenic *hxgprt*$^-$ parasite line stably expressing *Tg*CK-HA was labeled with the rat anti-HA (1:200) and mouse anti-*Tg*CK serum as primary antibodies (1:250) and protein A/gold (anti-rat, 5 nm; anti-mouse, 10 nm)-conjugated secondary antibodies to co-localize the native and ectopic isoforms of *Tg*CK. Mn, microneme; DG, dense granule; Rh, rhoptry; PV, parasitophorous vacuole; N, nucleus.

Further assays determined the role of the N-terminal hydrophobic peptide in formation of the enzyme clusters. To this end, we transfected *hxgprt*$^-$ tachyzoites with the C-terminally myc-tagged and truncated *Tg*CK lacking its first 20 residues (*Tg*CK$_S$-myc), and localized the protein with anti-myc antibody and anti-*Tg*CK serum. *Tg*CK$_S$-myc exhibited a more uniform distribution in the parasite cytosol confirming that the N-terminus of *Tg*CK is indeed required for its punctate distribution (Fig. 13). The *Tg*CK$_S$-myc expression was lost in most parasites during the transgenic selection, which indicated an apparent toxicity of the truncated *Tg*CK. Interestingly, we observed a redistribution of the full-length native as well as of ectopic HA-tagged *Tg*CK isoforms from clusters into a more uniform cytosolic pattern (Fig. 13) indicating that the hydrophobic peptide serves as an anchor to support the formation of enzyme clusters.

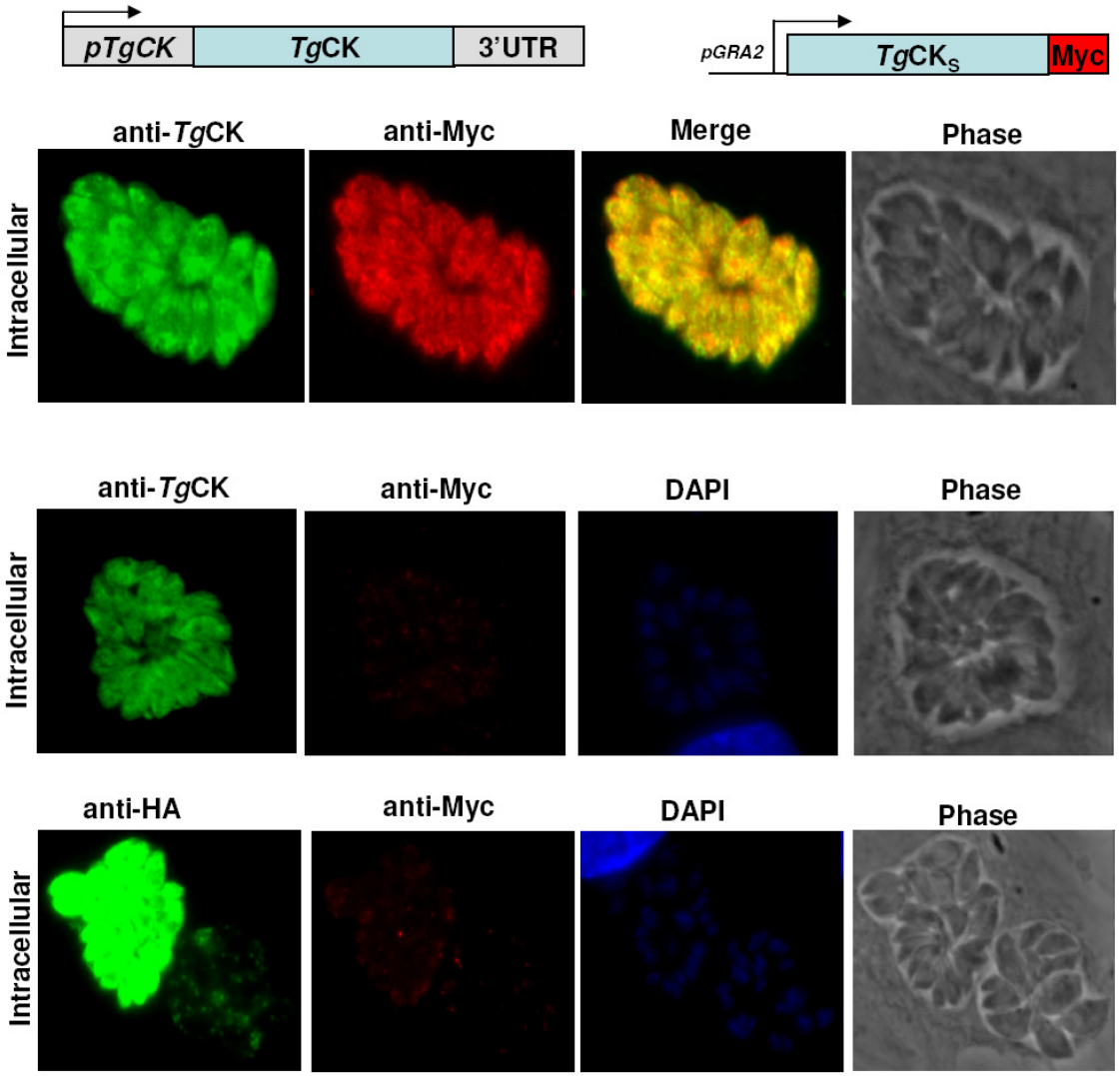

Fig. 13: **The *Tg*CK hydophobic N-terminus is required for enzyme clustering.** *Tg*CK lacking its N-terminal hydrophobic peptide (first 20 aa) and containing a myc-tag at the C-terminus (*Tg*CK$_s$-myc, red) was regulated by the *pGRA2* in *hxgprt*$^-$ tachyzoites. IFA was performed using mouse anti-*Tg*CK serum (1:200), mouse anti-HA (1:1000) and rabbit anti-myc (1:1000) antibodies 29 hrs post-infection.

3.5 *Tg*CK and *Tg*EK encode active choline and ethanolamine kinases

To classify the *Tg*CK and *Tg*EK proteins as choline and/or ethanolamine kinases according to their substrate specificity, we examined their activity by radioactive enzyme assay. *Tg*CK and *Tg*EK with the C-terminal 6xHis epitope were expressed and purified from *E. coli* Rosetta strain. *Tg*EK-6xHis could be purified to apparent homogeneity as deduced by a 60-kDa protein on SDS-PAGE (Fig. 14). The purified *Tg*CK-6xHis, however, contained two smaller species in addition to the expected 70-kDa band; these two smaller species were confirmed as alternative or degradation products of the *Tg*CK-6xHis ORF by western blot using the mouse anti-6xHis antibody or anti-*Tg*CK serum (Fig. 14).

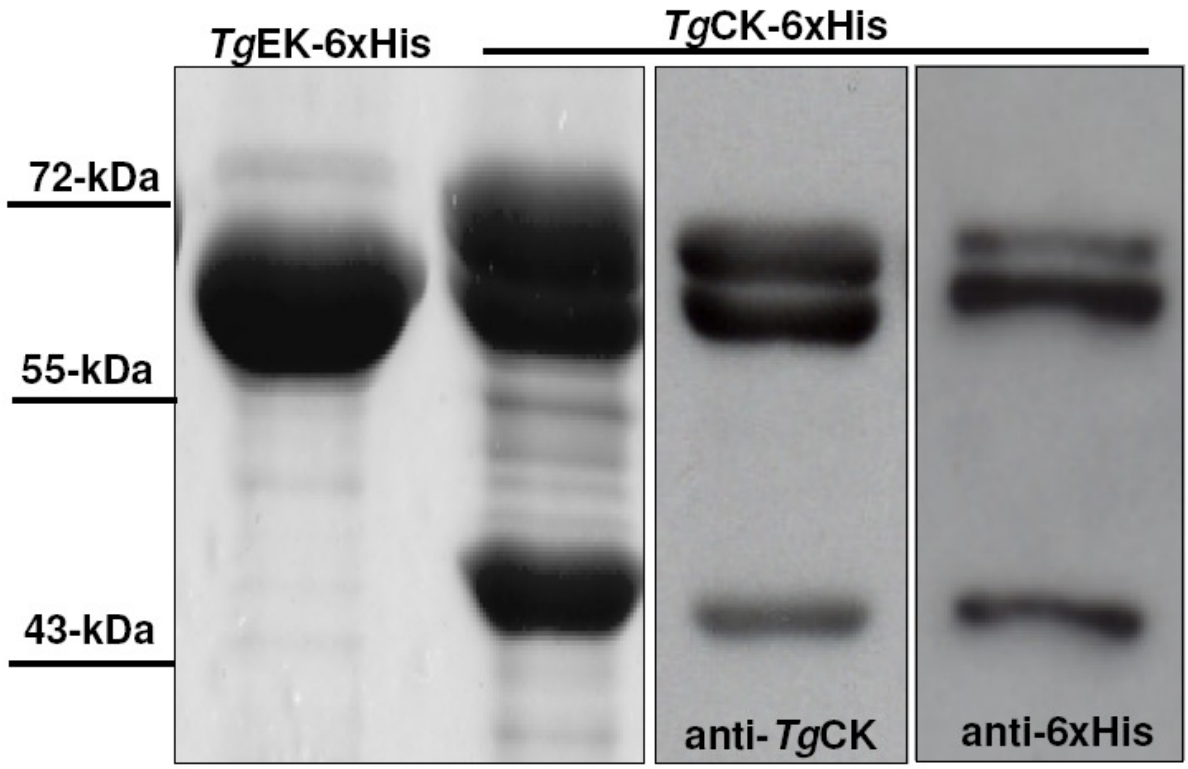

Fig. 14: **Purified recombinant *Tg*CK-6xHis and *Tg*EK-6xHis.** The full-length ORF of *Tg*CK and *Tg*EK with the C-terminal 6xHis tag in the *pET22b*$^{+}$ or *pET28b*$^{+}$ vector were expressed in *E. coli* Rosetta strain. The purity and identity of *Tg*CK was tested by coomassie-stained 12% SDS-PAGE (left) and western blot (right) using mouse anti-*Tg*CK serum (1:200) or mouse anti-6xHis antibody.

Both enzymes were tested for their ability to phosphorylate [^{3}H]-choline or [^{3}H]-ethanolamine and the reaction products were analyzed by thin layer chromatography (TLC). The choline and ethanolamine kinases of *S. cerevisiae* (*Sc*CK1, YLR133W; *Sc*EK1, YDR147W) were cloned into the galactose-inducible *pESC-Ura* vector and expressed in the *Δck1/Δek1* yeast mutant (KS106), which was used as a positive control. The yeast extract of the mutant transfected with the empty *pESC-Ura* served as a negative control. The recombinant *Tg*CK phosphorylated choline as a major and ethanolamine as its second substrate, as determined by co-migration of products with the corresponding controls (Fig. 15). By contrast, *Tg*EK displayed a kinase activity only for ethanolamine confirming its function as a substrate-specific kinase.

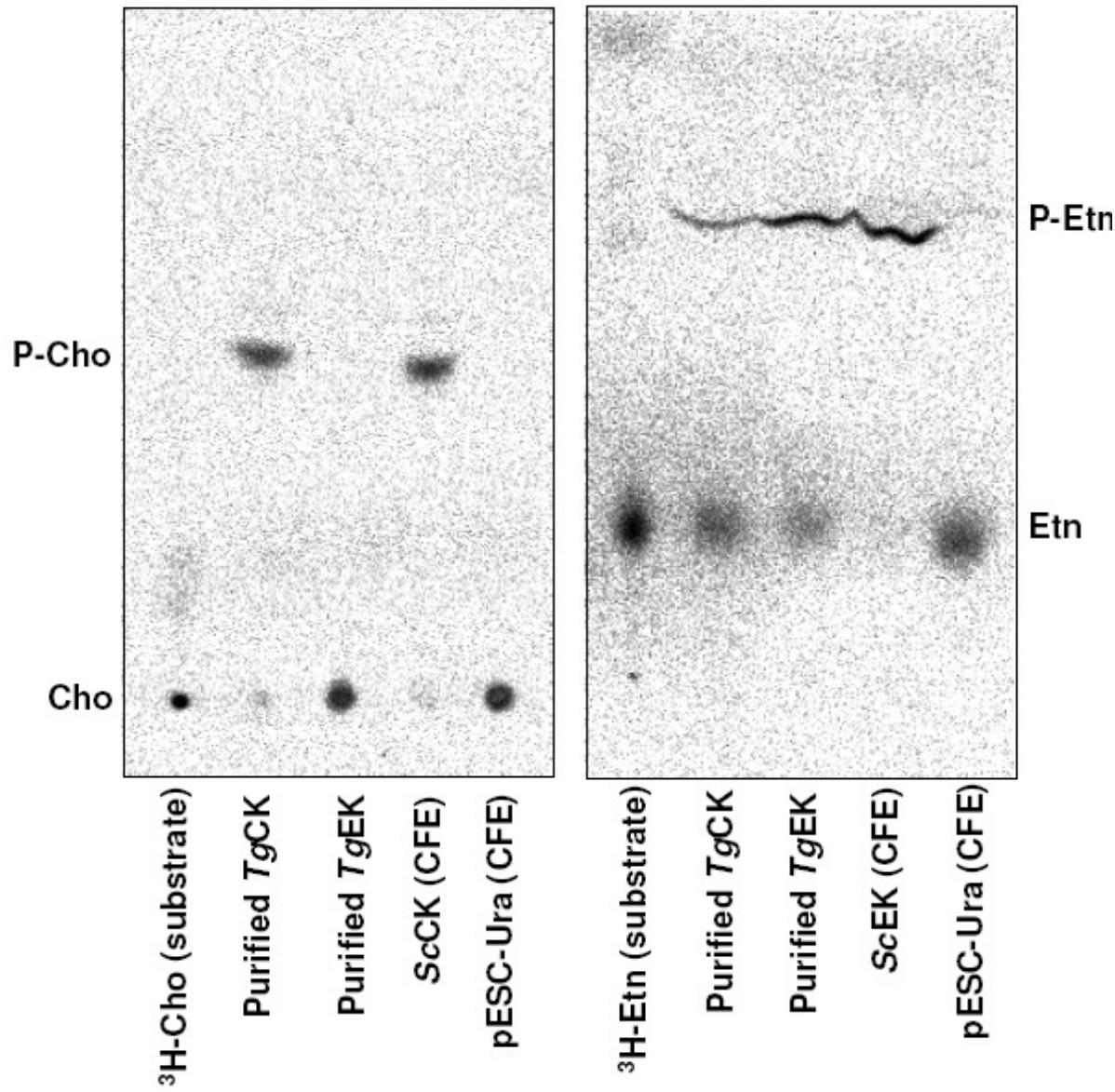

Fig. 15: ***Tg*CK phosphorylates choline and ethanolamine, whereas *Tg*EK is specific to ethanolamine.** Thin layer chromatography of resolved catalytic products of choline and ethanolamine kinases. The products (P-Cho, P-Etn) were identified by their co-migration with respective controls. Purified *Tg*CK-6xHis or *Tg*EK-6xHis was incubated with [^{3}H]-choline (Cho) or with [^{3}H]-ethanolamine (Etn) (37°C, 10 min) prior to TLC analysis (95%EtOH/2%NH_4OH, 1:1). The products were detected by phospho-imaging for 72 hrs at RT. Cell free extracts (CFE) from the *S. cerevisiae* KS106 (*Δck1*/*Δek1*) expressing *Sc*CK1 or *Sc*EK1 or harboring the empty vector (*pESC-Ura*) served as the positive and negative controls.

To determine the enzyme kinetics of *Tg*CK with choline, the assay was performed with increasing substrate concentrations (2.5 nCi/nmol, 0-3.2 mM), and reaction products were quantified by liquid scintillation counting. *Tg*CK-6xHis displayed a typical Michaelis-Menten kinetics with a relatively high K_m value of 0.77 mM (Fig. 16). Together, the data indicate that *Tg*CK is a low-affinity enzyme, which can phosphorylate choline and ethanolamine, whereas *Tg*EK is a substrate-specific ethanolamine kinase.

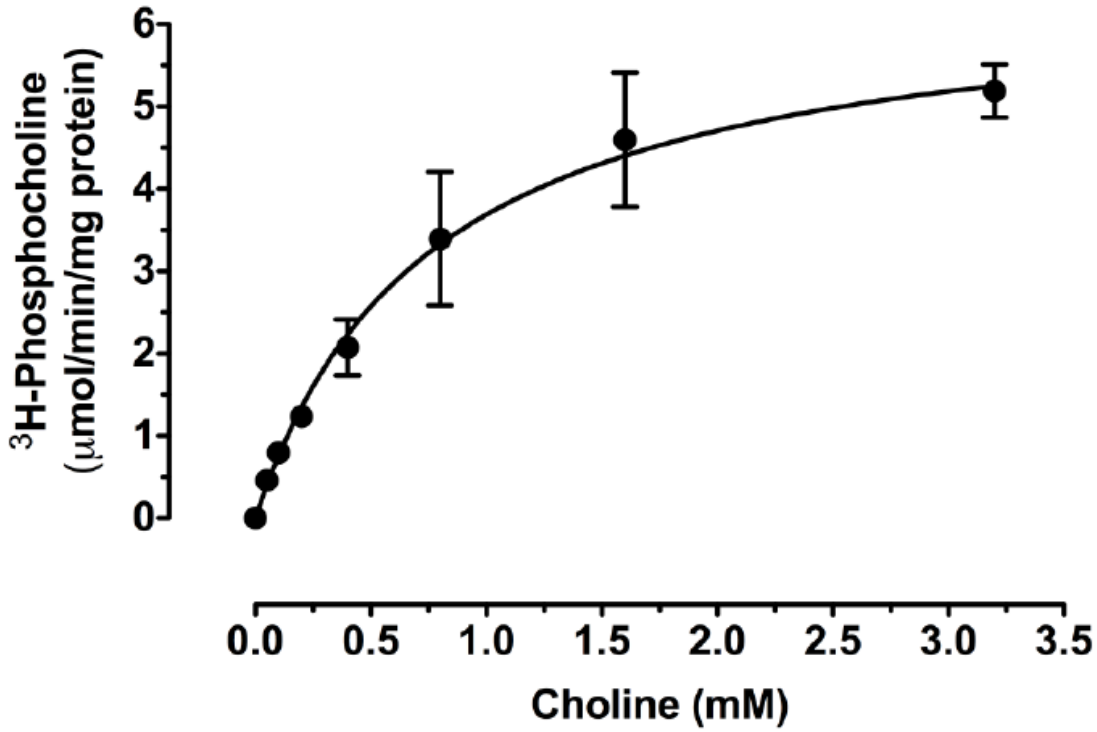

Fig. 16: **Michaelis-Menten kinetics of purified *Tg*CK-6xHis protein by radioactive choline kinase assay.** Activity was determined by scintillation counting of phosphocholine from [^{3}H]-choline chloride (2.5 nCi/nmol, 0–3.2 mM, 4 min, 37°C). For the assay details refer to section 2.4.4.

3.6 The N-terminal hydrophobic peptide is not required for function of *Tg*CK

To examine whether the hydrophobic peptide is important for *Tg*CK catalysis, we expressed a truncated protein lacking the first 20 amino acids with the N-terminal 6xHis-tag (6xHis-*Tg*CK$_S$) in *E. coli* Rosetta strain and purified the enzyme to apparent homogeneity (Fig. 17B).

Next, we established a 96-well-plate spectrophotometric assay for a user-friendly evaluation of the enzyme kinetics. The ATP-dependent catalysis by choline kinase initiates a cascade of three enzymatic reactions, the last of which involves the oxidation of NADH. Hence, monitoring a decline in the NADH absorbance (340 nm) allows an indirect monitoring of the choline phosphorylation (54). The full-length *Tg*CK-6xHis displayed a relatively low affinity for choline (K_m = 0.74 mM) (Fig. 17A), which is in accordance with the data obtained from radioactive assay. Quite noticeably, the 6xHis-*Tg*CK$_S$ displayed ~3-fold higher affinity for choline (K_m= 0.26 mM) when compared to full-length *Tg*CK-6xHis, which indicated a potential conformational change in 6xHis-*Tg*CK$_s$ (Fig. 17B), besides the fact that the N-terminal sequence is not necessary for *Tg*CK catalysis.

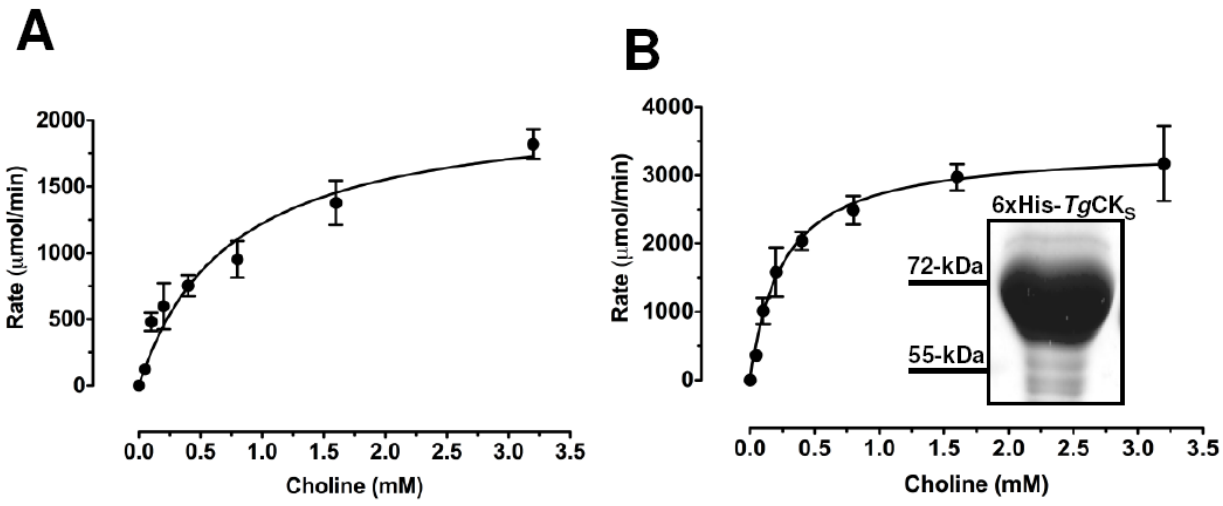

Fig. 17: **The N-terminal hydrophobic peptide is not required for catalysis by *Tg*CK.** Michaelis-Menten kinetics of *Tg*CK-6xHis (A) and 6xHis-*Tg*CK$_s$ (B) with choline using a pyruvate kinase/lactate dehydrogenase-coupled assay. Activity was monitored by decrease in the NADH absorbance (340 nm). For the assay details refer to section 2.4.4.

3.7 *Tg*CK is inhibited by a choline analog, dimethylethanolamine (DME)

The earlier work has shown that DME can block *in vitro* growth of *T. gondii* in HFF cells (38). Lipid analyses of the drug-treated parasites showed a time-dependent accrual of a PtdCho analog (PtdDME) and equivalent and concurrent (38) reduction in PtdCho, indicating that the anti-parasite effect of DME is due to interference with the PtdCho metabolism. *Tg*CK initiates the PtdCho biogenesis in *T. gondii*; therefore, it is also a likely enzyme being inhibited by DME. Hence, we first reconfirmed the anti-parasite effect of DME in plaque and replication assays. There was no plaque formation in the presence of 2 mM DME (Fig. 18A), and the drug treatment caused inhibition of the parasite replication as judged by formation of smaller vacuoles. About 80-100% of vacuoles harbored only 2-4 parasites. In contrast, the untreated sample contained 4-8 tachyzoites in ~80% of vacuoles (Fig. 18B).

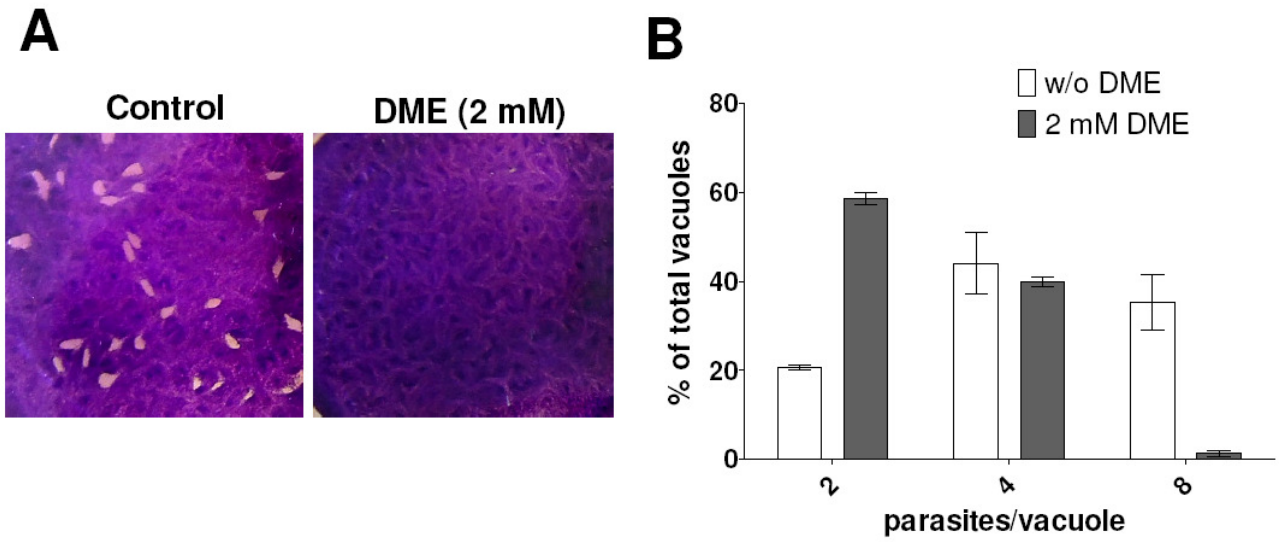

Fig. 18: **Intracellular replication of *T. gondii* is inhibited by a choline analog, dimethylethanolamine (DME).** (A) Confluent monolayers of human foreskin fibroblasts were infected with 200 parasites, and plaques were stained with crystal violet after 7 days of infection. (B) The number of parasites per vacuole was counted by anti-*Tg*Gap45 IFA (1:3000) 29 hrs post-infection with or without 2 mM DME treatment. In total, 3 independent assays, each with 50 vacuoles were evaluated.

We next determined the enzyme kinetics of *Tg*CK for choline and DME using the radioactive and photometric assays. Interestingly, *Tg*CK-6xHis phosphorylated DME with an apparent K_m value of 0.94 mM, which is similar to the K_m for its natural substrate choline (Fig. 19A). In accordance, DME inhibited phosphocholine formation by *Tg*CK-6xHis in radioactive assays exhibiting a K_i of 0.84 mM and IC_{50} of 0.95 mM (Fig. 19B). Likewise, the truncated 6xHis-*Tg*CK_S showed similar affinities for the analog (K_m, 0.25 mM) and for choline (Fig. 19C).

To evaluate the mechanism of DME inhibition, we compared the *Tg*CK-6xHis kinetics in the absence or presence of saturating amount of DME (2 mM). The radioactive assay revealed that the presence of DME increased the K_m of *Tg*CK for choline by about 3-fold without influencing the V_{max}, suggesting a competitive inhibition of *Tg*CK by the analog (Fig. 19D). The kinetic parameters of DME metabolism by *Tg*CK are consistent with the observed reduction of PtdCho synthesis and with the inhibition of parasite cultures by DME (IC_{50} ~0.5 mM) (38). These data suggest that the reported anti-parasite effect of DME is likely due to competitive inhibition of *Tg*CK activity.

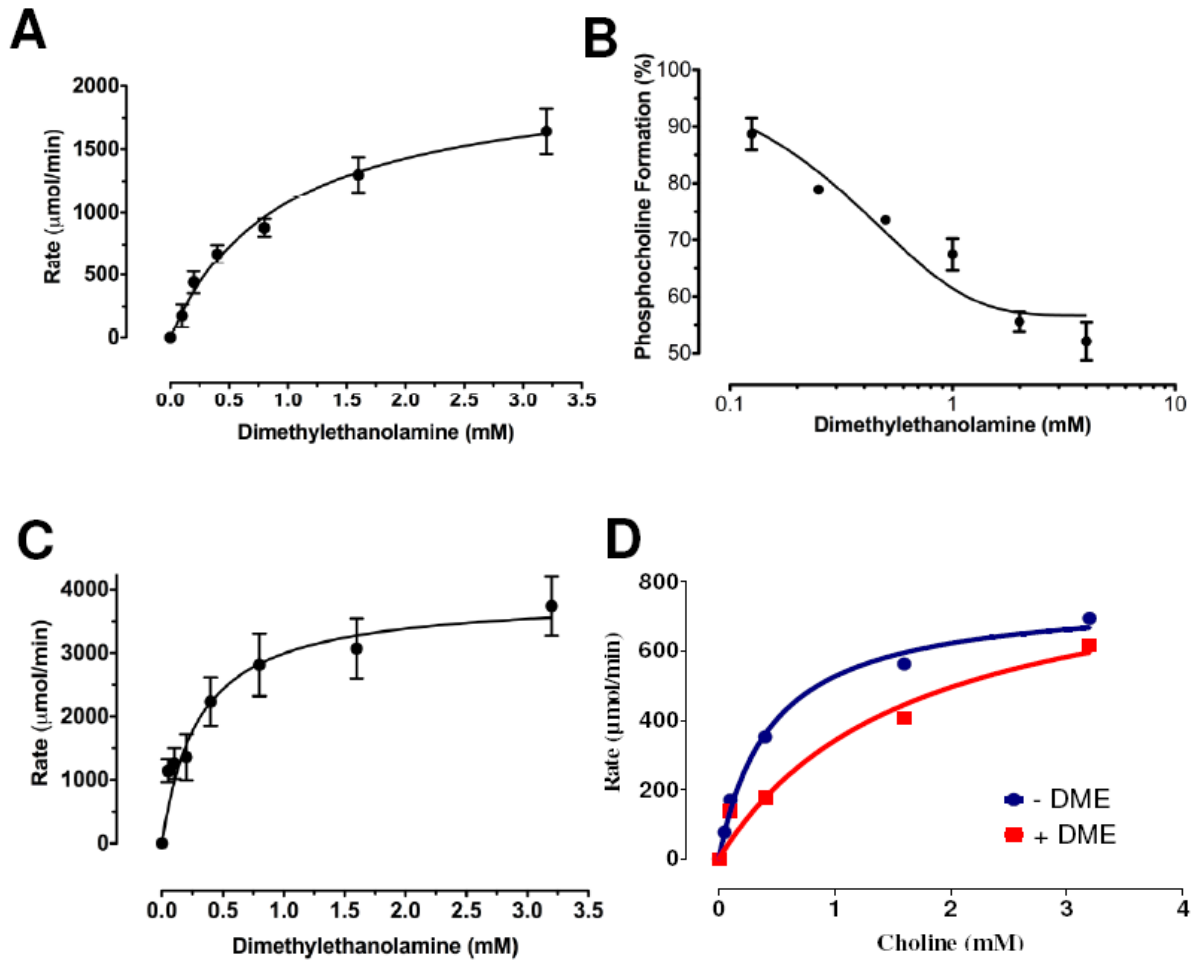

Fig. 19: **A choline analog DME can competitively inhibit the activity of the purified choline kinase.** (A) Michaelis-Menten kinetics of *Tg*CK-6xHis with DME was monitored by decrease in the NADH absorbance (340 nm) in a pyruvate kinase and lactate dehydrogenase-coupled assay. (B) Effect of DME (0-4 mM) on the formation of [^{3}H]-phosphocholine from [^{3}H]-choline (0.1 mM, 0.25 nCi/nmol) by purified *Tg*CK-6xHis was measured for 4 min at 37°C. (C) Michaelis-Menten kinetics of 6xHis-*Tg*CK$_S$ with DME (C) was monitored by decrease in the NADH absorbance (340 nm) in a coupled-enzyme assay. Values are means ±S.E. for three experiments. (D) Competitive inhibition of *Tg*CK in the presence of 2 mM DME was assayed for 4 min at 37°C (2.5 nCi/nmol, 0–3.2 mM choline).

3.8 Displacement of *pTgCK* by a conditional promoter

The susceptibility of parasite cultures and of endogenous PtdCho synthesis to an inhibitor of *Tg*CK implied an essential role of this enzyme for the parasite, which required verification by manipulation of the gene. Our attempts to directly delete the *TgCK* locus in *hxgprt*$^-$ and *Δku80* tachyzoites were futile. The recombination-specific PCR identified only single crossover events at the 5'- or 3'-end except for one clone, which had undergone double homologous recombination (Fig. 20A, B). Surprisingly, however, the PCR and sequencing revealed that

this putative knockout parasite still expressed *Tg*CK transcript (Fig. 20C). Similar results showing only 5'- or 3'-recombination events were obtained when using the crossover-efficient (*Δku80*) strain of *T. gondii*.

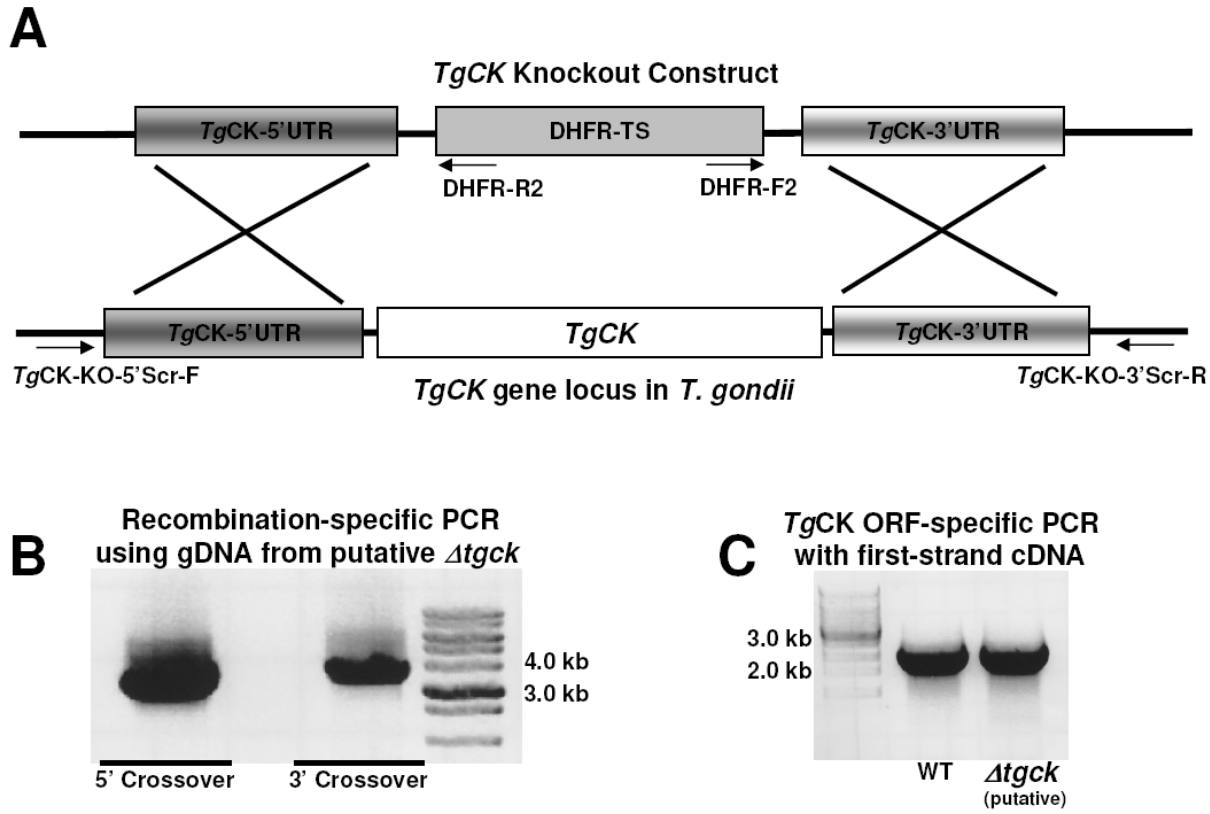

Fig. 20: **The direct knockout of the *Tg*CK gene *via* double homologous crossover.** (A) Scheme of the *Tg*CK deletion in the *Δku80* or *hxgprt*$^-$ strain of *T. gondii*. The 3.3-kb of the 5'- and 3'-UTRs of *Tg*CK were cloned into the *p2854-DHFR-TS* vector flanking the DHFR-TS resistance cassette. (B) The recombination-specific PCR using *Tg*CK-KO-5'Scr-F/DHFR-R2 and DHFR-F2/*Tg*CK-KO-3'Scr-R primers, respectively, revealed 5'- and 3'-crossover in a putative *Δtgck* mutant. (C) The mRNA was isolated from wild-type and the putative *Δtgck* parasites, which revealed presence of *Tg*CK transcript in the wild-type (WT) as well as in the putative *Δtgck* strain (Primer Table 1).

We, therefore, pursued conditional ablation of the *Tg*CK expression by means of the promoter displacement approach. In this regard, we made an inducible parasite line (*Δtgck*$_i$) *via* displacing the *pTgCK* promoter by the *pTetO7Sag4* in the TaTi-*Δku80* strain, which allows an efficient homologous recombination and tetracycline-regulatable expression. The promoter-displacement (PD) construct harbored the 5'UTR (2 kb) preceding the start codon and the partial *TgCK* gene fragment (1 kb), both inserts flanking the DHFR-TS (selection marker) and the *pTetO7Sag4* promoter (Fig. 21A). The pyrimethamine-resistant transgenic parasites were selected, cloned, and analyzed for displacement of the *pTgCK*. The construct-specific PCR of positive clones revealed the DHFR-TS cassette adjacent to the 5'- and 3'-UTRs in the genome

of the *Δtgck*$_i$ mutant and in the construct (control) but not in the parental gDNA (Fig. 21B). Likewise, PCRs for the 5'- and 3'-crossovers amplified the expected DNA bands in the promoter-displaced (*Δtgck*$_i$) parasites but not in the parental gDNA and control construct. Sequencing of the 5'- and 3'-bands confirmed the events of homologous crossover exactly at the *Tg*CK gene locus in the *Δtgck*$_i$ strain.

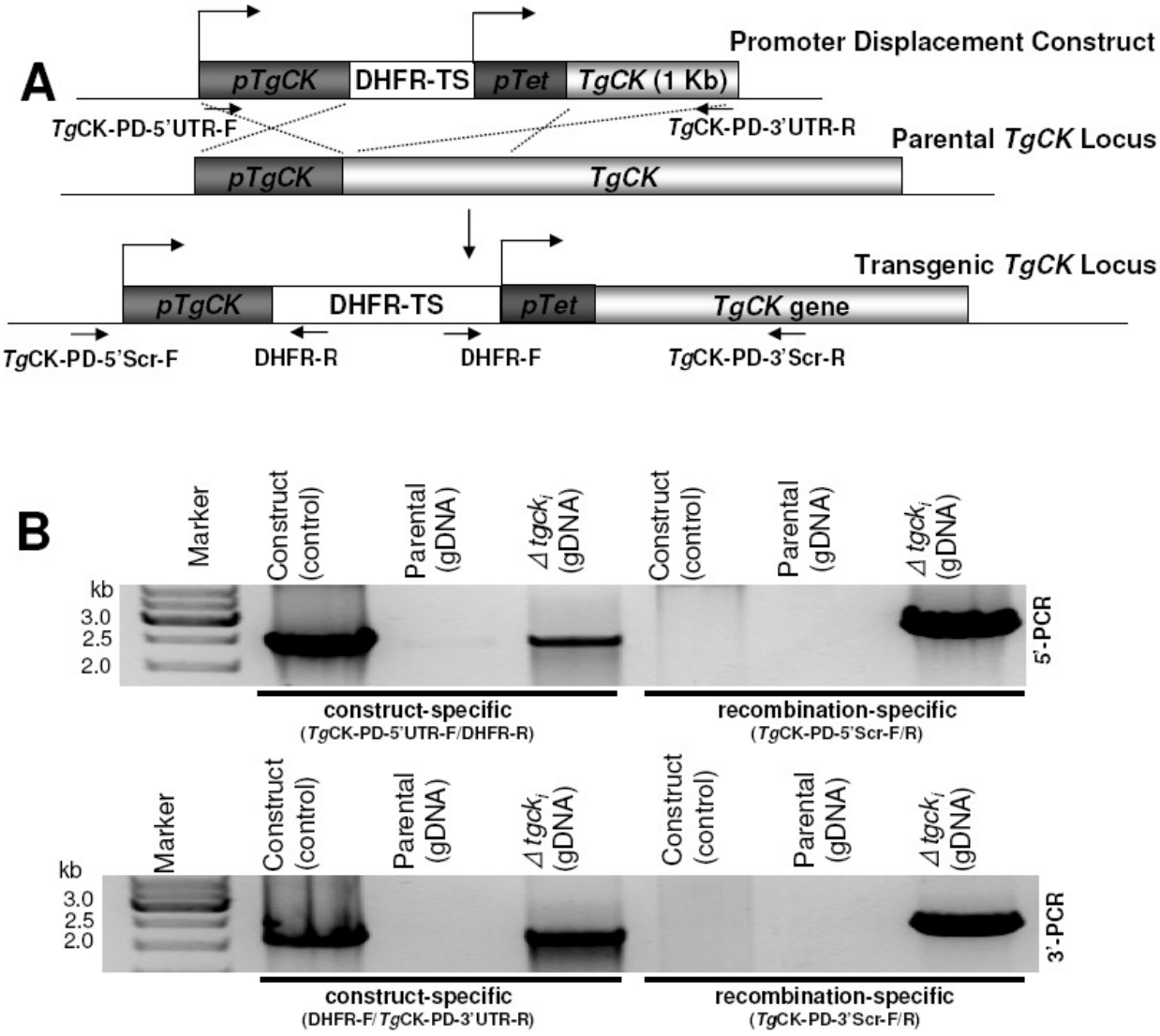

Fig. 21: **Conditional mutatgenesis of the *Tg*CK gene *via* promoter displacement method.** (A) Scheme of the *pTgCK* displacement by a tetracycline-regulatable *pTetO7Sag4* promoter in the TaTi-*Δku80* strain of *T. gondii*. The 2-kb of the promoter region and 1-kb following the initiating codon (ATG) of *Tg*CK were cloned flanking the *pTetO7Sag4* and DHFR-TS resistance cassette in the *pDT7S4* vector. (B) Construct-specific PCR (*Tg*CK-PD-5'UTR-F/DHFR-R and DHFR-F/*Tg*CK-PD-3'UTR-R) confirmed expected bands in the plasmid and in the *Δtgck*$_i$ gDNA, but not in the parental strain. The recombination PCR using *Tg*CK-PD-5'Scr-F/DHFR-R and DHFR-F/*Tg*CK-PD-3'Scr-R primers amplified 5'- and 3'-crossover products in the *Δtgck*$_i$ mutant but none with control construct or parental gDNA. The 5'- and 3'-PCR bands were confined by sequencing. For primers see Table 1.

3.9 PtdCho biogenesis can occur despite a major knockdown of full-length *Tg*CK in *T. gondii*

The IFA and western blot using the anti-*Tg*CK serum confirmed the anhydro-tetracycline (ATc)-mediated regulation of *Tg*CK in the promoter-displaced *Δtgck*$_i$ strain. The *Δtgck*$_i$ expressed a reduced level of choline kinase when compared to the parental strain indicating a depletion of the full-length *Tg*CK protein in the transgenic strain upon promoter displacement (Fig. 22A). The punctuate staining became undetectable following 48-hrs culture in ATc (Fig. 22A). Surprisingly, despite a reduction (control) or an apparent complete loss (ATc-treated) of *Tg*CK expression, the *Δtgck*$_i$ mutant exhibited no discerneable growth defect by plaque assay, which was confirmed by quantitative scoring of the plaque sizes (Fig. 22B). The transgenic strain also survived continued passage in cultures irrespective of the presence of ATc. Consistently, the replication assays also showed no difference in the vacuole size between the mutant and parental strain (Fig. 22C).

Next, we compared the major phospholipid profile of the mutant with the parental strain. Total lipids of the extracellular parasites were separated by TLC and visualized by iodine-staining. No apparent change in the iodine staining of PtdCho and other major phospholipids (PtdEtn and PtdSer) of the *Δtgck*$_i$ strain was observed in untreated cultures, and a reduction of about 30% was observed in the PtdCho content after ATc treatment (Fig. 22D). The individual phospholipids were also quantified by chemical phosphorous assay, which confirmed a similar (~30%) drop in PtdCho content (Fig. 22E).

These results demonstrate that despite a major knockdown of ~70-kDa *Tg*CK, *T. gondii* can ensure its survival and produce PtdCho for membrane biogenesis and ensure its survival. Moreover, a normal parasite growth despite a reduced PtdCho content in the *off state* indicates a compositional plasticity of the parasite membranes and the inability of parasite to scavenge host-derived PtdCho to trade off the knockdown of choline kinase.

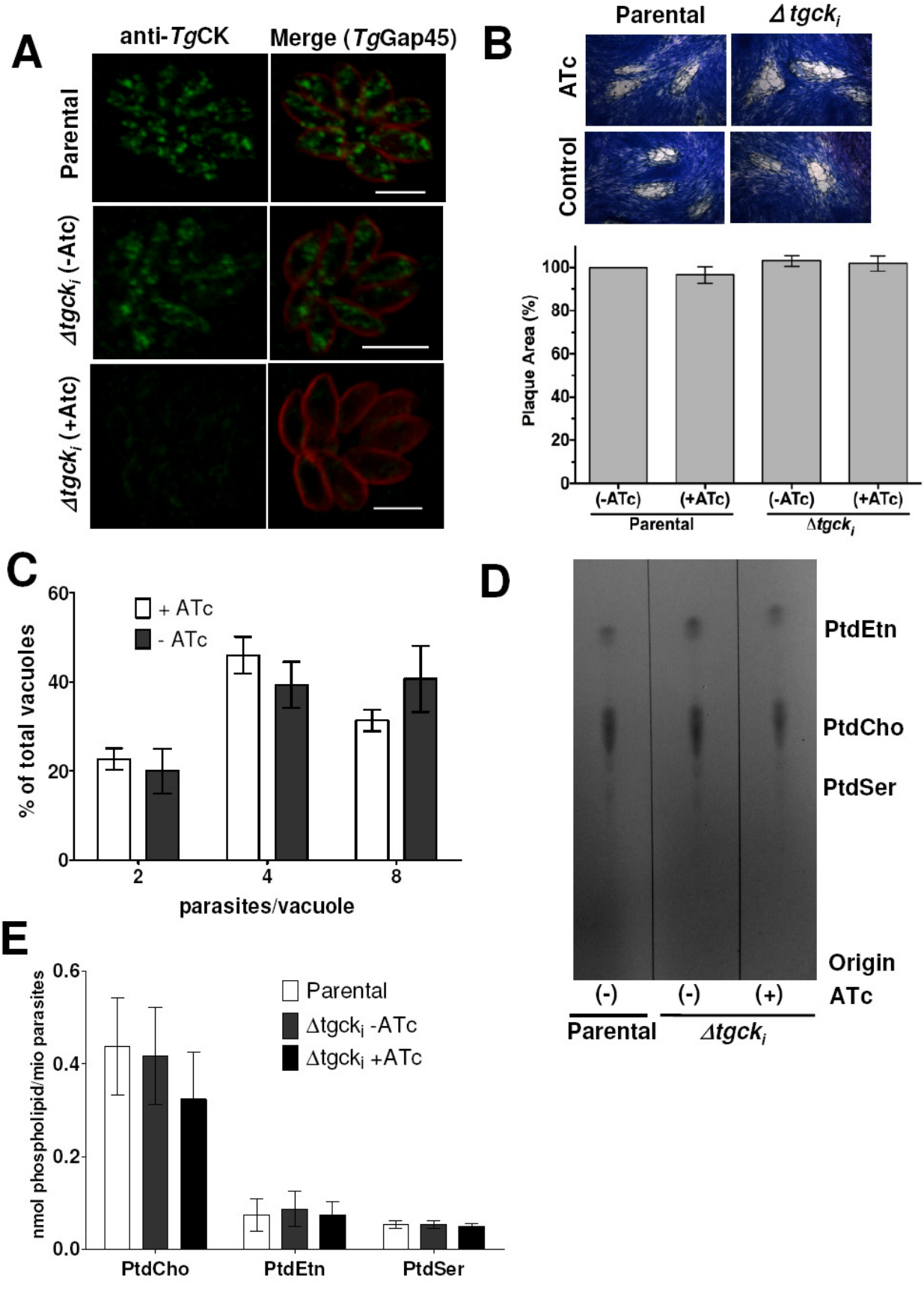
A
anti-TgCK
Merge (TgGap45)
Parental
Δtgcki (-Atc)
Δtgcki (+Atc)
B
Parental
Δ tgcki
ATc
Control
Plaque Area (%)
100
80
60
40
20
0
(-ATc)
(+ATc)
(-ATc)
(+ATc)
Parental
Δtgcki
C
+ ATc
- ATc
% of total vacuoles
60
40
20
0
2
4
8
parasites/vacuole
D
PtdEtn
PtdCho
PtdSer
Origin
(-)
(-)
(+)
ATc
Parental
Δtgcki
E
nmol phospholipid/mio parasites
0.6
0.4
0.2
0.0
Parental
Δtgcki -ATc
Δtgcki +ATc
PtdCho
PtdEtn
PtdSer

Fig. 22: **Knockdown of *Tg*CK does not affect the parasite growth and PtdCho biogenesis.** (A) *Tg*CK expression under the native promoter in the TaTi-*Δku80* strain or under the control of the conditional promoter (*pTetO7Sag4*) in the *Δtgck*$_i$ strain in the presence or absence of ATc (0.5 µM). Intracellular tachyzoites were stained 29 hrs post-infection using rabbit anti-*Tg*Gap45 antibody (red, 1:3000, inner membrane complex marker) and mouse anti-*Tg*CK serum (green, 1:200). Bar, 5 µm. (B) The representative plaques formed by the *Δtgck*$_i$ and the parental strain incubated with or without Atc (0.5 µM). Confluent monolayers of human foreskin fibroblasts were infected with 200 parasites, and plaques were stained with crystal violet 7 days post-infection. The size quantification was performed by ImageJ suite. (C) Replication of the *Δtgck*$_i$ strain with or without ATc (0.5 µM) was determined by IFA (anti-*Tg*Gap45, 1:3000) 29 hrs post-infection and counting of the parasites per vacuole. 50 vacuoles were counted each in 3 independent experiments. (D) Iodine staining of TLC-resolved phospholipids from the *Δtgck*$_i$ and parental strains. Lipids from equivalent numbers of parasites were extracted, separated by TLC ($CHCl_3/CH_3OH/H_2O$, 65:25:4), and then visualized by iodine vapors. The ATc (0.5 µM) treatment was performed for several passages in culture. (E) Phosphorous quantification of the *Δtgck*$_i$ lipid. Axenic tachyzoites of the TaTi-*Δku80* strain and the *Δtgck*$_i$ mutant in the *on* (-ATc) or *off* (+ATc) *state* were washed once with PBS and counted. Total phospholipids were extracted and resolved by TLC ($CHCl_3/CH_3OH/H_2O$, 65:25:4). Lipids were scraped off from the iodine-staned plate and quantified for their phosphorous content as desribed in section 2.4.7.

3.10 Choline kinase activity cannot be abolished in the *Δtgck*$_i$ mutant

Our further work focused on elucidating the mechanism underlying survival and membrane biogenesis in the *Δtgck*$_i$ mutant. We tested the *Tg*CK protein expression in the conditional mutant by western blot analysis. Surprisingly, in addition to the full-length ~70-kDa *Tg*CK, we observed the expression of a smaller protein (~53-kDa) recognized by anti-*Tg*CK serum in the *Δtgck*$_i$ mutant (Fig. 23A). The expression of this protein coincided with the disappearance of full-length *Tg*CK in the untreated sample and persisted despite the ATc treatment for 48 hrs. The high intensity images of the *Δtgck*$_i$ corroborated these findings, and identified a punctate cytosolic plus ATc-regulatable fluorescence representing the full-length *Tg*CK (Fig. 23B). The images also revealed a fluorescence in the mitochondrion and/or endoplasmic reticulum, which did not respond to regulation with ATc.

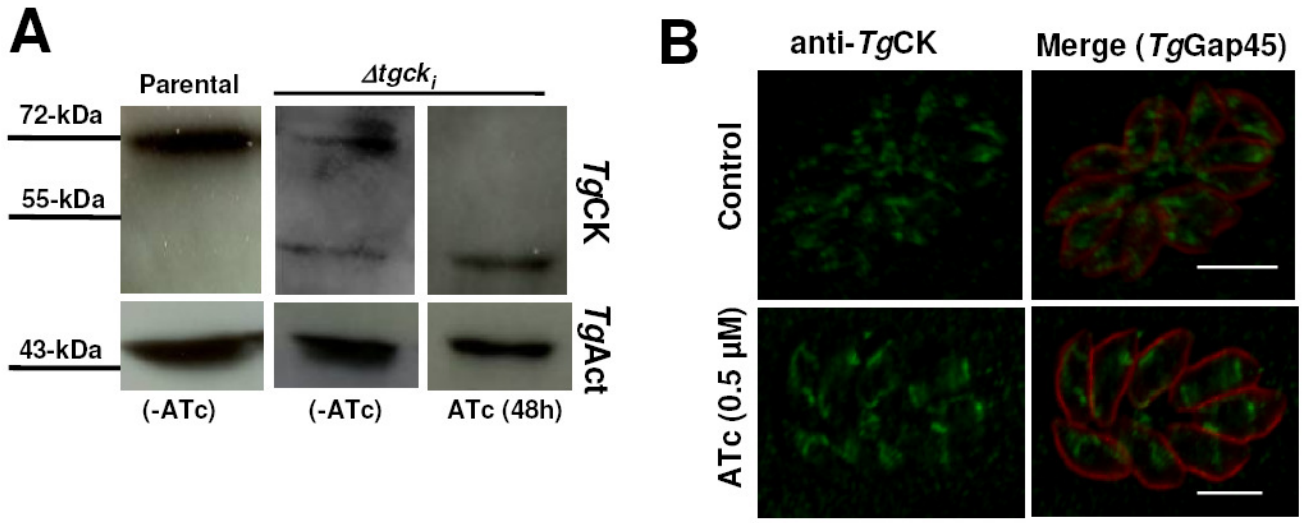

Fig. 23: **The *Δtgck*$_i$ mutant expresses a novel protein, recognized by anti-*Tg*CK serum.** (A) Western blot of the extract from the *Δtgck*$_i$ and TaTi-*Δku80* strains using the mouse anti-*Tg*CK serum (1:200). The parasite actin, identified by mouse anti-*Tg*Act (1:1000) served as a loading control. (B) High intensity fluorescent imaging of the *Δtgck*$_i$ mutant 29 hrs post-infection using rabbit anti-*Tg*Gap45 antibody (red, 1:3000) and mouse anti-*Tg*CK serum (green, 1:200). Bar, 5 μm.

We next examined the choline kinase activity in the total parasite extract of the *Δtgck*$_i$ mutant. The radioactive choline kinase assay was performed for 30 min and products were analyzed by scintillation counting (Fig. 24A) and TLC (Fig. 24B). In consistence with the western blot and immuno-fluorescence, the enzyme assay revealed synthesis of phosphocholine by the mutant extract, indicating the presence of a functional choline kinase. Only ~33% of the total kinase activity was regulatable with ATc (Fig. 24A). We next tested the *Δtgck*$_i$ mutant for its ability to metabolize choline into PtdCho during replication by labeling the intracellular parasite with [^{14}C]-choline and evaluating for the synthesis of radioactive lipids (Fig. 24C, D). Yet again ~35% decrease in the total lipid counts was observed in ATc-treated cultures (Fig. 24C, D). The persistence of choline kinase activity, and choline labeling of the parasite PtdCho confirm the presence of an active choline kinase in the *Δtgck*$_i$ strain.

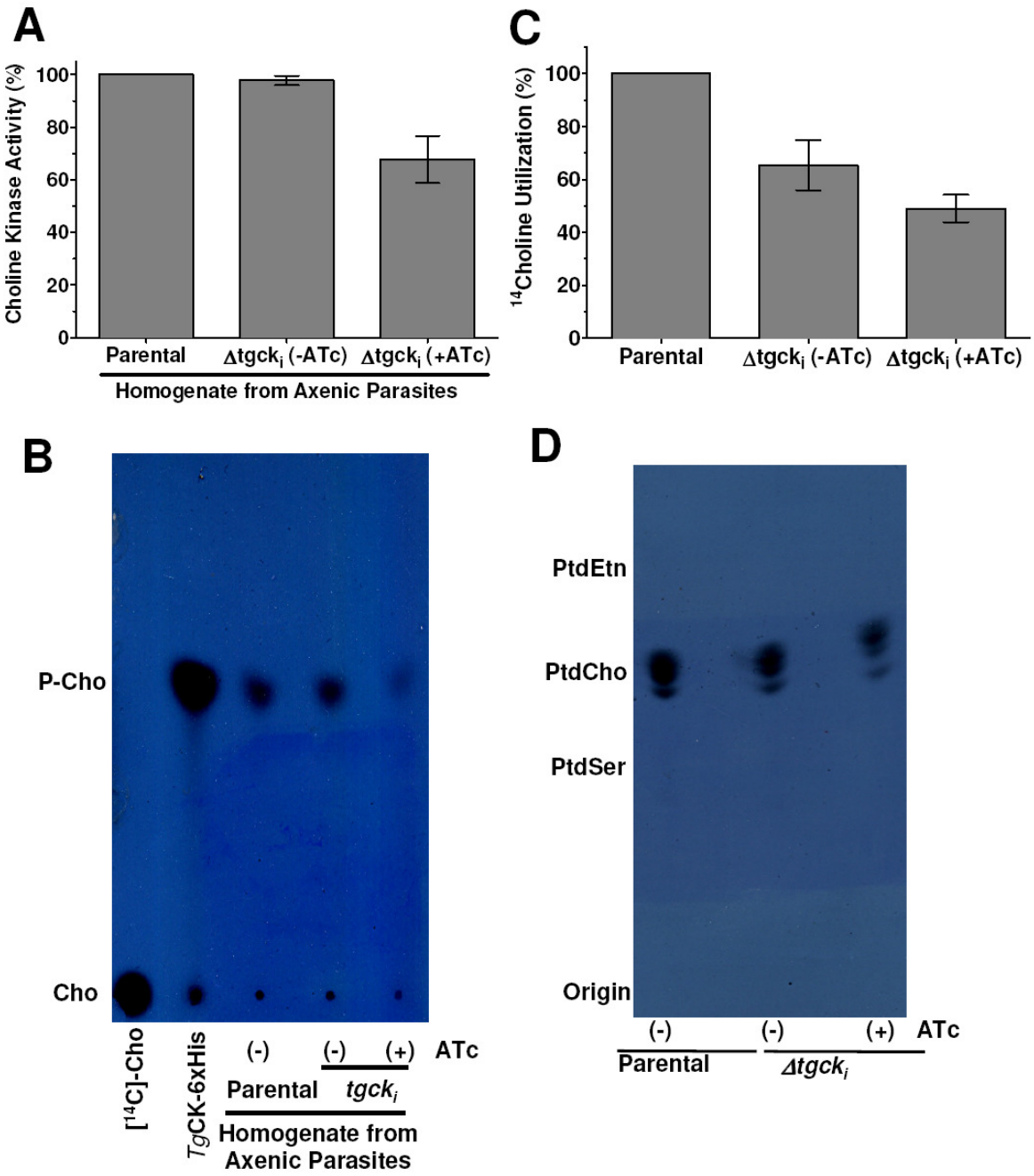

Fig. 24: ***Tg*CK activity and PtdCho synthesis cannot be abolished in *tgck*$_i$ mutant.** (A) Choline kinase activity was measured in the protein extract (25 µg) using [^{14}C]-choline (0.1 µCi, 10 µM, 30 min, 37°C) and phosphocholine formation was quantified or visualized by TLC (95% EtOH/2%NH_4OH, 1:1) and (B) X-ray exposure of the TLC plate at -80°C for 1 month. (C) The parasitized (MOI=3) monolayers of human foreskin fibroblasts were cultured for 40 hrs in media containing [^{14}C]-choline (0.1 µCi/ml). Parasites were washed twice with PBS, and lipids were extracted for TLC analysis ($CHCl_3/CH_3OH/H_2O$, 65:25:4). (C) [^{14}C]-Choline labeling into phospholipids was visualized by exposure of the TLC plate to X-ray film for 48 hrs (D) Quantification of lipid labeling by scintillation counting. The ATc (0.5 µM) treatment was performed for several passages in culture.

In accord, similar to the parental strain the *Δtgck*$_i$ mutant was susceptible to competitive inhibition of choline kinase activity by DME, which impaired the replication in both strains

(Fig. 25). The untreated control cultures displayed 4-8 tachyzoites in ~80% of vacuoles, and ~15-20% of them harbored 2 parasites. A prominent decrease in the number of parasites per vacuole was observed in DME-treated samples, where vacuoles showed only 2-4 tachyzoites.

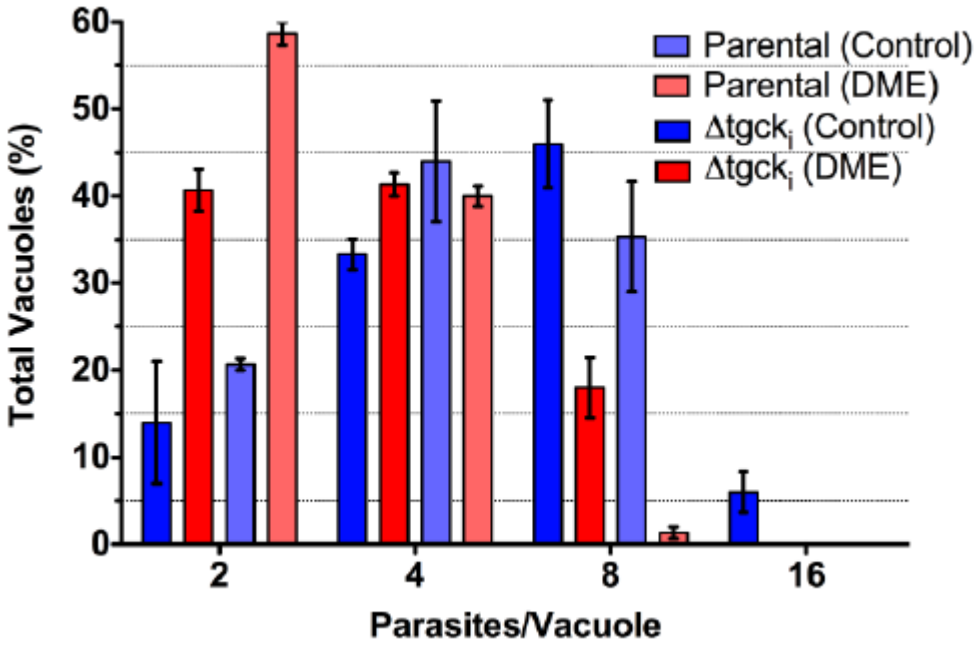

Fig. 25: **The *Δtgck$_i$* mutant is susceptible to inhibition by DME.** Parasites in their vacuoles were counted in the parasitized HFF (29 hrs post-infection) following staining with rabbit anti-*Tg*Gap45 antibody (1:3000). Values are means ±S.E. for 3 independent experiments, each with 50 parasitophorous vacuoles.

3.11 The exon1 of the *Tg*CK gene harbors a potential promoter

Next, we attempted to identify the source of choline kinase activity in the mutant. A weak expression of the 53-kDa protein detected by anti-*Tg*CK serum hampered its identification by mass spectrometry. The *Toxoplasma* genome harbors 2 additional choline/ethanolamine kinases, one of which (*Tg*EK) was confirmed as an ethanolamine-specific kinase in this work. This protein should not contribute to the observed choline kinase activity in the *Δtgck$_i$*. Besides, our attempts to amplify the third putative choline/ethanolamine kinase (TGGT1_058210) using the mRNA isolated from wild-type tachyzoites or from the *Δtgck$_i$* mutant were not successful. The RNA sequencing and proteomic data (www.ToxoDB.org) also show no evidence for expression of this gene in *T. gondii* tachyzoites.

Alternatively, the observed activity could be due to use of an alternative (secondary) promoter and/or an alternative start codon in the *Tg*CK gene. To test this, we performed quantitative PCR of the *Δtgck*$_i$ mRNA following treatment with Atc (Fig. 26). Three different

primer pairs were used, two of which annealed in the first exon and the third amplified a fragment of the exon 6 (Appendix 6). Interestingly, the EST corresponding to Exon1-2 primer pair (binding in the first half of exon1) was less abundant and appeared at cycle 25. The other two ESTs (Exon1-1 binding in the second half of exon1, and primer pair annealing in exon6) were more abundant and visible at cycle 22. These data indicated the presence of at least two type of transcripts comprising of two in-frame start codons present in the exon1 (1-1893 bp and 493 -1893 bp). These transcripts would code for proteins of 630 amino acids (~70-kDa) and 466 amino acids (~53-kDa), the latter corresponding to the smaller protein observed in the *Δtgck*$_i$ mutant. Different levels of transcript also imply the presence of an alternative promoter. All three ESTs responded to regulation with ATc. However, a modestly stronger downregulation by ATc was observed with the primers annealing in the first half of the exon1 (primer Exon1-2 in Fig. 26). Collectively, these data indicate the presence of a weakly active alternative promoter within the first exon, which is not regulatable by Atc, and produces a shorter transcript translating into a functional choline kinase of ~53-kDa.

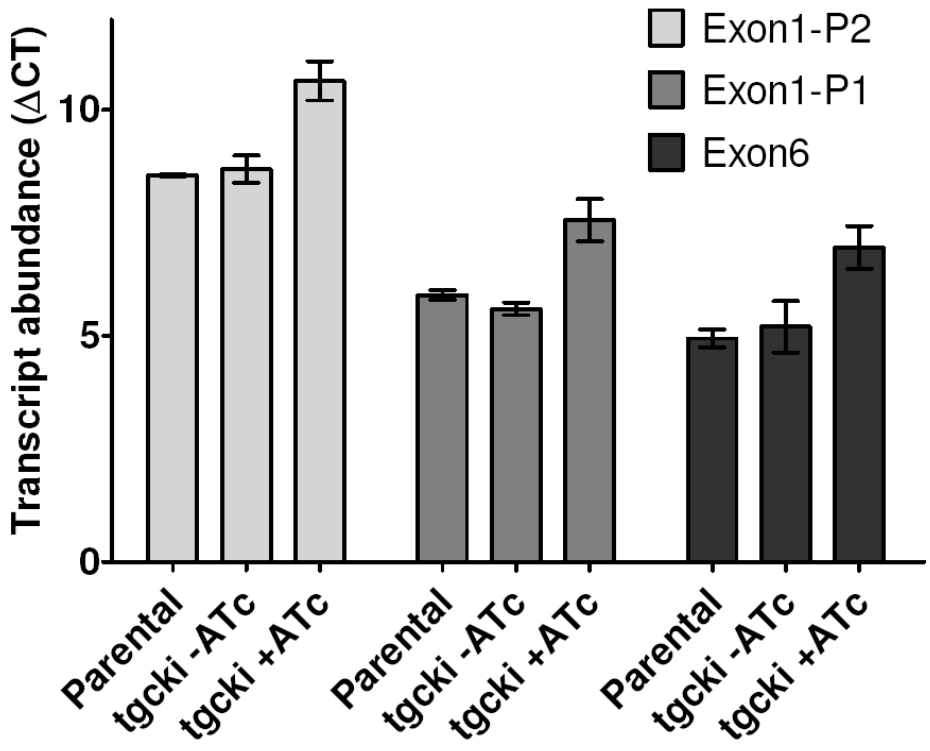

Fig. 26: E**xpression analysis of *Tg*CK transcript by real-time PCR.** The total RNA was isolated from the *Δtgck*$_i$ mutant in the absence or presence of ATc (0.5 µM, 148 hrs) and the parental strain cultures. 100 ng of total RNA were transcribed into the first-strand cDNA using Oligo(dT) and random hexamer primers at T_a of 60°C. qPCR was performed using primers annealing in exon-1 or -6 of *Tg*CK and the transcript abundance was calculated as *Δct* by subtracting the ct from the housekeeping transcripts (TGGT1_124740, *Tg*GT1; TGGT1_037840, *Tg*Elf1a).

3.12 The Knockdown of a putative *Tg*CCT causes a growth defect in *T. gondii*

The conditional mutagenesis of *Tg*CK could not convincingly adress the essentiality of CDP-choline pathway. Therefore, a conditional knockout of the rate-limiting enzyme, *Tg*CCT, was generated in the TaTi-*Δku80* strain to further test the essentiality of *de novo* PtdCho synthesis. The C-terminally HA-tagged *Tg*CCT ORF (*Tg*CCT$_i$-HA) under the control of the *pTetO7Sag1* promoter and *NTP3*-3'UTR was cloned into plasmid *pTetUPKO*. The expression cassette was flanked by 800 bp of the 5'- and 3'-UTRs of the *Tg*UPRT (uracil phosphoribosyl transferase) gene for the insertion of *Tg*CCT$_i$-HA at the locus by double crossover (Fig. 27A). Disruption of the UPRT locus renders the parasite insensitive to FUDR (5-fluorodeoxyuridine), which otherwise blocks the parasite replication by interfering with the DNA synthesis (18). Stable transgenic parasites were selected for 3-4 weeks using 5 µM FUDR and the expression plus tetracycline-regulation of *Tg*CCT$_i$-HA was verified by IFA. The *Tg*CCT$_i$-HA strain was then transfected with the *Tg*CCT knockout construct. To this end, the 1 kb of 5'- and 3'-UTRs of the *Tg*CCT gene were cloned into *p2854-DHFR-TS* flanking the resistance cassette, which allowed selection of stable parasites with 1 µM pyrimethamine (Fig. 27A). The clonal parasites obtained by dilution plating were analyzed for the double crossover events at the *Tg*CCT locus by PCR. As described above for the *Δtgck$_i$* mutant, recombination-specific PCRs for the 5'- and 3'-ends amplified the expected DNA bands in the knockout parasites (*Δtgcct*/*Tg*CCT$_i$-HA) but not in the parental gDNA and in control construct (Fig. 27B). The homologous integration event was confirmed by sequencing of both PCR products. The absence of endogenous *Tg*CCT locus was verified further by PCR using the ORF-specific primers (Fig. 27C), which yields a 2 kb fragment corresponding to the size of the genomic *Tg*CCT locus in wild-type parasite gDNA. The parental strain which, besides the endogenous gene, also expressed *Tg*CCT$_i$-HA, displayed a second PCR fragment of 1 kb. Whereas, as expected, the *Δtgcct*/*Tg*CCT$_i$-HA mutant lacked the larger 2 kb fragment corresponding to the gene locus, and showed expression of only the 1 kb cDNA, which validated the deletion of the *Tg*CCT locus.

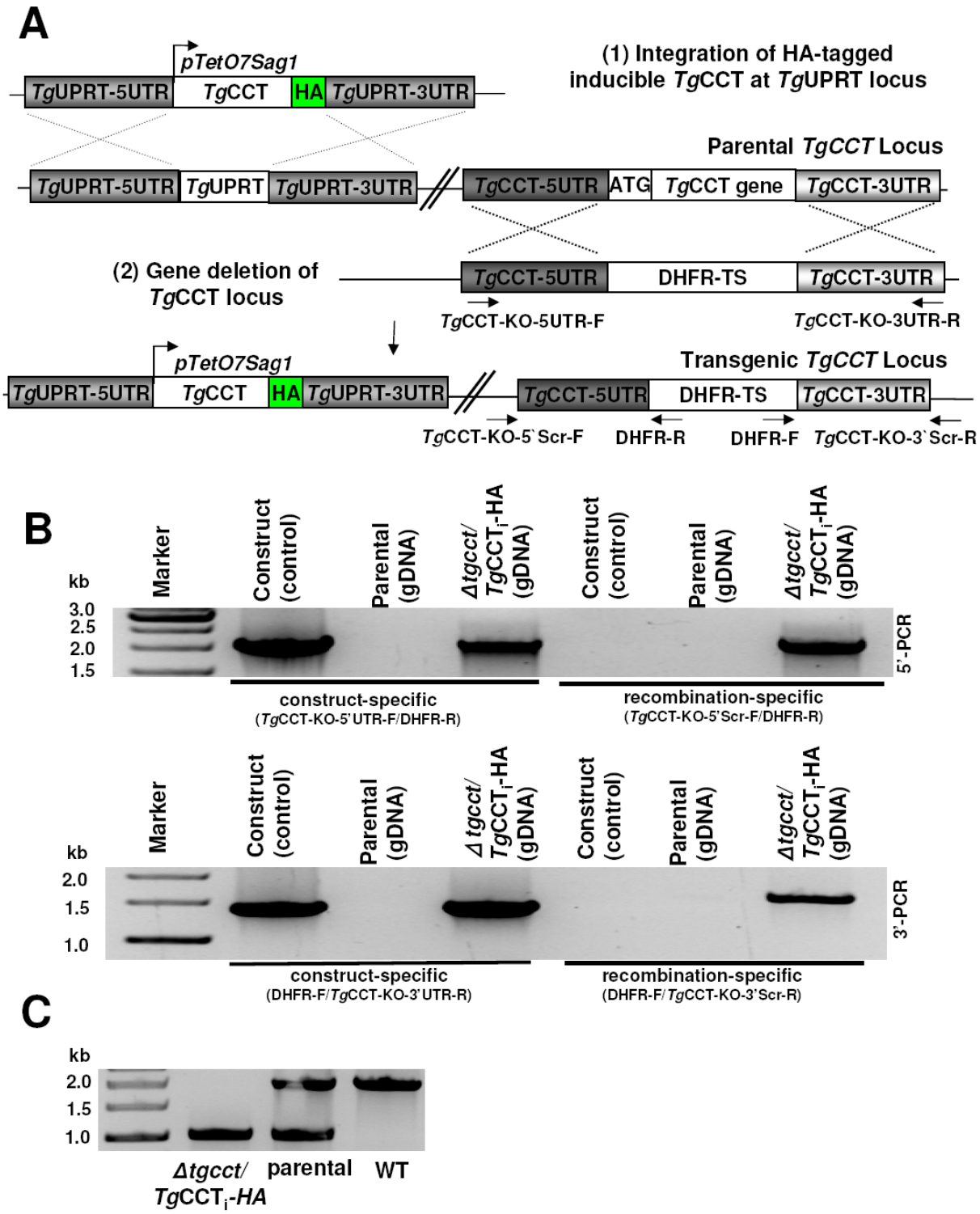
A
pTetO7Sag1
TgUPRT-5UTR
TgCCT
HA
TgUPRT-3UTR
(1) Integration of HA-tagged inducible TgCCT at TgUPRT locus
Parental TgCCT Locus
TgUPRT
TgCCT-5UTR
ATG
TgCCT gene
TgCCT-3UTR
(2) Gene deletion of TgCCT locus
DHFR-TS
TgCCT-KO-5UTR-F
TgCCT-KO-3UTR-R
Transgenic TgCCT Locus
TgCCT-KO-5`Scr-F
DHFR-R
DHFR-F
TgCCT-KO-3`Scr-R
B
kb
Marker
Construct (control)
Parental (gDNA)
Δtgcct/ TgCCTi-HA (gDNA)
5'-PCR
construct-specific
(TgCCT-KO-5'UTR-F/DHFR-R)
recombination-specific
(TgCCT-KO-5'Scr-F/DHFR-R)
3'-PCR
(DHFR-F/TgCCT-KO-3'UTR-R)
(DHFR-F/TgCCT-KO-3'Scr-R)
C
Δtgcct/ TgCCTi-HA
parental
WT

Fig. 27: **Conditional mutagenesis of the *Tg*CCT locus.** (A) Schematic depiction of a regulatable *Tg*CCT knockout generated in two steps. *Tg*CCT-HA under the control of the *pTetO7Sag1* promoter (*Tg*CCT_i-HA) was cloned into *pTetUPKO* plasmid, which allows the selection of transgenic parasites with FUDR for stable integration at the *Tg*UPRT locus. In the next step, the 1kb of 5'- and 3'-UTRs of *Tg*CCT were introduced into *p2854-DHFR-TS* flanking the resistance cassette, and the *NotI*-linearized construct was transfected into the TaTi-*Δku80* strain of *T. gondii* expressing the *Tg*CCT_i-HA. Stable parasites were selected with 1 µM pyrimethamine and cloned by limiting dilution. (B) Construct-specific PCR using *Tg*CCT-KO-5'UTR-F/DHFR-R and DHFR-F/*Tg*CCT-KO-3'UTR-R confirmed expected bands in the plasmid and in the *Δtgcct/Tg*CCT_i-HA gDNA, but not in the parental strain. The recombination PCR using *Tg*CCT-KO-5'Scr-F/DHFR-R and DHFR-F/*Tg*CCT-KO-3'Scr-R primers, revealed 5'- and 3'-crossovers in the *Δtgcct/Tg*CCT_i-HA mutant but none with control construct or the parental gDNA. (C) *Tg*CCT ORF-specific primers revealed expression of the 1kb cDNA and 2kb genomic locus in the TaTi-*Δku80* strain expressing the regulatable *Tg*CCT_i-HA (parental). PCR on *hxgprt*$^-$ parasites results in 2kb amplicon, whereas the genomic locus is absent in the *Δtgcct/Tg*CCT_i-HA mutant, which expresses only the 1kb cDNA.

Next, we examined the knockdown of *Tg*CCT_i-HA expression following treatment with ATc (Fig. 28A, B). Two protein bands of 40- and 37-kDa, of which the lower band corresponds to the predicted size of *Tg*CCT protein, were observed. Both isoforms were substantially downregulated following 24 hrs treatment, and disappeared completely after 72 hrs of treatment (Fig. 28A). This was confirmed by IFA, where the protein was detectable in the nucleus 29 hrs post-infection, and it was barely detectable at 110 hrs post-infection (Fig. 28B).

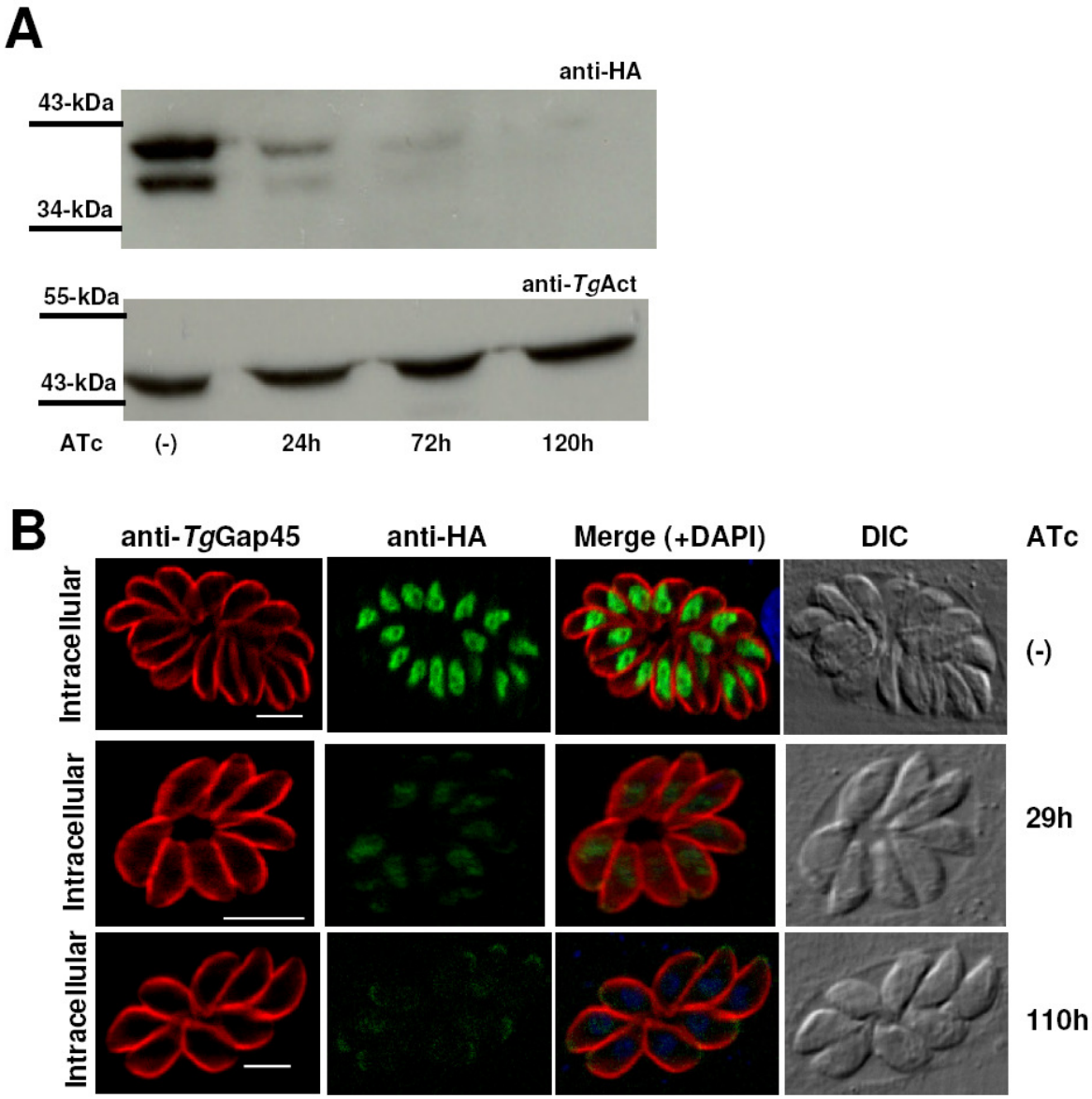

Fig. 28: **Regulation of *Tg*CCT expression in the *Δtgcct/Tg*CCT$_i$-HA mutant.** (A) Western blot of total parasite extract prepared following Atc (1 µM) treatment as indicated. The rabbit anti-HA antibody (1:1000) revealed depletion of *Tg*CCT$_i$-HA in the *Δtgcct/Tg*CCT$_i$-HA mutant after ATc treatment. Actin served as the loading control. (B) IFA of the *Δtgcct/Tg*CCT$_i$-HA mutant cultured without or with ATc (1 µM) for 29 or 110 hrs post-infection (mouse anti-HA, green, 1:1000; rabbit anti-*Tg*Gap45, red, 1:3000; DAPI, blue). Bar, 5 µm.

The Atc treatment of the *Δtgcct/Tg*CCT$_i$-HA mutant caused a marked growth defect as deduced by plaque and replication assays. The plaque size of the *Δtgcct/Tg*CCT$_i$-HA was similar to the parental strain in the absence of ATc, whereas in the *off state* the plaque size in the mutant was reduced to about 50% (Fig. 29A, B). This was mirrored by the formation of smaller vacuoles in replication assays, where about 70% of the parental vacuoles harbored 8-16 parasites per vacuole. Whereas ~56% of the mutant vacuoles contained 2-4 parasites in contrast to ~30% in the parental strain (Fig. 29C).

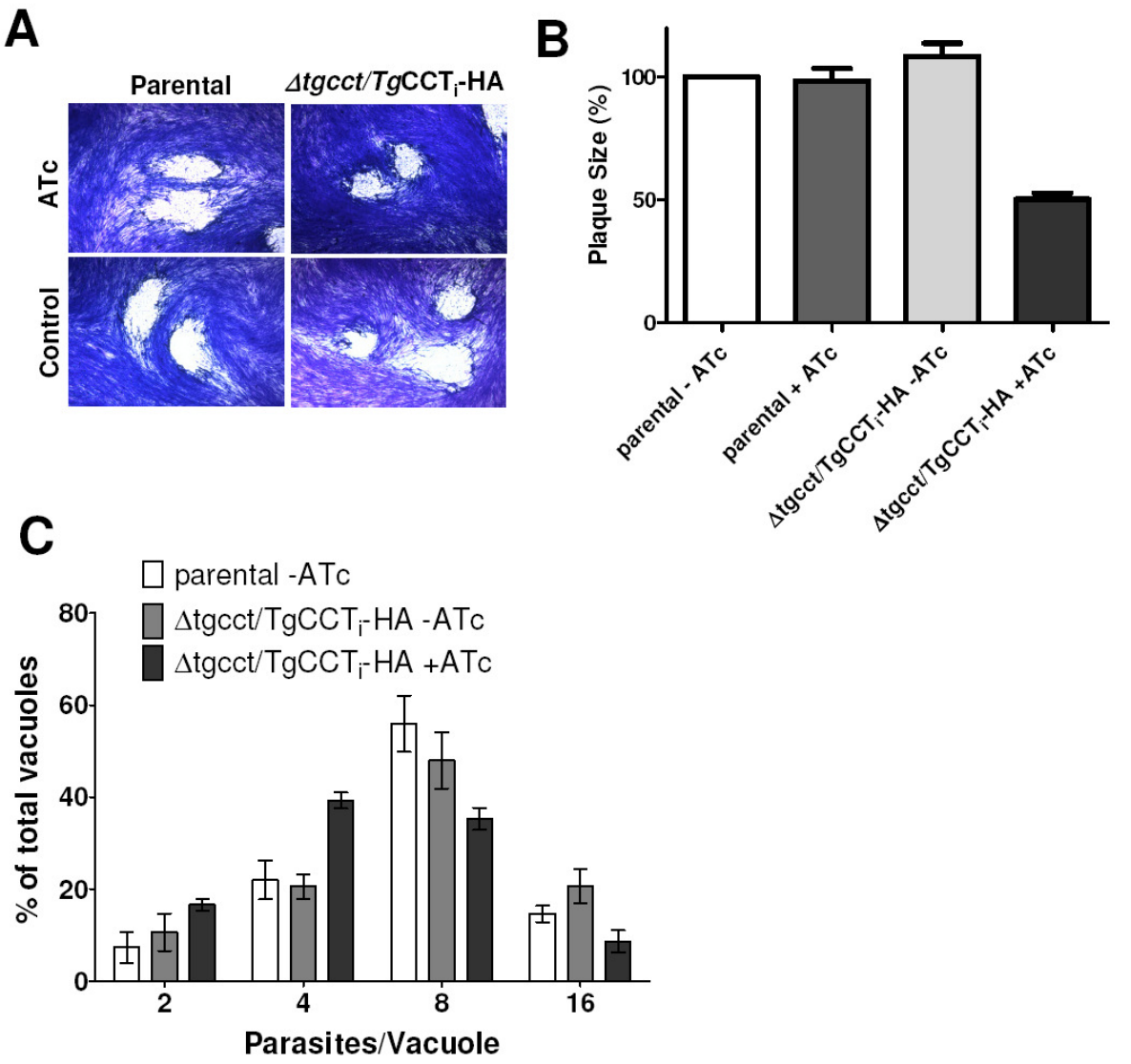

Fig. 29: **The knockdown of *Tg*CCT reduces the parasite replication.** (A) The representative plaques formed by the *Δtgcct*/*Tg*CCT$_i$-HA and the parental strain. Confluent monolayers of HFFs infected with 200 parasites were cultured without or with 1 µM ATc, and plaques were stained with crystal violet 7 days post-infection. (B) Quantification of plaque size of *Δtgcct*/*Tg*CCT$_i$-HA and the parental strain using the ImageJ suite. (C) Intracellular replication of the *Δtgcct*/*Tg*CCT$_i$-HA mutant was measured by counting the number of parasites per vacuole 29 hrs post infection. The parasites were stained using rabbit anti-*Tg*Gap45 (1:3000) antibody. 50 vacuoles per assay were counted from three independent experiments.

4 Discussion

4.1 CDP-choline and CDP-ethanolamine pathways of *T. gondii*

Similar to other eukaryotes, PtdCho and PtdEtn are the two most abundant phospholipids in the membranes of *Toxoplasma gondii* (38). The *T. gondii* genome (www.ToxoDB.org) harbors the predictions for the CDP-choline and the CDP-ethanolamine pathway, which are the major routes of PtdCho and PtdEtn biogenesis in mammalian cells (Fig. 30). Similarly, the parasite is competent in utilizing choline and ethanolamine into PtdCho and PtdEtn, respectively (38), but, however, lacks a PtdEtn methyltransferase to make PtdCho from PtdEtn (Fig. 30).

The three enzymes of the CDP-choline pathway in *T. gondii* – *Tg*CK, *Tg*CCT and *Tg*CPT – display a differential localization in the cytosol, nucleus and ER membrane, respectively (Fig. 30). The first reaction is catalyzed by *Tg*CK, which besides its major substrate choline can also phosphorylate ethanolamine. An anti-parasite choline analog DME can competitively inhibit *Tg*CK (Fig. 30). A truncated enzyme, lacking the N-terminal hydrophobic peptide, shows about 3-fold increased activity towards choline and DME. The *Tg*CCT showed best homology to the mammalian CCT-alpha isoform, and localizes to the parasite nucleus. However, unlike mammalian CCTs, which regulate their activity by a reversible attachment to the nuclear membrane (59), the *Tg*CCT showed a persistent nuclear staining in the intracellular and extracellular tachyzoite. This implies a different mechanism regulating the *Tg*CCT activity, which probably does not require the protein re-localization. *Tg*CPT localizes to the ER membrane as also known for its orthologs (27). The differential subcellular distribution of *Tg*CK, *Tg*CCT and *Tg*CPT raises the obvious question of how their catalytic products are transported to yield PtdCho biogenesis in the ER of *T. gondii*.

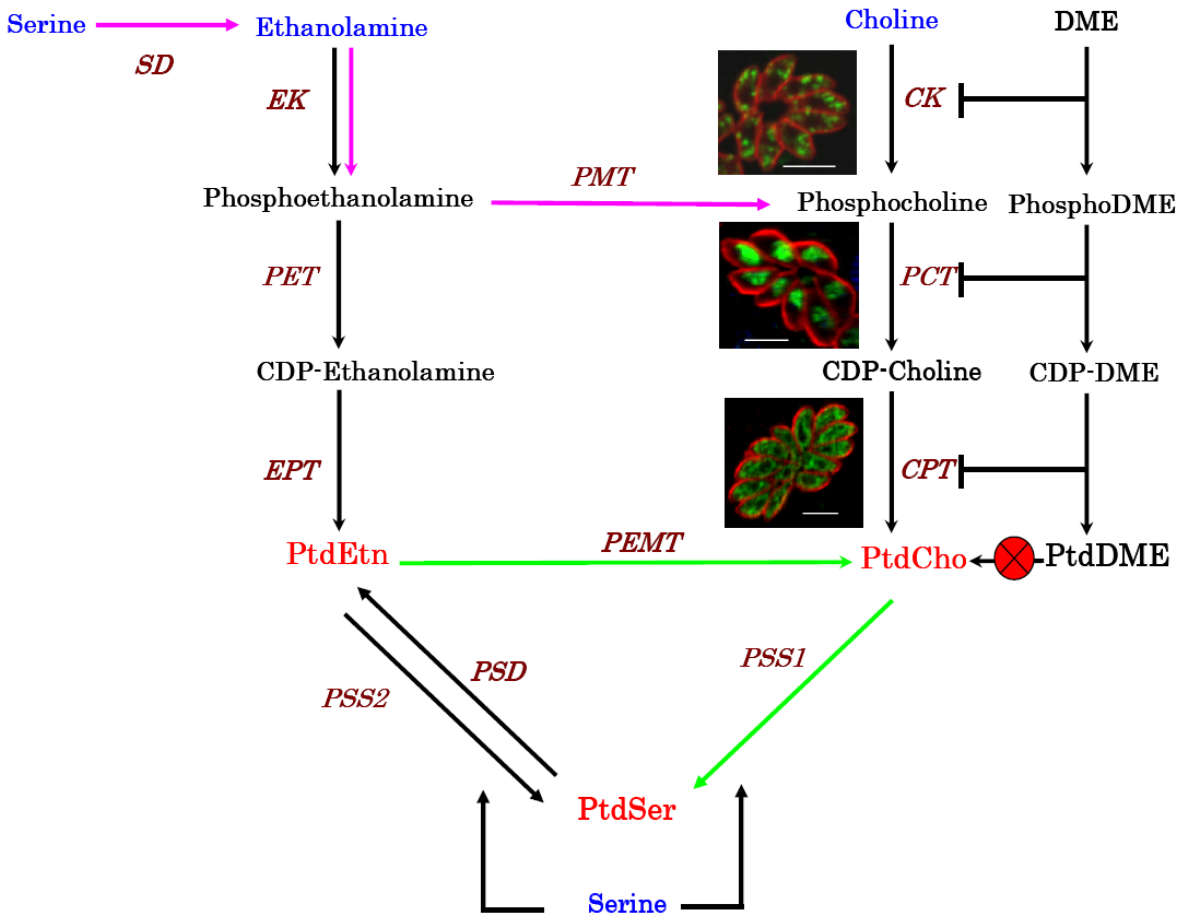

Fig. 30: ***De novo* synthesis of phospholipids in *T. gondii*.** The *H. sapiens* and *P. falciparum* pathways are adapted from literature, and of *T. gondii* are constructed based on the reported enzyme activities and annotations in the parasite database (www.ToxoDB.org). The pathways, common to all organisms, are shown in black; and those specific to human, are depicted in green. The SDPM-pathway, shown in purple, denotes a plant-type route for PtdEtn and PtdCho synthesis, and is exclusive to *P. falciparum*. Initial precursors are shown in blue; the intermediates of lipid synthesis are in black; phospholipids are in red, and the enzymes are depicted in brown color. DME is metabolized *via* the CDP-choline route and produces PtdDME, which is not methylated to PtdCho in *T. gondii* causing disruption of membrane biogenesis. The treatment of parasite cultures with DME leads to a reduction in PtdCho and an accumulation of PtdDME. CK, choline kinase; PCT, phosphocholine cytidylyltransferase; CPT, CDP-choline phosphotransferase; EK, ethanolamine kinase; PET, phosphoethanolamine cytidylyltransferase; EPT, CDP-ethanolamine phosphotransferase; PEMT, phosphatidylethanolamine methyltransferase; PMT, phosphoethanolamine methyltransferase; SD, serine decarboxylase; PSS, phosphatidylserine synthase; PSD, phosphatidylserine decarboxylase; DME, dimethylethanolamine.

Our futile attempts to generate a *Tg*CK knockout parasite line by direct deletion suggest that choline kinase activity is required for PtdCho biogenesis, and thereby also for the parasite survival. Despite an apparent knockdown of the full-length *Tg*CK in a conditional mutant, choline kinase activity could not be abolished in the *on* and *off states*. The choline kinase activity in the mutant was reduced only by ~33%, which translated into ~27% reduction in the PtdCho content of tachyzoites. Surprisingly, despite a reduction in total PtdCho, the parasite

growth was not influenced. *T. gondii* appears not to be capable of salvaging PtdCho or its intermediates from the host cell, which would otherwise alleviate the reduction in PtdCho content. This implies a strict dependence of *T. gondii* on its CDP-choline pathway (i.e. choline auxotrophy). Moreover, these results suggest that the reported anti-parasite effect of DME is likely not a consequence of decline in PtdCho content but an effect of accumulated PtdDME, which due to absence of a PtdEtn methyltransferase in *T. gondii* is not further methylated to form PtdCho and eventually causes a disruption of the membrane integrity and inhibits the parasite replication (Fig. 30). *Toxoplasma* also lacks a serine-decarboxylase phosphoethanolamine methyltransferase pathway (SDPM), a second plant-type route of PtdCho synthesis in *P. falciparum*. Disruption of the PtdCho synthesis by chemical inhibition of *Pf*CK or by the genetic deletion of *Pf*PMT are detrimental to the *P. falciparum* growth (40,60). Despite an apparent redundancy of PtdCho biogenesis, disruption of either pathway strongly reduces the growth of the malaria parasite suggesting their role in formation of different pools of PtdCho. In contrast, this work indicates that the related parasite *Toxoplasma* depends on *de novo* CDP-choline pathway for PtdCho biogenesis.

4.2 Novel features of *Tg*CK and its therapeutic exploitation

The use of anti-parasite choline analogs is an effective approach to block growth of a variety of parasites including *T. gondii* (38,60,61). Quite notably, the K_m of full-length choline kinase encoded by *Tg*CK (0.77 mM) for choline is many-fold higher than parasite (*Pf*CK, 0.14 mM, (60); *Tb*CK, 0.032 mM, (61)) and non-parasite (*Hs*CKα1, 0.2 mM, (62); *Sc*CK, 0.27 mM, (63)) peers. In addition, *Tg*CK protein harbors a novel hydrophobic sequence at the N-terminus that is nonessential for catalysis but appears to be required for its clustering in the cytosol. The deletion of the N-terminal peptide presumably changes the conformation of *Tg*CK and increases the protein affinity by 3-fold (0.26 mM), which is in range of other choline kinases. Formation of choline kinase oligomers has been reported in *S. cerevisiae* (63). Moreover, the three isoforms of mouse choline kinase (α1, α2, β) can form *in vitro* homo-/hetero-oligomers, which have been attributed to enzyme regulation (64). The closely related parasite *P. falciparum* with a monomeric cytosolic choline kinase, however, appears to represent an exception (65). Whether the clustered form of *Tg*CK in the cytosol is more efficient in phosphorylating choline, or if the enzyme clusters can compensates for low affinity by sequestered catalysis of substrate should be investigated. Irrespective of the mechanism, disruption of PtdCho synthesis by competitive inhibition of CDP-choline

pathway is an effective strategy to disrupt the membrane biogenesis and replication of *T. gondii*.

4.3 Plasticity of PtdCho biogenesis in *T. gondii*

The ability to tolerate a perturbation of the PtdCho biogenesis varies between organisms. The mutation of CCT and reduction in PtdCho content has been reported to be lethal in CHO cells. A temperature-sensitive mutant of CHO cells could only be rescued by exogenous PtdCho. Interestingly, PtdEtn methyltransferase cannot circumvent the disruption of the CDP-choline pathway in CHO cells (66,67). Conversely, PtdCho and N-methylated lipids in *S. cerevisiae* are considered as non-essential on non-fermentable carbon sources (68). The results presented here suggest that the PtdCho biogenesis in *T. gondii* likely occurs *via* the CDP-choline route. Similar to yeast, however, the decline in PtdCho is tolerated by *Toxoplasma* without affecting its replication and viability.

Toxoplasma appears to harbor different mechanisms to circumvent or compensate for the loss of individual enzyme activities to ensure biogenesis of PtdCho. Interestingly, displacement of the *Tg*CK promoter by a conditional promoter coincides with the detection of a 53-kDa non-regulatable protein in/on mitochondrion or endoplasmic reticulum of the $\Delta tgck_i$ mutant. Assuming that there is no other choline kinase expressed in tachyzoites, our data would suggest a shorter isoform of full-length *Tg*CK being responsible for the residual activity in the $\Delta tgck_i$ mutant. Our qPCR data imply the presence of a promoter within the exon1, which produces a shorter and non-regulatable transcript. There are two in-frame start codons (amino acid position 165 and 244), which may lead to the synthesis of of 53-kDa and 45-kDa proteins, respectively (Appendix 6). The detection of the shorter isoforms in the parental strain may have been hampered by the higher abundance of the full-length *Tg*CK (~70-kDa). Affinity purification of the *Tg*CK antibody from the here-reported antiserum might increase the specificity and may allow the detection of the isoform(s) with lower abundance. The short isoform(s) arising from the second promoter and/or alternative start codon contain the predicted choline kinase and Brenner's motifs, and therefore should encode funtional enzymes. Testing this notion would require expression of a reporter protein (e.g. GFP) under the control of the first exon and expression cloning of shorter variants of *Tg*CK.

The conditional mutagenesis of putative *Tg*CCT caused a slower replication, which resulted in formation of 50% smaller plaques as compared to the parental strain. The enzymatic activity of *Tg*CCT towards phosphocholine, however, remains to be proven that is necessary to

correlate the observed growth defect to a disruption of PtdCho synthesis in the mutant. The assumption that *Tg*CCT is involved in PtdCho synthesis suggests yet another mechanism in *T. gondii* to compensate for its depletion as discussed below. The *Toxoplasma* genome also encodes for a putative ECT (TGGT1_008370). Whether *T. gondii* ECT and CCT have overlapping activity could not be extablished during this work. Moreover, transcriptomic studies have shown an upregulation of human CCT in parasitized cells (69), which may provide CDP-choline for PtdCho biogenesis in *T. gondii*.

Finally, sphingomyelin can be degraded by sphingomyelinases to yield phosphocholine. The presence of a putative sphingomyelinase (TGGT1_081220) in *Toxoplasma* provides a second source of phosphocholine in *T. gondii*, which could dispense the function of *Tg*CK (Fig. 31). These pathways together can provide an unexpected flexibility of PtdCho biogenesis to the parasite, which may contribute to the survival of *T. gondii* as a promiscuous pathogen.

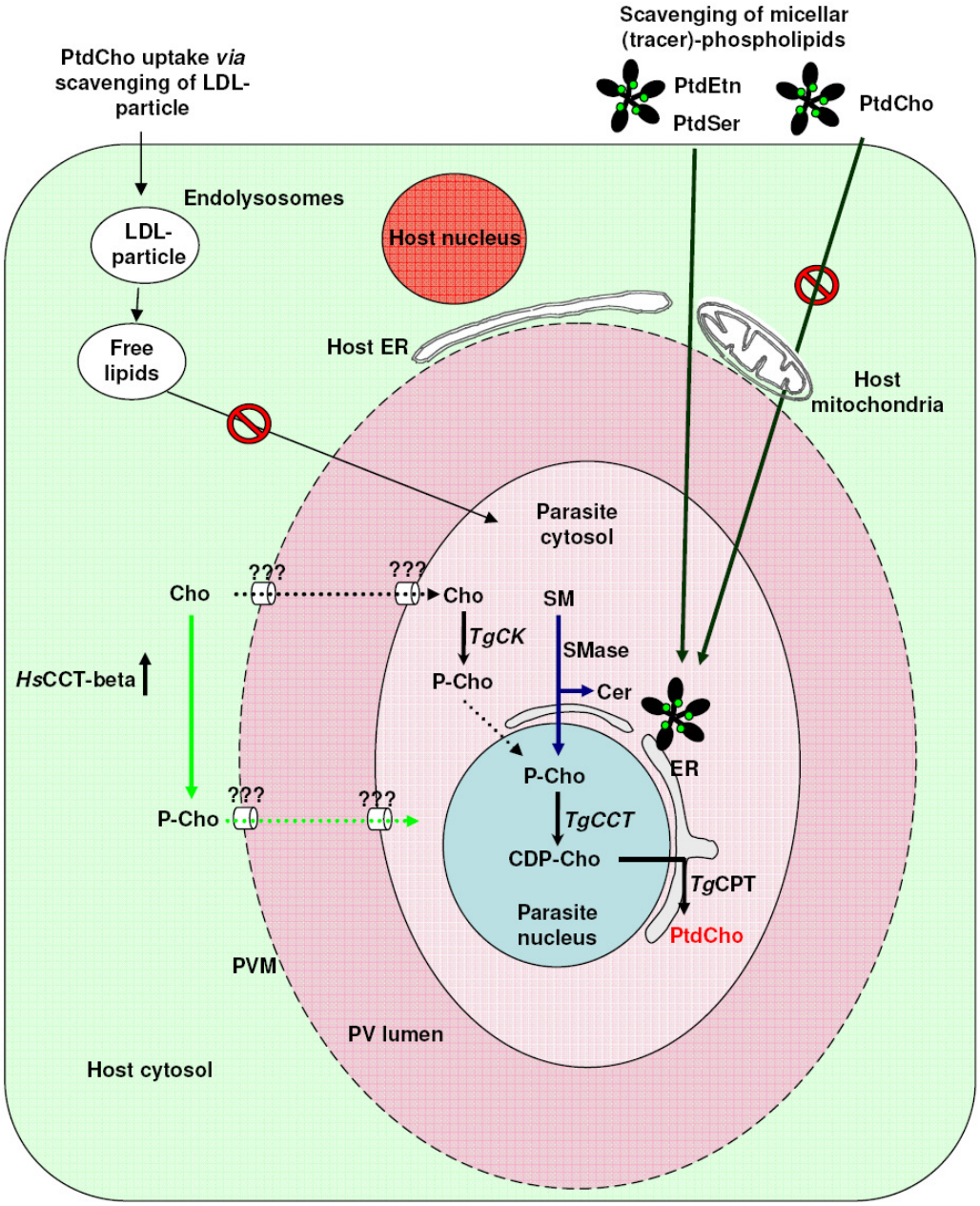

Fig. 31: **Current model of the PtdCho biogenesis in *T. gondii*.** The scavenging of NBD-PtdCho (micellar or LDL-conjugated) likely does not contribute to the PtdCho biogenesis in *T. gondii*, whereas NBD-PtdEtn and NBD-PtdSer are salvaged, which may involve lipid transfer from the host ER and mitochondria juxtaposed to the PVM. The parasite appears to be a choline auxotroph, utilizing choline into PtdCho *via* the *de novo* CDP-choline pathway. Activity of *Tg*CK can potentially be made dispensable by a sphingomyelinase (SMase), which cleaves sphingomyelin (SM) into ceramide (Cer) and phosphocholine (P-Cho). Host CCT (*Hs*CCT) is upregulated in parasitized HFFs and might provide CDP-choline to the replicating parasite. *Tg*CK, *Tg*CCT and *Tg*CPT localize in the parasite cytosol, nucleus and ER, respectively. Therefore, synthesis of PtdCho in the ER would require trafficking of its intermediates (P-Cho, CDP-Cho) from the cytosol to nucleus and ER. LDL, low-densitiy lipoprotein; PV, parasitophorous vacuole; PVM, PV membrane

4.4 Potential redundancy of PtdEtn biogenesis and enzyme activities in *T. gondii*

The ability of *Toxoplasma* to utilize ethanolamine into PtdEtn suggests the presence of a functional CDP-ethanolamine pathway, which should involve the activity of *Tg*EK, *Tg*ECT and *Tg*EPT enzymes (38). Although not proven in this work, the CDP-ethanolamine pathway appears to be a major route of PtdEtn synthesis in *Toxoplasma*. PtdEtn can also be derived *via* decarboxylation of PtdSer by a PtdSer decarboxylase (PSD). Similar to *Saccharomyces cerevisiae*, the *Toxoplasma* genome harbors predictions for two types of PSDs (TGGT1_108460, TGGT1_080780). Whereas the yeast PSD1 and PSD2 localize in the mitochondria and Golgi membrane, respectively, and produce compartment-specific lipid pools (70), more experiments are required to characterize the *Tg*PSD proteins in detail. *Plasmodium* and *Trypanosoma* species possess a dual-specificity choline kinase and a substrate-specific ethanolamine kinase (60,61), whereas in *S. cerevisiae* both enzymes have interchangeable function (71,63). In this respect, the *Tg*CK is akin to its parasite peers. It is possible that *Tg*CK can compensate for the loss of *Tg*EK activity, and thereby support PtdEtn synthesis in the parasite. *T. gondii*, therefore, harbors a variety of potentially redundant pathways to synthesize and/or salvage its second most abundant phospholipid, PtdEtn.

Interchangeable activities have also been reported for CPT and EPT. Human, *S. cerevisiae* and *Plasmodium* are known to harbor choline- and/or ethanolamine-phosphotransferases, which are capable of utilizing CDP-choline and/or CDP-ethanolamine as the phosphobase donors (72,73,74). The substrate specificity is probably regulated by the availability of certain co-factors, such as Mg^{2+} or Mn^{2+}. In addition, *S. cerevisiae* also possess a CPT protein restricted to CDP-choline (71). It remains to be seen wether *Tg*CPT and *Tg*EPT have redundant catalytic activity. To this end, we attempted the functional expression of *Tg*CK, *Tg*CCT, *Tg*CPT (and *Tg*EPT) in various expression models, namely *E. coli* and *S. cerevisiae* mutants to assess their specific enzymatic activities. Our attempts to express the C-terminally 6xHis-tagged isoforms in *E. coli* were not fruitful. No protein expression was detectable in the coomassie-stained gel or by western blot upon induction with IPTG (Appendix 5A). We also performed the heterologous expression in *S. cerevisiae* mutants, which were also not successful in confirming the enzyme activity (Appendix 5B).

All proteins were also over-expressed as their C-terminally V5-tagged isoforms under the *pCMV* promoter in COS-7 cells. The transgenic expression confirmed the aforementioned localization of *Tg*CK, *Tg*CCT and *Tg*CPT/*Tg*EPT to the cytosol, nucleus and ER, respectively

(Fig. 32). None of the transgenic extracts expressing *Tg*CCT, *Tg*CPT/EPT yielded CDP-choline formation with radioactive phosphocholine in the CCT assay (Appendix 5C). Due to the unavailability of the head-group (choline) labeled CDP-choline, we were unable to assess *Tg*CPT/*Tg*EPT activity. Finally, we over-expressed the C-terminally HA-tagged *Tg*CCT (*Tg*CCT-HA) under the *pNTP3* promoter in *T. gondii* and tested the parasite extract for CCT activity. Yet again, no activity was observed in the transgenic or control samples (Appendix 5D).

Taken together, the functional expression of the *Tg*CCT/*Tg*ECT and *Tg*CPT/*Tg*EPT remains unsolved and requires future assay optimization.

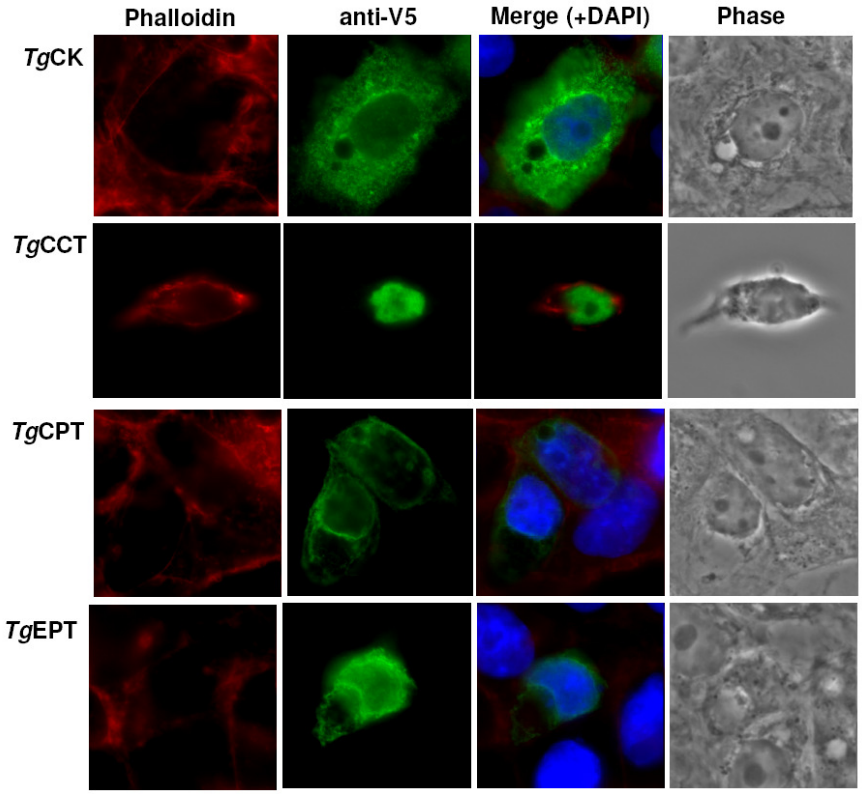

Fig. 32: **Heterologous expression of *Tg*CK, *Tg*CCT, *Tg*CPT (and *Tg*EPT, Accession number TGGT1_008370) in COS-7 cells.** The cDNAs of *Tg*CK, *Tg*CCT, *Tg*CPT and *Tg*EPT with the C-terminal V5-epitope were cloned at *XbaI*/*HindIII* sites into plasmid *pcDNA3.1*$^{+}$ under the control of the *pCMV* promoter. The *BglII*-linearized constructs were transfected into COS-7 cells using the lipofectamine method (section 2.4.9). IFA was performed 24 hrs post-infection using the rabbit anti-V5 antibody (green, 1:1000; co-stained with Phalloidin-Alexa595 (1:40) labeling the cellular F-Actin, red, and with DAPI, shown in blue).

4.5 Contribution of lipid scavenging to membrane biogenesis in *T. gondii*

The axenic parasite can synthesize sufficient amount of PtdEtn required for one cell doubling, whereas the rates of PtdSer and PtdCho synthesis are sufficient only for 50% and 9% of the parasite lipid requirement, respectively (38). This discrepancy between the demand and supply of PtdCho and PtdSer is possibly resolved by an increased rate of synthesis and/or scavenging of lipids by the intracellular tachyzoites. The PVM-recruitment of host endoplasmic reticulum and mitochondria offers potential sources of host cell lipids to the parasite. The majority of choline-containing lipids, such as PtdCho and sphingomyelin, reside in the exoplasmic membrane leaflet of eukaryotic membranes (34), therefore, the inward-directed movement and import of PtdCho is probably not favored. The CHO cells have been shown to bypass a suppression of their CDP-choline pathway by uptake of PtdCho or lyso-PtdCho from the media (66). *S. cerevisiae* can also internalize exogenous PtdCho and PtdEtn (75). Whereas PtdEtn is internalized solely *via* transbilayer transport, the translocation of PtdCho involves endocytosis, as opposed to the former mechanism (76,77). The parasite genome harbors predictions for P4-type ATPases, specific transport proteins involved in phospholipid translocation across membranes in yeast and mammalian cells (35). Whether *Toxoplasma* is capable of endocytosis, which may be necessary for the transport of lipids from the PVM lumen to the parasite interior, remains to be investigated (78). Our data (Marquardt S, unpublished data) using the tracer lipids in their micellar form exclude the prospect of PtdCho scavenging by *T. gondii*. Wheras PtdSer and PtdEtn were trafficked across the parasite membranes, PtdCho was largely excluded by the parasites (Fig. 31). The recruitment of low-density protein (LDL) by *T. gondii* can supply cholesterol to the parasite (79), which makes then use of the Host Organelle-Sequestering Tubulo-structures (H.O.S.T.). Being rich in PtdCho (80), LDL also offers a route to obtain this lipid. The labeling of intracellular parasites with NBD-conjugated lipids (PtdCho, PtdEtn or PtdSer) loaded onto human LDL-particles yielded only a weak NBD signal in the parasite membranes and/or vacuolar space with all three samples (Fig. 33), but no staining was apparent within the parasite body. These preliminary data indicate that LDL-derived phospholipids likely provide only a minor contribution to the parasite membranes.

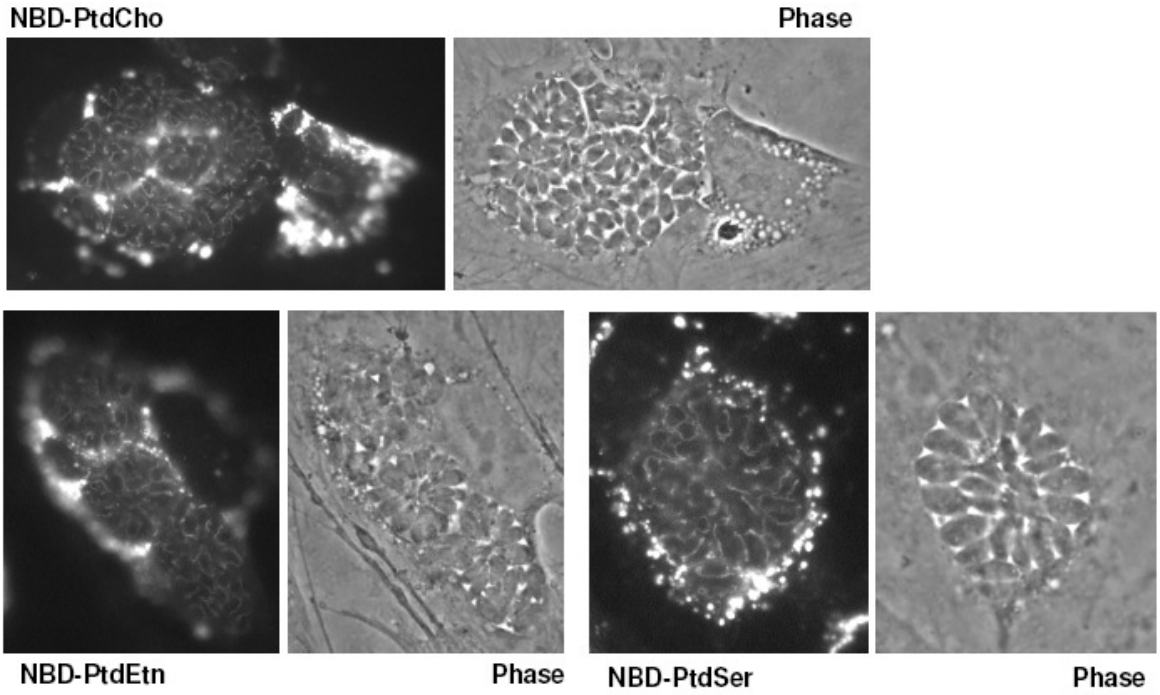

Fig. 33: **Scavenging of host LDL-derived phospholipids by intracellular *T. gondii* tachyzoites.** The C6-NBD-phospholipids were conjugated to human LDL-particles (37°C overnight) prior to LDL isolation by zonal density gradient ultracentrifugation. Confluent HFF monolayers grown on glass coverslips in the lipoprotein-deficient serum were infected (MOI = 3), and 28 hrs post infection NBD-loaded LDL particles (0.1 mg/ml) were added. Samples were fixed following 1 hr incubation at 37°C, and lipid trafficking was analyzed by fluorescence microscopy.

4.6 Outlook

This work suggests *T. gondii* as being a choline auxotroph, which utilizes choline into PtdCho *via* the *de novo* CDP-choline pathway (Fig. 31). The parasite shows an unexpected robustness to the genetic perturbation of the *Tg*CK and *Tg*CCT, which indicates alternative routes of PtdCho biogenesis in *T. gondii* as highlighted in Figure 33. The low affinity of choline kinase offers a potential target for therapeutic application and our plate-based spectrometric assay offers a cost-effective platform to screen for *Tg*CK inhibitors.

Future experiments should include the functional characterization of CDP-choline phosphotransferase (*Tg*CPT) and deletion of *Tg*CCT to confirm the essentiality of the CDP-choline pathway. The substrate specificities of *Tg*CCT/*Tg*ECT and *Tg*CPT/*Tg*EPT should also be assessed for and unambiguous interpretation of the observed phenotypes in the two mutants. Insertional tagging of the *Tg*CK gene with a destabilization domain offers an alternative technique to confirm the essential nature of choline kinase.

Transcriptomic studies can reveal potential pathways used by the parasite mutants to circumvent the mutagenesis of *Tg*CK and *Tg*CCT. The reported data on the contribution of host-derived lipids via rerouting of LDL-pathway require validation with internal control such as the LDL-NBD-cholesterol. Potential host candidates, which may provide the intermediates of PtdCho or the lipid itself, should also be investigated. This requires detailed studies genetic and biochemical studies on lipid transport from the host cell to the parasite.

Appendix 1

A

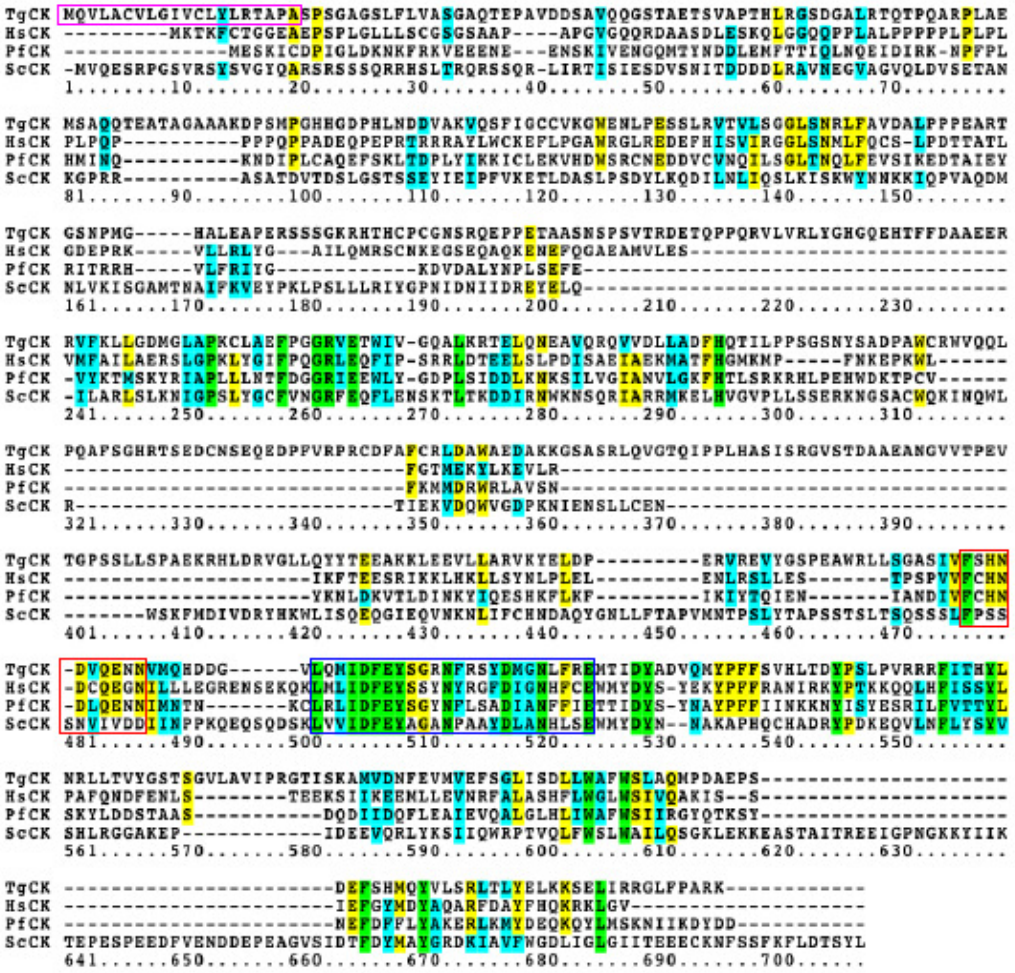

B

	*Tg*CK	*Sc*CK	*Pf*CK
*Hs*CK	19	14	23
*Pf*CK	16	12	
*Sc*CK	10		

Appendix 1: **The *Tg*CK cDNA encodes a choline kinase with 630 residues, which shows 19%, 16% and 10% identity with *Hs*CKα, *Pf*CK and *Sc*CK1, respectively.** The best homologies are found in the Brenner's (red box) and choline kinase (blue box) motives. *Tg*CK also harbors an N-terminal hydrophobic peptide (first 20 amino acids; magenta box) with no homology to a known protein in the NCBI database. The NCBI accession numbers are: *Hs*CKα, NP_001268.2; *Pf*CK, PF14_0020; *Sc*CK1, YLR133W.

Appendix 2

A

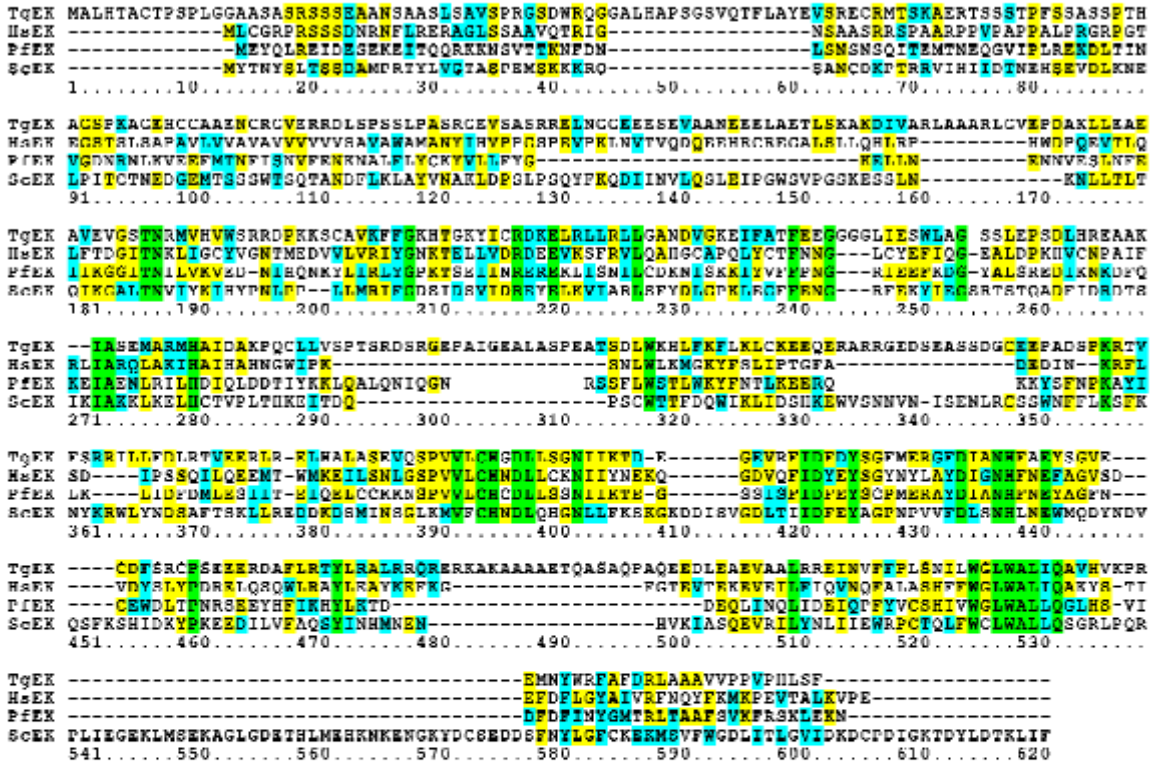

B

	*Tg*EK	*Sc*EK	*Pf*EK
*Hs*EK	21	16	23
*Pf*EK	20	15	
*Sc*EK	14		

Appendix 2: **The *Tg*EK cDNA encodes an ethanolamine kinase with 547 residues, which shows 21%, 20% and 14% identity with *Hs*EK1α, *Pf*EK and *Sc*EK1, respectively**. The NCBI accession numbers are: *Hs*EK1α, NP_061108.2; *Pf*EK, PF11_0257; *Sc*EK1, YDR147W.

Appendix 3

A

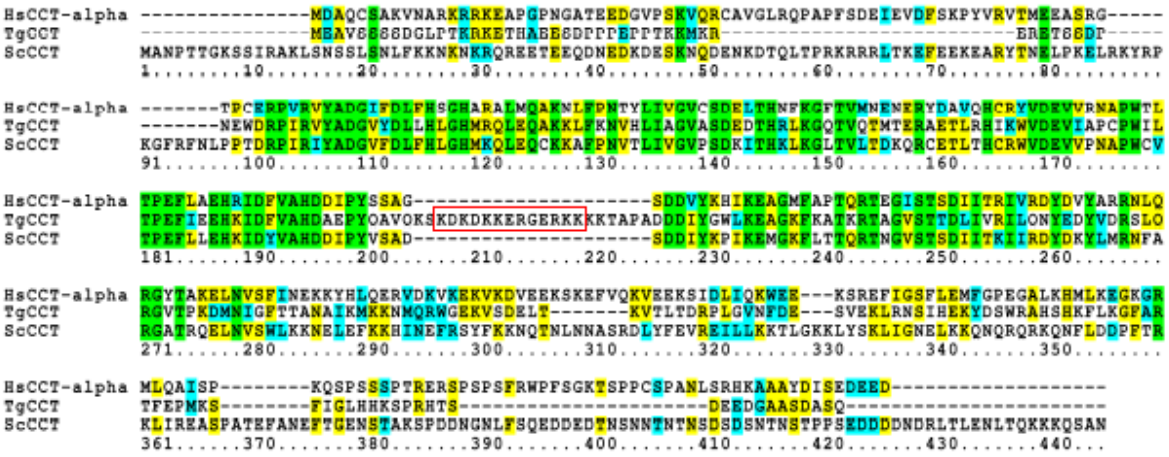

B

	*Tg*CCT	*Sc*CCT
*Hs*CCT-alpha	30	32
*Sc*CCT	26	

Appendix 3: **The *Tg*CCT cDNA encodes a protein of 329 amino acids with 30% and 26% homology to *Hs*CCT-alpha and *Sc*CCT, respectively.** *Tg*CCT possesses a putative nuclear localization signal (NLS) between the residues 154 and 166 (red box). Accession numbers: *Hs*CCT-alpha, NP_005008.2; *Sc*CCT, YGR202C.

Appendix 4

A

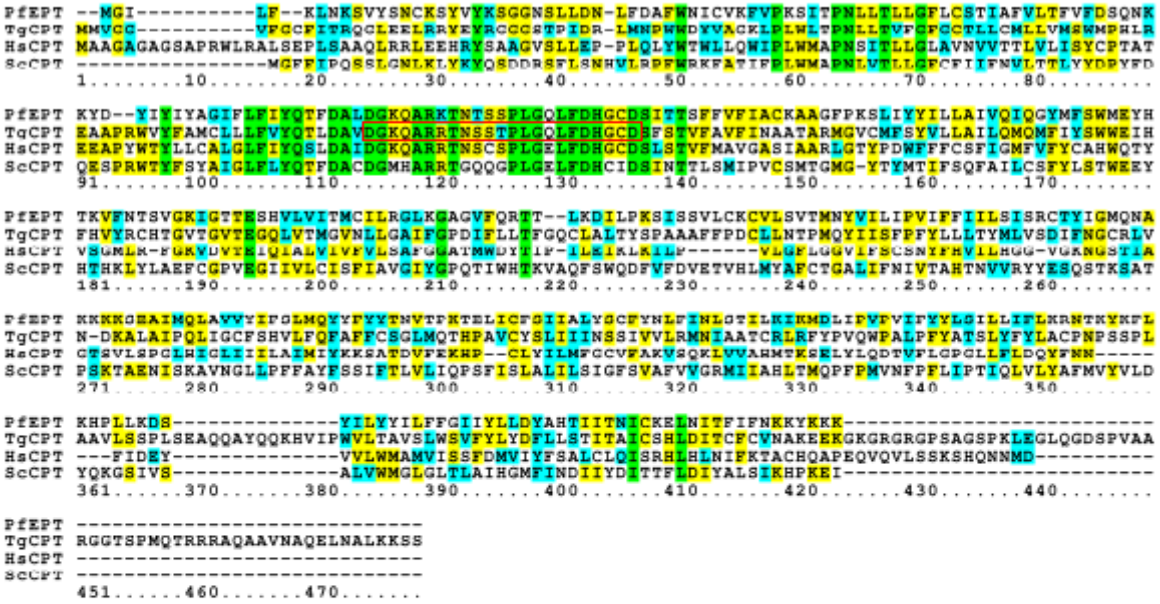

B

	*Tg*CPT	*ScCPT*	*PfEPT*
*Hs*CPT	20	19	21
*Pf*EPT	26	21	
*Sc*CPT	19		

Appendix 4: **The *Tg*CPT cDNA encodes a protein with 467 residues.** *Tg*CPT shows 20%, 26% and 19% homology to *Hs*CPT, *Pf*EPT and *Sc*CPT respectively. The catalytic domain $DG(X)_2AR(X)_8G(X)_3D(X)_3D$ is highlighted in the red box. Accession numbers: *Hs*CPT, NP_006081.1; *Pf*EPT, PFF1375c-b; *Sc*CPT, YNL130C.

Appendix 5

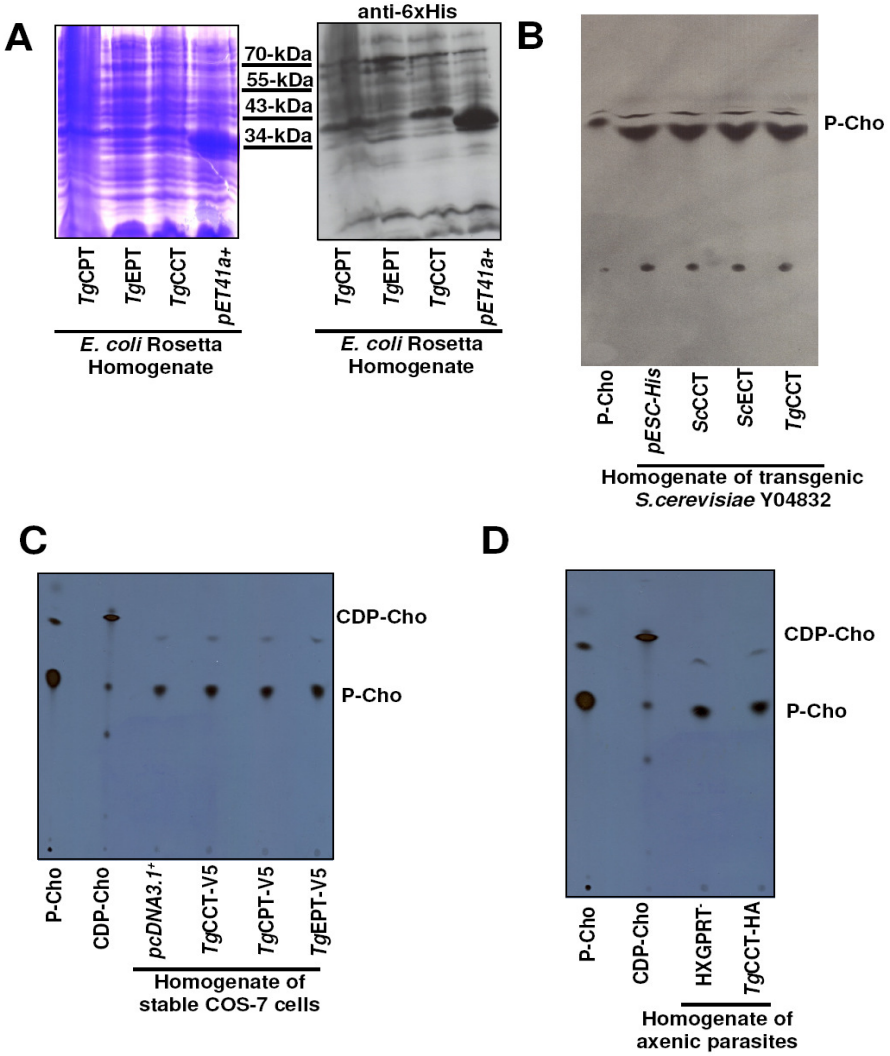

Appendix 5: **Expression of *Tg*CCT, *Tg*CPT and *Tg*EPT in transgenic models.** (A) The ORF of *Tg*CCT (38-kDa), *Tg*CPT (52-kDa) and *Tg*EPT (49-kDa) were cloned as their C-terminally 6xHis-tagged isoforms into plasmid *pET41b+* (*NdeI*/*NotI*). Expression in the *E. coli* Rosetta strain was induced with 1 mM IPTG overnight at 30°C. The total protein extract (10 µg) was separated on 12% SDS-PAGE and stained with coomassie blue or subjected to western blot using the anti-6xHis antibody (1:10000). The empty plasmid *pET41b+* served as the negative control. (B) The *Tg*CCT ORF was cloned in *pESC-His* (*NotI*/*NotI*) under the galactose-inducibe promoter *pGAL10* and expressed in *S. cerevisiae* mutants Y04832 (*Δcct1*) or Y04637 (*Δect1*). The *Sc*CCT and *Sc*ECT served as the positive controls. Yeast extract of transfected Y04832 and Y04637 was generated using 0.45 – 0.6 mm glass beads, and 100 µg of total extract was supplemented with 100 µl reaction buffer (final concentration 58 mM Tris (pH 7.5), 40 mM NaCl, 1.8 mM EDTA, 8.9 mM magnesium acetate), 3 mM CTP and 0.1 µCi [^{14}C]-phosphocholine (P-Cho). The assay was performed for 5 min at 30°C (*Sc*CCT, *Sc*ECT) or at 37°C (*Tg*CCT). The reaction was stopped by 2 min heating, and the formation of radiolabeled CDP-choline (CDP-Cho) was analyzed by TLC (95% EtOH/2%NH_4OH, 1:1). X-ray film was exposed overnight at -80°C. (C) The *Tg*CCT, *Tg*CPT and *Tg*EPT were expressed with the C-terminal V5-tag under the *pCMV* promoter in plasmid *pcDNA3.1*$^+$. All constructs and the empty plasmid were linearized with *BglII*, transfected into COS-7 cells using the lipofectamine method (section 2.4.9) and stable cells were achieved by selection with geneticin. 100 µg of total protein extract was prepared and tested for *Tg*CCT activity for 30 min at 37°C. (D) *Tg*CCT-HA was expressed under the *pNTP* promoter in *hxgprt*$^-$ parasites and stable parasites were obtained by selection with 1 µM pyrimethamine. 100µg of total parasite extract was assayed for *Tg*CCT activity for 30 min at 37°C as described in panel B.

Appendix 6

*Tg*CK Coding Sequence with Introns

ATGCAGGTACTCGCGTGTGTGCTGGGCATTGTCTGCCTCTATTTAAGGACCGCTCCTGCGTCCCCTTCAGGCGCTGGCTCTTTGTTTCTGGTGGCCAGTGGCGCGCAGACA
GAGCCAGCAGTGGACGACTCCGCTGTACAGCAAGGGTCGACCGCGGAAACCTCTGTCGCGCCGACGCATTTGCGTGGAAGTGATGGAGCTCTTCGCACACAAACGCCGCAG
GCGCGGCCGCTCGCTGAGATGTCTGCACAGCAGACGGAAGCCACAGCTGGCGCCGCGGCGAAGGATCCGAGTATGCCAGGGCACCATGGTGACCCGCATCTGAATGATGAC
GTTGCTAAAGTGCAGTCGTTTATCGGGTGCTGCGTAAAGGGCTGGGAAAACCTTCCGGAAAGCTCTCTGCGCGTCACCGTTCTCTCTGGCGGCCTCAGCAATCGCCTTTTT
GCGGTAGATGCCCTCCCACCGCCGGAGGCGCGCACTGGCAGCAACCCCATGGGCCATGCGCTTGAAGCGCCGGAACGAAGTTCGTCCGGGAAAAGGCACACGCATTGTCCG
TGTGGAAATTCGAGGCAAGAGCCGCCGGAGACCGCCGCCTCGAATTCACCCTCCGTAACGAGGGATGAAACCCAACCGCCGCAGCGAGTGCTCGTTCGGCTGTACGGTCAT
GGCCAAGAACATACTTTCTTTGATGCAGCTGAGGAACGTCGCGTGTTCAAACTTTAGGGGATATGGCCTTGCCCCGAAATGTCTCGCTGAGTTTCCAgtgagtggatag
cgcgaaaacgcttctgcgtactacattttgccgattctaggttgtattcgaatacagaagccggtactgagggctgtgtaactcacttccgcaaggcgaaacataactggc
cggtggagggttgtagccttcaagtctgacaaaaaaaggattgcagtggagtgcggttatccctcgtattgcctctgatcggaaacagcgtaggctttcactatgatcact
gccatctgactgggggatgacggtctctggaacagcaggatttatacgcttttctacggagagtgtagactacctgatggagtacccgttcagatctcggatgtcagcgtat
ccctccaccgcccccctacctgatccgagtcaggtgccttccatatgtaacggaaacacactcattcttgtcgtacgatggacctgcctgtacccgtctctcagtccgt
gtctgcttgtttcttctgacggggagtctccggcctgaaccatgagctttcaacgaattctgtgttaacagGGTGGCCGAGTCGAGACCTGGATCGTAGGACAAGCTCTGA
AGCGGACGGAATTGCAGAACGAGGCGGTGCAGAGACAGGTTGTTGATCTTgtaagatttccttttcaacttgaacgcttcccgacctaccggcatcttccacatctcaggac
tagtgttagtgagggatgctgccgagttcggatttgtgtgtcagctggttgcccgcaattgctcgtggtttggcgtcttaggcgctgctttgactctcgtggatgcacgac
agaggactacttacaagtatgtttctggggaatgtggtgccggcgcagctcgttgctgcagcgtcgtcttctttatctgctgtgtccttgtttttctcagCTCGCGGACTTC
CACCAAACCATTCTGCCTCCGTCGGGAAGTAACTACTCGGCCGACCCAGCTTGGTGCCGGTGGGTGCAGCAATTGCCACAGGCGTTTAGTGGGCATCGAACCAGCGAGGAC
TGCAACTCCGAGCAGGAAGACCCCTTCGTCCGCCCGCGTTGCGACTTTGCGTTCTGTCGCCTTGATGCATGGGCCGAAGATGCGAAGAAAGGTTCTGCGTCGCGGCTCCAA
GTCGGCACTCAGATTCCTCCTTTGCATGCATCCATTTCTCGAGGAGTTTCGACCGACGCCGCTGAGGCGAACGGTGTTGTCACACCTGAGGTAACGGGTCCTTCCTCGCTG
TTGTCTCCCGCGGAGAAGCGTCATCTCGATCGTGTCGGCCTGCTTCAGTATTACACCGAGGAAGCGAAGAAGCTCGAGGAGgtacgccagggaatgcttgtgatggggttc
ggcgaaacagtttcgcatccccgtatggagttcctgatcggtgatttataggtcgtctttccggtgtttctgagacgacagtgtcccctgaacggctaacagtggtgcata
gggtgccacgacgcgctttggtttcgagttccttgactcgggcagtagcaacaacggagagaaatgatggggaggaacgagtatggctcatgagctgcgaggcatccgtta
cccgtttgctgtatctgcctcatgtattagaaatcgcgatcgagttgagttctttcaaactcccgaatccctctcgccacccgcgttctgtggtgcgccaggacttggcat
ggtggccttctcttggttgcttgcaactgggtgacggctgagaatcttcattccgcaactgtccgcaggatctctggtatccgcgtccccacactatgtcattgtgttttt
gtgcgtttctcatagGTATTGCTCGCACGGGTGAAGTACGAACTTGACCCAGAGAGAGTGAGGGAAGTCTACGGAAGTCCTGAGGCGTGGCGACTGCTGTCTGGTGCGTCG
ATTGTGTTCTCTCACAACGACGTACAGGAGAACAATGTGATGCAGgtaggcaagaggtcctgcgaaggacgctcgcggcgctcgctgctctcggcacaggcccagaagaac
gtgatcttgtcgtcgcttaaacaggcaaagcgaaaacgagtatagaacaggcgaagtcgcgtcatgagtactcagtgaacgtcaatgttcgatttgaagtttatgggaatt
ttaagattgttgacccgatcgaggtccacccacatgcaagaacatgcagacgacactttcacggtggatacaacatcagatgtcgcgtagggcatgcagaatgatactcca
agtatccccagacgttatgaggagcagcctcggcctcgatgtcacctgtgatggtcggagggtcgctcgaggtgctacagcggtggcaagcaagataaactgtagcgtgt
acaatctgtccgtcgagaagatttcgattttgatggttctgccgcgaatgtgtcttgacgcagCACGATGACGGCGTTCTGCAGATGATCGATTTCGAGTACTCGGGCAGA
AATTTCCGAAGCTATGACATGGGCAACTTATTTCGGGAGATGACGATTGACTATGCAGACGTTCAAAgtaagggcaaagctgctggtcacgaagccggtgcggaggtcttg
aggttttccctgagatgggcctgtgacatgcagtctccgttctctgggtatagaggctgtgtggcagggtattgtgaattacggatcattgttatggatatttcatgacac
gcaaagaaagcaccgccagccgaccggttttggatggcattggttttgactccgcgtaatatgctggagaacgtttatcagaaattcgagctttggatgcccagatgatgt
ctattcgtctgtaggtcattcaagggtagagaccagaggggtggcgagtgaaaacaggtggtgcggaaccggcgacccagttcgtgctacggtttctgctgtcgtatcat
aaagaaactcctacagtgtagtcgtctgtttcctgtaacgcatacgttacgcataacaatgcgatctgtccgcagTGTACCCTTTCTTCTCCGTCCACTTGACCGACTACC
CCTCGCTGCCGGTTCGACGACGCTTCATCACGCACTATTTGAATCGCCTGCTCACAGTCTACGGTTCCACGTCCGGTGTCTTGGCAGTTATTCCGCGGGGAACCATTTCCA
AGGCTATGGTGGACAACTTTGAAGTTATGgtaagcctttgaatgtgcggtcatgcctgcgtctggctcctccagaggggcgggggtcaagttgtacggtggcaaggc
gcgcgtttcatggggatggttcagggagagccggaggcggcattctagagtcggtgggtgtcgaggacggtcaattggacggtgattctgagccgttttccgagtaacct
gttctgcacttgcttggactctgtcaacagGTGGAGTTCAGCGGCCTGATTTCCGATCTTCTGTGGGCCTTCTGGTCTCTTGCTCAgtgagtttcttcgtcacacgctcgca
tcaggttcacaaatcctatggaaacgatatgcatctgaaacaccggcagttcgggcgcttgccgaatgaccgcgtgtatctgtgtctgtctatttctgatccattacatct
ctatctctcaaaatcaatctagagctgattacggcgcgtggtgtgcgcgttgagacacttggtggattgctcgcaggggtactttgtgagcatgacgttatttgtagatct
tgtaggcaaatgtaggatctccaaataaacgcctaataccgttcgcttcctaatgcacttcctgccatcatgagagaggcaaaatatagggcgattcgtgacgtcttaaccc
aagacaccggacattctgagccgttctcaagagagcatgcggttccacgcgacacggagccaatgttgatcaatgggattcttctttttgcggaatttctacgggatttca
aatgcggttcgtgtgtgtgcagGATGCCAGATGCCGAACCATCGGACGAGTTCTCCCACATGCAGTACGTTTTGTCCCGgtaagtgttttcgctccacctttaggttttgt
gaggtggcagttattgccgaaggggttttacaccccgtggtgctttcgaaacctccggctatgtgcccgctattttggtaggatgtttgcttggtgcagatggcgcagaaa
atacctctctctttgtatatctgtacatttctctcttttttatttctgtattcagttttatttgtacgtctgcgtgtatacctctgttcagctatgcctgtcttcaccaata
tatacatatacatatatatgtgtatgtctgtataatattcgtgccagcattcgggggtttctgtgtgaggagtgtcacagccacagtatcgagatgagtgagggacagcga
ggtcgcatgcaggtggagtcacgcgccttgagctgagggctgtacatatttgcgtgtgactggggcaccgccatgaagggagacctggccagcgccacagttcgaccctgt
aaaacgctccgcaggtatctgtacttaactcggataacacagtggaacttggattcaatgaagatctcagtttgtagtcgagagcgtgtactctcgtggtttgtccgtgct
gtgtgtgtgtgaatgtcggcagACTGACCCTCTATGAGCTTAAGAAAAGCGAGCTTATTCGGCGTGGACTCTTCCCGGCTCGAAAGTGA

*Tg*CK-Ex1-F1/R1 Primers for qPCR

*Tg*CK-Ex1-F2/R2 Primers for qPCR

*Tg*CK-Ex6-F1/R1 Primers for qPCR

Protein synthesis with alternative start codons

MGHALEAPERSSSGKRHTHCPCGNSRQEPPETAASNSPSVTRDETQPPQRVLVRLYGHGQEHTFFDAAEERRVFKLLGDMGLAPKCLAEFPGGRVET
WIVGQALKRTELQNEAVQRQVVDLLADFHQTILPPSGSNYSADPAWCRWVQQLPQAFSGHRTSEDCNSEQEDPFVRPRCDFAFCRLDAWAEDAKKGS
ASRLQVGTQIPPLHASISRGVSTDAAEANGVVTPEVTGPSSLLSPAEKRHLDRVGLLQYYTEEAKKLEEVLLARVKYELDPERVREVYGSPEAWRLL
SGASIVFSHNDVQENNVMQHDDGVLQMIDFEYSGRNFRSYDMGNLFREMTIDYADVQMYPFFSVHLTDYPSLPVRRRFITHYLNRLLTVYGSTSGVL
AVIPRGTISKAMVDNFEVMVEFSGLISDLLWAFWSLAQMPDAEPSDEFSHMQYVLSRLTLYELKKSELIRRGLFPARK

Appendix 6: **Sequence of the gDNA depicting *Tg*CK cDNA.** *Tg*CK-Ex1-F2/R2 primers (grey) bind in the first half of exon1; *Tg*CK-Ex1-F1/R1 primers (brown) anneal in the second half of exon1; *Tg*CK-Ex6-F1/R1 primers (green) anneal in exon6. These primer pairs were used to amplify the corresponding ETSs by qPCR on the *Δtgck*$_i$ mutant and parental strain. The start codon coding for the full-length *Tg*CK (70-kDa), and the possible shorter isoforms (53-kDa and 45-kDa) are depicted in yellow and turquoise.

REFERENCES

[1] Black MW, Boothroyd JC (2000): Lytic cycle of Toxoplasma gondii, Microbiol Mol Biol Rev (vol. 64), pp. 607-23.

[2] Tenter AM, Heckeroth AR, Weiss LM (2000): Toxoplasma gondii: from animals to humans., Int J Parasitol (vol. 30), pp. 1217-58.

[3] Jones JL, Kruszon-Moran D, Wilson M, McQuillan G, Navin T, McAuley JB (2001): Toxoplasma gondii infection in the United States: seroprevalence and risk factors, Am J Epidemiol (vol. 154), pp. 357-65.

[4] Blackman MJ, Bannister LH (2001): Apical organelles of Apicomplexa: biology and isolation by subcellular fractionation, Mol Biochem Parasitol (vol. 28), pp. 11-25.

[5] Mogi T, Kita K (2010): Diversity in mitochondrial metabolic pathways in parasitic protists Plasmodium and Cryptosporidium, Parasitol Int (vol. 59), pp. 305-12.

[6] Mann T, Beckers C (2001): Characterization of the subpellicular network, a filamentous membrane skeletal component in the parasite Toxoplasma gondii, Mol Biochem Parasitol (vol. 115), pp. 257-68.

[7] Morrissette NS, Sibley LD (2002): Cytoskeleton of apicomplexan parasites, Microbiol Mol Biol Rev (vol. 66), pp. 21-38.

[8] Wilson RJ, Williamson DH (1997): Extrachromosomal DNA in the Apicomplexa, Microbiol Mol Biol Rev (vol. 61), pp. 1-16.

[9] Nishi M, Hu K, Murray JM, Roos DS (2008): Organellar dynamics during the cell cycle of Toxoplasma gondii, J Cell Sci (vol. 121), pp. 1559-68.

[10] Hu K, Mann T, Striepen B, Beckers CJ, Roos DS, Murray JM (2002): Daughter cell assembly in the protozoan parasite Toxoplasma gondii, Mol Biol Cell (vol. 13), pp. 593-606.

[11] Pelletier L, Stern CA, Pypaert M, Sheff D, Ngô HM, Roper N, He CY, Hu K, Toomre and D, Coppens I, Roos DS, Joiner KA, Warren G (2002): Golgi biogenesis in Toxoplasma gondii, Nature (vol. 418), pp. 548-52.

[12] Striepen B, Crawford MJ, Shaw MK, Tilney LG, Seeber F, Roos DS (2000): The plastid of Toxoplasma gondii is divided by association with the centrosomes, J Cell Biol (vol. 151), pp. 1423-34.

[13] Soldati D, Boothroyd JC (1993): Transient transfection and expression in the obligate intracellular parasite Toxoplasma gondii, Science (vol. 260), pp. 349-52.

[14] Kim K, Weiss LM (2004): Toxoplasma gondii: the model apicomplexan, Int J Parasitol (vol. 34), pp. 423-32.

[15] Kim K, Soldati D, Boothroyd JC (1993): Gene replacement in Toxoplasma gondii with chloramphenicol acetyltransferase as selectable marker, Science. (vol. 262), pp. 911-4.

[16] Donald RG, Roos DS (1993): Stable molecular transformation of Toxoplasma gondii: a selectable dihydrofolate reductase-thymidylate synthase marker based on drug-resistance mutations in malaria, Proc Natl Acad Sci U S A (vol. 90), pp. 11703-7.

[17] Donald RG, Carter D, Ullman B, Roos DS (1996): Insertional tagging, cloning, and expression of the Toxoplasma gondii hypoxanthine-xanthine-guanine phosphoribosyltransferase gene. Use as a selectable marker for stable transformation, J Biol Chem (vol. 271), pp. 14010-9.

[18] Pfefferkorn ER, Pfefferkorn LC (1977): Toxoplasma gondii: characterization of a mutant resistant to 5-fluorodeoxyuridine, Exp Parasitol (vol. 42), pp. 44-55.

[19] Meissner M, Brecht S, Bujard H, Soldati D (2001): Modulation of myosin A expression by a newly established tetracycline repressor-based inducible system in Toxoplasma gondii, Nucleic Acids Res (vol. 29), p. E115.

[20] Meissner M, Schlüter D, Soldati D (2002): Role of Toxoplasma gondii myosin A in powering parasite gliding and host cell invasion, Science (vol. 298), pp. 837-40.

[21] B, Striepen (2007): Switching parasite proteins on and off, Nat Methods (vol. 4), pp. 999-1000.

[22] Banaszynski LA, Chen LC, Maynard-Smith LA, Ooi AG, Wandless TJ (2006): A rapid, reversible, and tunable method to regulate protein function in living cells using synthetic small molecules, Cell (vol. 126), pp. 995-1004.

[23] Huynh MH, Carruthers VB (2009): Tagging of endogenous genes in a Toxoplasma gondii strain lacking Ku80, Eukaryot Cell (vol. 8), pp. 530-9.

[24] Fox BA, Ristuccia JG, Gigley JP, Bzik DJ (2009): Efficient gene replacements in Toxoplasma gondii strains deficient for nonhomologous end joining, Eukaryot Cell (vol. 8), pp. 520-9.

[25] Critchlow SE, Jackson SP (1998): DNA end-joining: from yeast to man, Trends Biochem Sci (vol. 23), pp. 394-8.

[26] Fox BA, Falla A, Rommereim LM, Tomita T, Gigley JP, Mercier C, Cesbron-Delauw MF, and Weiss LM, Bzik DJ (2011): Type II Toxoplasma gondii KU80 Knockout Strains Enable Functional Analysis of Genes Required for Cyst Development and Latent Infection, Eukaryot Cell (vol. 10), pp. 1193-206.

[27] Vance JE, Vance DE (2004): Phospholipid biosynthesis in mammalian cells, Biochem Cell Biol (vol. 82), pp. 113-28.

[28] Li Z, Vance DE (2008): Phosphatidylcholine and choline homeostasis, J Lipid Res (vol. 49), pp. 1187-94.

[29] Ott DB, Lachance PA (1981): Biochemical controls of liver cholesterol biosynthesis, Am J Clin Nutr (vol. 34), pp. 2295-306.

[30] Maxfield FR, van Meer G (2010): Cholesterol, the central lipid of mammalian cells, Curr Opin Cell Biol (vol. 22), pp. 422-9.

[31] WA, Prinz (2010): Lipid trafficking sans vesicles: where, why, how?, Cell (vol. 143), pp. 870-4.

[32] DR, Voelker (2009): Genetic and biochemical analysis of non-vesicular lipid traffic, Annu Rev Biochem (vol. 78), pp. 827-56.

[33] Gaigg B, Simbeni R, Hrastnik C, Paltauf F, Daum G. (1995): Characterization of a microsomal subfraction associated with mitochondria of the yeast, Saccharomyces cerevisiae. Involvement in synthesis and import of phospholipids into mitochondria., Biochim Biophys Acta. (vol. 1234), pp. 214-20.

[34] A, Zachowski (1993): Phospholipids in animal eukaryotic membranes: transverse asymmetry and movement, Biochem J (vol. 294), pp. 1-14.

[35] Pomorski T, Menon AK (2006): Lipid flippases and their biological functions, Cell Mol Life Sci (vol. 63), pp. 2908-21.

[36] Maréchal E, Azzouz N, de Macedo CS, Block MA, Feagin JE, Schwarz RT, Joyard J (2002): Synthesis of chloroplast galactolipids in apicomplexan parasites, Eukaryot Cell (vol. 1), pp. 653-6.

[37] Welti R, Mui E, Sparks A, Wernimont S, Isaac G, Kirisits M, Roth M, Roberts CW, Botté C, Maréchal E, McLeod R (2007): Lipidomic analysis of Toxoplasma gondii reveals unusual polar lipids, Biochemistry (vol. 46), pp. 13882-90.

[38] Gupta N, Zahn MM, Coppens I, Joiner KA, Voelker DR (2005): Selective disruption of phosphatidylcholine metabolism of the intracellular parasite Toxoplasma gondii arrests its growth, J Biol Chem (vol. 280), pp. 16345-16353.

[39] Charron AJ, Sibley LD (2002): Host cells: mobilizable lipid resources for the intracellular parasite Toxoplasma gondii, J Cell Sci (vol. 115), pp. 3049-59.

[40] Witola WH, El Bissati K, Pessi G, Xie C, Roepe PD, Mamoun CB (2008): Disruption of the Plasmodium falciparum PfPMT gene results in a complete loss of phosphatidylcholine biosynthesis via the serine-decarboxylase-phosphoethanolamine-methyltransferase pathway and severe growth and survival defects, J Biol Chem (vol. 283), pp. 27636-43.

[41] Labruyere E, Lingnau M, Mercier C, Sibley LD (1999): Differential membrane targeting of the secretory proteins GRA4 and GRA6 within the parasitophorous vacuole formed by Toxoplasma gondii, Mol Biochem Parasitol (vol. 102), pp. 311-24.

[42] Sibley LD, Niesman IR, Parmley SF, Cesbron-Delauw MF (1995): Regulated secretion of multi-lamellar vesicles leads to formation of a tubulo-vesicular network in host-cell vacuoles occupied by Toxoplasma gondii, J Cell Sci (vol. 108), pp. 1669-77.

[43] Caffaro CE, Boothroyd JC (2011): Evidence for host cells as the major contributor of lipids in the intravacuolar network of toxoplasma-infected cells, Eukaryot Cell (vol. 10), pp. 1095-9.

[44] Schwab JC, Beckers CJ, Joiner KA (1994): The parasitophorous vacuole membrane surrounding intracellular Toxoplasma gondii functions as a molecular sieve, Proc Natl Acad Sci U S A (vol. 91), pp. 509-13.

[45] Sinai AP, Webster P, Joiner KA (1997): Association of host cell endoplasmic reticulum and mitochondria with the Toxoplasma gondii parasitophorous vacuole membrane: a high affinity interaction, J Cell Sci (vol. 110), pp. 2117-28.

[46] Plattner, F., Yarovinsky, F., Romero, S., Didry, D., Carlier, M.F., Sher, A., Soldati-Favre, D. (2008): Toxoplasma profilin is essential for host cell invasion and TLR11-dependent induction of an interleukin-12 response. , Cell Host Microbe (vol. 3), pp. 77-87.

[47] Dubremetz, J.F., Achbarou, A., Bermudes, D., Joiner, K.A. (1993): Kinetics and pattern of organelle exocytosis during Toxoplasma gondii/host-cell interaction., Parasitol Res (vol. 79), pp. 402-408.

[48] Kim, K., and Boothroyd, J.C (1995): Toxoplasma gondii: stable complementation of sag1 (p30) mutants using SAG1 transfection and fluorescence-activated cell sorting., Exp Parasitol (vol. 80), pp. 46-53.

[49] Bastin, P., Bagherzadeh, Z., Matthews, K.R., and Gull, K. (1996): A novel epitope tag system to study protein targeting and organelle biogenesis in Trypanosoma brucei. , Mol Biochem Parasitol (vol. 77), pp. 235-239.

[50] MM, Bradford (1976): A rapid and sensitive method for the quantitation of microgram quantities of protein utilizing the principle of protein-dye binding, Anal Biochem (vol. 72), pp. 248-54.

[51] Rotureau, B., Gego, A., and Carme, B. (2005): Trypanosomatid protozoa: a simplified DNA isolation procedure. , Exp Parasitol (vol. 111), pp. 207-209.

[52] Fölsch H, Pypaert M, Schu P, Mellman I (2001): Distribution and function of AP-1 clathrin adaptor complexes in polarized epithelial cells., J. Cell Biol. (vol. 152), pp. 595-606.

[53] Porter TJ, Kent C (1992): Choline/ethanolamine kinase from rat liver. , Methods Enzymol. (vol. 209), pp. 134-46.

[54] Uchida T, Yamashita S (1992): Choline/ethanolamine kinase from rat brain. , Methods Enzymol. (vol. 209), pp. 147-53.

[55] Bligh EG, Dyer WJ (1959): A rapid method of total lipid extraction and purification, Can. J. Biochem. Physiol. (vol. 37), pp. 911-7.

[56] Poumay Y, Ronveaux-Dupal MF (1985): Rapid preparative isolation of concentrated low density lipoproteins and of lipoprotein-deficient serum using vertical rotor gradient ultracentrifugation, J Lipid Res (vol. 26), pp. 1476-80.

[57] S, Brenner (1987): Phosphotransferase sequence homology, Nature (vol. 329), p. 21.

[58] Jackowski S, Fagone P (2005): CTP: Phosphocholine cytidylyltransferase: paving the way from gene to membrane, J Biol Chem (vol. 280), pp. 853-6.

[59] Cornell RB, Northwood IC (2000): Regulation of CTP:phosphocholine cytidylyltransferase by amphitropism and relocalization, Trends Biochem Sci (vol. 25), pp. 441-7.

[60] Alberge B, Gannoun-Zaki L, Bascunana C, Tran van Ba C, Vial H, Cerdan R (2009): Comparison of the cellular and biochemical properties of Plasmodium falciparum choline and ethanolamine kinases, Biochem J (vol. 425), pp. 149-58.

[61] Gibellini F, Hunter WN, Smith TK (2008): Biochemical characterization of the initial steps of the Kennedy pathway in Trypanosoma brucei: the ethanolamine and choline kinases, Biochem J (vol. 415), pp. 135-44.

[62] Gallego-Ortega D, Ramirez de Molina A, Ramos MA, Valdes-Mora F, Barderas MG, Sarmentero-Estrada J, Lacal JC (2009): Differential role of human choline kinase alpha and beta enzymes in lipid metabolism: implications in cancer onset and treatment. , PLoS One (vol. 4: e7819).

[63] Kim KH, Voelker DR, Flocco MT, Carman GM (1998): Expression, purification, and characterization of choline kinase, product of the CKI gene from Saccharomyces cerevisiae, J Biol Chem (vol. 273), pp. 6844-52.

[64] Aoyama C, Ohtani A, Ishidate K (2002): Expression and characterization of the active molecular forms of choline/ethanolamine kinase-alpha and -beta in mouse tissues, including carbon tetrachloride-induced liver, Biochem J (vol. 363), pp. 777-84.

[65] Choubey V, Guha M, Maity P, Kumar S, Raghunandan R, Maulik PR, Mitra K, Halder and UC, Bandyopadhyay U (2006): Molecular characterization and localization of Plasmodium falciparum choline kinase, Biochim Biophys Acta (vol. 1760), pp. 1027-38.

[66] Esko JD, Nishijima M, Raetz CR (1982): Animal cells dependent on exogenous phosphatidylcholine for membrane biogenesis, Proc Natl Acad Sci U S A (vol. 79), pp. 1698-702.

[67] Houweling M, Cui Z, Vance DE (1995): Expression of phosphatidylethanolamine N-methyltransferase-2 cannot compensate for an impaired CDP-choline pathway in mutant Chinese hamster ovary cells, J Biol Chem (vol. 270), pp. 16277-82.

[68] Choi JY, Martin WE, Murphy RC, Voelker DR (2004): Phosphatidylcholine and N-methylated phospholipids are nonessential in Saccharomyces cerevisiae, J Biol Chem (vol. 279), pp. 42321-30.

[69] Fouts AE, Boothroyd JC (2007): Infection with Toxoplasma gondii Bradyzoites Has a Diminished Impact on Host Transcript Levels Relative to Tachyzoite Infection, INFECTION AND IMMUNITY (vol. 75), pp. 634-642.

[70] DR, Voelker (1997): Phosphatidylserine decarboxylase, Biochim Biophys Acta (vol. 1348), pp. 236-44.

[71] Hosaka K, Kodaki T, Yamashita S (1989): Cloning and characterization of the yeast CKI gene encoding choline kinase and its expression in Escherichia coli, J Biol Chem (vol. 264), pp. 2053-9.

[72] Henneberry AL, McMaster CR (1999): Cloning and expression of a human choline/ethanolaminephosphotransferase: synthesis of phosphatidylcholine and phosphatidylethanolamine, Biochem J (vol. 339), pp. 291-8.

[73] Vial HJ, Thuet MJ, Philippot JR (1984): Cholinephosphotransferase and ethanolaminephosphotransferase activities in Plasmodium knowlesi-infected erythrocytes. Their use as parasite-specific markers, Biochim Biophys Acta (vol. 795), pp. 372-83.

[74] Hjelmstad RH, Bell RM (1988): The sn-1,2-diacylglycerol ethanolaminephosphotransferase activity of Saccharomyces cerevisiae. Isolation of mutants and cloning of the EPT1 gene, J Biol Chem (vol. 263), pp. 19748-57.

[75] Grant AM, Hanson PK, Malone L, Nichols JW. (2001): NBD-labeled phosphatidylcholine and phosphatidylethanolamine are internalized by transbilayer transport across the yeast plasma membrane., Traffic. (vol. 2), pp. 37-50.

[76] Kean LS, Fuller RS, Nichols JW (1993): Retrograde lipid traffic in yeast: identification of two distinct pathways for internalization of fluorescent-labeled phosphatidylcholine from the plasma membrane, J Cell Biol (vol. 123), pp. 1403-19.

[77] Kean LS, Grant AM, Angeletti C, Mahé Y, Kuchler K, Fuller RS, Nichols JW (1997): Plasma membrane translocation of fluorescent-labeled phosphatidylethanolamine is controlled by transcription regulators, PDR1 and PDR3, J Cell Biol (vol. 138), pp. 255-70.

[78] Robibaro B, Hoppe HC, Yang M, Coppens I, Ngô HM, Stedman TT, Paprotka K, Joiner and KA (2001): Endocytosis in different lifestyles of protozoan parasitism: role in nutrient uptake with special reference to Toxoplasma gondii, Int J Parasitol (vol. 31), pp. 1343-53.

[79] Coppens I, Sinai AP, Joiner KA (2000): Toxoplasma gondii exploits host low-density lipoprotein receptor-mediated endocytosis for cholesterol acquisition, J Cell Biol (vol. 149), pp. 167-80.

[80] Goldstein JL, Brown MS (1977): The low-density lipoprotein pathway and its relation to atherosclerosis, Annu Rev Biochem (vol. 46), pp. 897-930.

LIST OF PUBLICATIONS AND PRESENTATIONS

The following publications and presentations resulted from the here-presented work:

Articles in international peer-reviewed journals	Vera Sampels, Isabelle Dietrich, Isabelle Coppens, Lilach Sheiner, Boris Striepen, Andreas Herrmann, Richard Lucius and Nishith Gupta "The knockdown of a Novel Choline Kinase Demonstrates the Metabolic Plasticity of Membrane Biogenesis in *Toxoplasma gondii*" In Preparation
Oral presentations in international conferences	European Congress on Protistology (ECOP), 2011, Berlin, Germany "Knockdown of a Novel Choline Kinase Demonstrates the Metabolic Plasticity of Membrane Biogenesis in *Toxoplasma gondii"* 11th International Meeting on Toxoplasmosis, 2011, Ottawa, Canada "A Novel Choline Kinase, *Toxoplasma gondii* is not Capable Living Without" DGP Conference, 2010, Düsseldorf, Germany "Endogenous Synthesis *vs.* Scavenging of Phospholipids in *Toxoplasma gondii*"
Poster presentations in international conferences	Gordon Research Conference "Biology of Host-Parasite Interaction", 2010, Newport, Rhode Island, USA "Membrane Biogenesis in *Toxoplasma gondii*: *De novo* Synthesis *versus* Selective Scavenging of Major Phospholipids by the Parasite" 10th International Conference on Toxoplasmosis, 2009, Kerkrade, Netherlands "*Toxoplasma gondii* Secretes a Novel Choline Kinase into its Parasitophorous Vacuole"

Berlin, 22.09.2011 Vera Sampels